Study of Interchange Instabilities and Anomalous Transport Based on Reduced Two-Fluid Model

Hideo Sugama

1988

Study of Interchange Instabilities and Anomalous Transport Based on Reduced Two-Fluid Model

Hideo Sugama

1988

Abstract

In this thesis, theoretical studies of interchange instabilities and anomalous transport in a stellarator/heliotron plasma are reported. We derive the reduced two-fluid model in order to describe high temperature large aspect ratio toroidal plasmas. Our new model is more general than the conventional reduced MHD (RMHD) model. It contains diamagnetic drifts and ion parallel motion, which are neglected in RMHD, and it is applicable to both stellarator/heliotron and tokamak. Based on the reduced two-fluid model, we study stabilizing effects of the ion diamagnetic drift on the ideal interchange instability both analytically and numerically. Improvement of beta limit due to the ion finite Larmor radius stabilization is discussed in the case of Heliotron E. Considering a low beta plasma, in which ideal interchange modes are stable, we study the resistive interchange instabilities coupled to the electron diamagnetic drift under the electrostatic assumption. These resistive electrostatic instabilities are considered as candidates to explain the edge turbulence observed in stellarator/heliotron plasmas. Linear growth rates are given as a function of collision frequency and mode structures are shown. Nonlinear time evolution of the ideal and resistive interchange modes are numerically investigated. We show that ion diamagnetic drift lowers the saturation level of the ideal interchange modes and decreases the kinetic energy distribution on higher harmonic modes. In the simulation of the electrostatic turbulence driven by the resistive interchange modes coupled to the electron diamagnetic drift, we find the condensation of the mode energy to the $m = 0$ mode accompanied with the production of the stationary radial electric field, which is not seen in the resistive interchange mode driven turbulence based on the RMHD model. The decrease of the energy distributed over the high poloidal mode numbers due to the energy condensation to the $m = 0$ mode is expected to improve the particle confinement.

We give a new formulation of renormalized theories to describe strong turbulence and the resultant anomalous transport. In our formulation, considering the general model equation with convective nonlinearity, we derive the exact integral equation for the nonlinear propagator, from which the renormalized expression of the propagator is obtained by the iterative method and the one-point (coherent) and two-point (incoherent) renormalized theories are given in a unified manner. We apply our formulation to the RMHD and the reduced two-fluid equations. For both models, the wavenumber

spectrum of the pressure or density fluctuations and the turbulent diffusivity are obtained. The results based on the latter two-fluid model seem to be appropriate for explaining the edge turbulence in Heliotron E.

Acknowledgements

It is a great pleasure to thank Emeritus Professor Koji Uo and Professor Atsuo Iiyoshi for affording me the opportunity to study fusion plasma and write this thesis.

I would like to express my special gratitude to Professor Masahiro Wakatani for teaching and guiding me over the several years. Without his patient encouragement and many productive suggestions, this thesis would not have been completed.

I am very grateful to Doctor Kimitaka Itoh and Doctor Katsumi Kondo for their useful comments and suggestions on the manuscript.

I would like to acknowledge helpful discussions with Doctor Akira Hasegawa and Doctor Benjamin A. Carreras during their visit to Kyoto.

I wish to thank Doctor Yuji Nakamura, Katsuji Ichiguchi and Masatoshi Yagi for their support in computational work and useful discussions. I am also indebted to Doctor Hiroyuki Okada and Takeshi Suzuki for helping me in using a computer system to type this thesis.

Finally, I thank all members of Plasma Physics Laboratory in Kyoto University for their warm friendship and support.

Contents

Chapter 1

Introduction

In magnetically confined plasmas inhomogeneities of magnetic fields, currents, pressure, density and temperature cause a variety of instabilities, which give limitation to stable plasma confinement and also produce complex dynamical behavior of the plasmas. Fluid models such as magnetohydrodynamics (MHD) have made the most successful contributions to the theoretical research of the magnetized plasmas including those spatial inhomogeneities. Analyses of equilibrium and stability based on the ideal MHD equations are one of the basic methods in designing a magnetic configuration of a new device. The reduced MHD (RMHD) model,[1]–[3] which was derived from the full MHD equations, is also useful in the theoretical description of plasma dynamics including the effects of nonlinearity and dissipation. However the MHD model does not include kinetic effects such as finite Lamor radius (FLR) effect, Landau damping and particle trapping. These phenomena becomes important in the high temperature rare collisional plasmas. In this thesis, we concentrate our attention on the FLR effect, which can be included through diamagnetic drifts of ions and electrons in the two-fluid model. One of main topics in this thesis is to study the effects of the ion and electron diamagnetic drifts on interchange instabilities which are driven by pressure gradients combined with bad magnetic field curvature.

Construction of the reduced fluid model based on the two-fluid equations and its application to stability analysis of interchange modes in stellarator/heliotron configuration[4],[5] are presented in the first part of this thesis. Our new model is more general than RMHD. It contains diamagnetic drifts and ion parallel motion, which are neglected in RMHD model, and

it can describe both tokamak and stellarator/heliotron plasmas. After the derivation of the reduced two-fluid equations, we will use them to investigate the interchange instabilities, which degrade plasma confinement in stellarator/heliotron configuration. As an example, stabilizing effects of the ion diamagnetic drift on the ideal interchange instability are examined. We will also study the resistive interchange instability including the electron diamagnetic drift effect. These instabilities with properties which are not predicted by the ideal or resistive single fluid MHD equations are considered to be the cause of turbulence and the related anomalous transport in high temperature plasma.

The anomalous transport is a problem of great interest both experimentally and theoretically.[6] The transport phenomena are directly related to the dependence of the particle and energy cofinement time on the plasma parameters and therefore the reliable estimation of them are essentially important in the future reactor design. Since the measured microscopic fluctuations in a plasma show strong turbulence character e.g. broad spectra of wavenumbers and frequencies,[7]-[9] the perturbative approach of quasilinear or weak turbulence theories fails to describe them and the turbulence theories treating the strong nonlinearity are required. Theoretically it is impossible to explain the observed transport in terms of classical collisional mechanisms, which is called anomalous transport. Many efforts have been made to explain it based on turbulence theories in these years. For estimating the transport coefficients theoretically, we usually use mixing length arguments[23] in which a diffusion coefficient is given by $D \sim \gamma/k_\perp^2$ using a perpendicular wavenumber $k_\perp$ and a linear growth rate of the concerning instability γ as characteristic space and time scales. We also use dimensional analysis technique based on scale transfomation symmetries of the basic nonlinear equations.[10]-[14] In the approaches to the strong plasma turbulence, the renormalized theories[6],[15]-[26] quantitatively describe the macroscopic statistical averages of the fluctuations. By using the renormalized theories, diffusion coefficients enhanced by the turbulent fluctuations are derived, which is comparable with the anomalous transport observed in experiments. In the renormalized theories discussed in this thesis, the two-point correlation or incoherent structure called 'clumps'[18] is considered, which enables one to calculate the wavenumber or frequency spectra of the fluctuations. In the second part of this thesis, we give a new formulation of the renormalized theories and apply it to the analyses of the turbulence

driven by the resistive interchange instabilities in stellarator/heliotron. We will show how the electron diamagnetic drift makes the parameter dependence of the turbulent diffusivity different from that obtained by the RMHD model.

This dissertation is organized in the following manner. In Chapter 2, the reduced two-fluid equations are derived and their general properties are discussed. The significant difference between the one-fluid MHD equations and the two-fluid equations is that in the latter the generalized Ohm's law and the ion gyroviscosity are contained to describe the electron and ion diamagnetic drifts correctly. In the derivation of the reduced two-fluid equations, we consider application to stellarator/heliotron. Our model also includes the evolution equation of the ion fluid velocity along the magnetic field line, which makes it possible to describe the ion acoustic wave. It is shown that our model conserves the total energy in the case of no dissipation. Reduced fluid models such as RMHD, Hasegawa-Wakatani[27] and Hasegawa-Mima equations[28] are derivable as limiting forms of our model.

In Chapter 3, we study the stabilizing effects of the ion diamagnetic drift on the ideal interchange instability[29]–[31] both analytically and numerically based on the reduced two-fluid model. Using the sheared-slab geometry and the method of asymptotic matching, analytical expressions of the linear dispersion relation and the stability criterion are obtained. The analytical results for the slab geometry are checked by the numerical calculation for the cylindrical plasma using the shooting method. Inprovement of beta limit due to the ion FLR stabilization of the ideal interchange mode is discussed.

In Chapter 4, the resistive interchange instabilities coupled to the electron diamagnetic drift are studied.[32] Here we consider a low beta plasma, in which ideal interchange modes are stable and the electrostatic approximation is applicable. These resistive electrostatic instabilities are considered as candidates to explain the turbulence observed in the peripheral region of stellarator/heliotron plasmas. Linear growth rates are given as a function of collision frequency and mode structures are shown.

In Chapter 5, time evolution of the nonlinear ideal and resistive interchange modes, which are studied in Chapter 3 and Chapter 4, respectively, are numerically investigated. By using single-helicity calculations, nonlinear saturation of the ideal interchange modes are studied. We show the ion diamagnetic drift effects on the saturation level and the poloidal mode number (m) spectrum of the fluctuation energy. The multi-helicity calculations of the

electrostatic turbulence driven by the resistive interchange modes coupled to the electron diamagnetic drift are given. We find the condensation of the mode energy to the $m = 0$ mode accompanied with the production of the stationary radial electric field, which is not seen in the resisitive interchange mode driven turbulence based on the RMHD model.

In Chapter 6, our formulation of renormalized theories is presented. Considering the general model equation with convective nonlinearity, we derive the integral equation for the nonlinear propagator, from which the renormalized expession of the propagator is obtained by the iterative method and the one-point (coherent) and two-point (incoherent) renormalized theories are given in a unified manner. Our formulation is based on the real space representation instead of the wavenumber space. We also discuss the clump lifetime approximation[18]–[24] to the solution of the two-point renormalized equation. An application of the renormalized theories is illustrated by using the Vlasov-Poisson equations and the results obtained by Dupree[15]–[18] are reproduced.

In Chapter 7, the resistive interchange mode driven turbulence is studied analytically using the renormalized theories given in Chapter 6. We apply the formulation to the RMHD equations and the the reduced two-fluid equations in Chapter 4. For both models, the wavenumber spectrum of the pressure or density fluctuations and the turbulent diffusivity in a stellarator/heliotron plasma are obtained.

Finally in Chapter 8, concluding remarks are given. Main results and future studies relating to this thesis are discussed.

Chapter 2

Reduced Two-Fluid Model

2.1 Introduction

In this chapter, the reduced two-fluid model, which describes the dynamics of large aspect ratio toroidal plasmas including tokamak and stellarator/heliotron, is derived and its properties are discussed. Strauss derived the reduced magnetohydrodynamics (RMHD) equations for tokamak plasmas[1]–[2] from the full MHD equations by the ordering in terms of the inverse aspect ratio, $\epsilon = a/R_0$, where a and R_0 are the minor and major radii of the torus, respectively. He also obtained the RMHD equations for stellarator plasmas[3], using the stellarator ordering where the expansion parameter is $\lambda = \epsilon^{1/2}$. Here λ denotes the ratio of the magnitude of the external helical magnetic field to the toroidal magnetic field. RMHD is a set of simple nonlinear equations, which includes only three field variables, i.e., stream function (or electrostatic potential), poloidal magnetic flux and pressure; however RMHD can describe much of dynamics which the full MHD equations do. As the shortest time scale of RMHD, the shear Alfven dynamics is included; therefore, the phenomina which occur in a shorter time scale than the shear Alfven wave, such as compressional Alfven dynamics, are eliminated. The ion accoustic waves, which propagate dominantly in the direction of the magnetic field, are not included in RMHD since the flow along the magnetic field lines can be decoupled from the shear Alfven dynamics. Furthermore, two-fluid dynamics such as drift waves cannot be treated in RMHD based on the one-fluid model. For studying turbulent fluctuations driven by these drift

waves or kinetic unstable modes, we need extension of RMHD. Here we construct a new reduced fluid model to include the ion and electron diamagnetic drift motion as important kinetic effects in high temperature plasma by keeping two-fluid nature of plasma. The reduced two-fluid model presented in the following sections have the four field variables, where the flow along the magnetic field lines is added to the three field variables in RMHD.

In Sec.2.2, we discuss the two-fluid equations, from which our reduced model is derived. In Sec.2.3, the derivation of the reduced two-fluid model is presented and the properties of that are discussed. In Sec.2.4, conclusions are given.

2.2 Two-Fluid Equations

Here we assume that the plasma consists of electrons and protons. By taking the first and second order moments of the Boltzmann equation for each species of particle, the continuity and momentum equations for electron and ion fluids are given in the following expressions,

$$\frac{\partial n_e}{\partial t} + \nabla \cdot (n_e \boldsymbol{v}_e) = 0 \tag{2.1}$$

$$n_e m_e \left(\frac{\partial}{\partial t} + \boldsymbol{v}_e \cdot \nabla \right) \boldsymbol{v}_e + \nabla \cdot \mathsf{P}_e = -n_e e \left(\boldsymbol{E} + \frac{\boldsymbol{v}_e}{c} \times \boldsymbol{B} \right) + \boldsymbol{F} \tag{2.2}$$

$$\frac{\partial n_i}{\partial t} + \nabla \cdot (n_i \boldsymbol{v}_i) = 0 \tag{2.3}$$

$$n_i m_i \left(\frac{\partial}{\partial t} + \boldsymbol{v}_i \cdot \nabla \right) \boldsymbol{v}_i + \nabla \cdot \mathsf{P}_i = n_i e \left(\boldsymbol{E} + \frac{v_i}{c} \times \boldsymbol{B} \right) - \boldsymbol{F} \tag{2.4}$$

where n_α is the particle density, $\boldsymbol{v}_\alpha$ the fluid velocity, P_α the pressure tensor, m_α the mass, $\alpha(= e, i)$ the species label, $-e$ the electron charge, $+e$ the ion charge. $\boldsymbol{E}$ and $\boldsymbol{B}$ are the electric and magnetic fields, respectively, and $\boldsymbol{F}$ represents the friction force i.e. the momentum transfer per unit volume and unit time due to collisions from the ion fluid to the electron fluid.

It is convenient to use the average fluid velociy $\boldsymbol{v}$ and the current density $\boldsymbol{J}$ as in the MHD description instead of using $\boldsymbol{v}_i$ and $\boldsymbol{v}_e$. Here we neglect the electron inertia since $m_e/m_i \ll 1$. We consider the phenomina which occur sufficiently slower than plasma oscillations and therefofe we can assume the quasineutrality condition, $n_e = n_i = n$. Thus the average velocity $\boldsymbol{v}$ and the current density $\boldsymbol{J}$ are written as

$$\boldsymbol{v} \equiv \frac{n_i m_i \boldsymbol{v}_i + n_e m_e \boldsymbol{v}_e}{n_i m_i + n_e m_e} \simeq \boldsymbol{v}_i \tag{2.5}$$

and

$$\boldsymbol{J} \equiv n_i e \boldsymbol{v}_i - n_e e \boldsymbol{v}_e = ne(\boldsymbol{v}_i - \boldsymbol{v}_e), \tag{2.6}$$

respectively. From Eqs.(2.5) and (2.6), the electron fluid velocity $\boldsymbol{v}_e$ is given by

$$\boldsymbol{v}_e = \boldsymbol{v} - \frac{\boldsymbol{J}}{ne}. \tag{2.7}$$

From Eqs.(2.1) and (2.3) and the quasineutrality condition, we obtain

$$\frac{\partial n}{\partial t} = -\nabla \cdot (n\boldsymbol{v}) = -\nabla \cdot (n\boldsymbol{v}_e). \tag{2.8}$$

Then Eqs.(2.6) and (2.8) yield

$$\nabla \cdot \boldsymbol{J} = 0. \tag{2.9}$$

The friction force $\boldsymbol{F}$ is given by

$$\boldsymbol{F} = ne(\eta_{\parallel}\boldsymbol{J}_{\parallel} + \eta_{\perp}\boldsymbol{J}_{\perp}) \tag{2.10}$$

where η is the electrical resistivity and the subscripts $\parallel$ and $\perp$ refer to directions parallel and perpendicular to the magnetic field line.

We assume that the pressure tensors $\mathsf{P}_\alpha (\alpha = e, i)$ take the form

$$\left.\begin{aligned} \mathsf{P}_e &= P_e \mathsf{I} \\ \mathsf{P}_i &= P_i \mathsf{I} + \Pi_{gi} \end{aligned}\right\} \tag{2.11}$$

where I is the unit tensor and the scalar pressure $P_\alpha = nT_\alpha$. Here T_α is the temperature assuming the isotropic thermalization. Π_{gi} denotes the ion gyroviscousity tensor, which is assumed to be determined by P_i, $\boldsymbol{B}$ and $\boldsymbol{v}$ here. The expression of Π_{gi} will be given in the next section, since its explicit form is not required here. The gyroviscosity is due to the gyromotion of the particles and remains in the collisionless limit. The electron gyroviscosity is negligible because of small gyroradii of electrons. Collisional viscosity is smaller than the gyroviscosity for both electrons and ions. Inclusion of Π_{gi} becomes essential when the effect of the ion diamagnetic drift is considered.

Adding Eqs.(2.2) and (2.4) gives

$$nm_i \left(\frac{\partial}{\partial t} + \boldsymbol{v} \cdot \nabla\right) \boldsymbol{v} + \nabla(P_e + P_i) + \nabla \cdot \Pi_{gi} = \frac{1}{c}\boldsymbol{J} \times \boldsymbol{B} \tag{2.12}$$

by assuming charge neutrality. Eq.(2.2) is rewritten as

$$\boldsymbol{E} + \frac{1}{c}\boldsymbol{v}_e \times \boldsymbol{B} + \frac{1}{ne}\nabla P_e = \eta_{\parallel}\boldsymbol{J}_{\parallel} + \eta_{\perp}\boldsymbol{J}_{\perp}. \tag{2.13}$$

Here Eqs.(2.5), (2.10) and (2.11) are used and the electon inertia terms are neglected. Equation (2.13) is called the generalized Ohm's law in which,

compared with the usual Ohm's law in MHD, the average fluid velocity $\boldsymbol{v}$ is replaced with the electron fluid velocity $\boldsymbol{v}_e$ and the electron pressure P_e is included, which is related to the diamagnetic drift motion.

In order to obtain a closed set of equations describing the two-fluid plasma, we need Maxwell's equations and two equations of state connecting the pressures with the density. In summary of the two-fluid model, the plasma is descried by n, $\boldsymbol{v}$, $\boldsymbol{v}_e$, $\boldsymbol{J}$, $\boldsymbol{E}$, $\boldsymbol{B}$, P_e, P_i as functions of the position $\boldsymbol{x}$ and the time t governed by the equations

$$\frac{\partial n}{\partial t} = -\nabla \cdot (n\boldsymbol{v}) = -\nabla \cdot (n\boldsymbol{v}_e) \tag{2.14}$$

$$nm_i \left(\frac{\partial}{\partial t} + \boldsymbol{v} \cdot \nabla \right) \boldsymbol{v} + \nabla (P_e + P_i) + \nabla \cdot \Pi_{gi} = \frac{1}{c} \boldsymbol{J} \times \boldsymbol{B} \tag{2.15}$$

$$\boldsymbol{E} + \frac{1}{c} \boldsymbol{v}_e \times \boldsymbol{B} + \frac{1}{ne} \nabla P_e = \eta_{\parallel} \boldsymbol{J}_{\parallel} + \eta_{\perp} \boldsymbol{J}_{\perp} \tag{2.16}$$

$$\boldsymbol{v}_e = \boldsymbol{v} - \frac{\boldsymbol{J}}{ne} \tag{2.17}$$

$$\frac{\partial \boldsymbol{B}}{\partial t} = -c \nabla \times \boldsymbol{E}, \qquad \nabla \cdot \boldsymbol{B} = 0 \tag{2.18}$$

$$\frac{4\pi}{c} \boldsymbol{J} = \nabla \times \boldsymbol{B} \tag{2.19}$$

$$P_e = f_e(n), \qquad P_i = f_i(n) \tag{2.20}$$

where the displacement current term $\partial \boldsymbol{E}/\partial t$ is neglected and the Ampere's law (2.19) is employed, which is consistent with the quasineutrality condition or Eq.(2.9). The equations of state are represented by Eqs.(2.20). Hereafter we may assume that the electron and ion fluids obey the ideal gas law and Eqs.(2.20) take the form

$$P_\alpha = C_\alpha n_\alpha^{\gamma_\alpha} \qquad (\alpha = e, i). \tag{2.21}$$

Here, if the changes of state are adiabatic, then $C_\alpha = \exp[(S - S_0)/C_v] =$ const. and $\gamma_\alpha = C_p/C_v$, where C_v is the specific heat at constant volume, C_p is that at constant pressue, S and S_0 are the entropy and its standard

point, respectively. All these quantities are given for each species α and assumed to be constant. In the case of the isothermal process, we may take $C_\alpha = T_\alpha = \text{const.}$ and $\gamma_\alpha = 1$. Examining the two-fluid equations (2.14)–(2.20), we note that, three field quantities n, $\boldsymbol{v}$, and $\boldsymbol{B}$ are sufficient to determine uniquely the momentary state of the system and the other field quantities P_e, P_i, $\boldsymbol{J}$, $\boldsymbol{v}_e$, and $\boldsymbol{E}$ are represented by the above three quantities at every instant of time, which is similar to the usual MHD equations. Then the evolution of the system is principally described by Eqs.(2.14), (2.15) and (2.18). The quantities n, $\boldsymbol{v}$ and $\boldsymbol{B}$ have seven field components and also the equations include nonlinear terms. Thus it is impossible to solve them analytically. Since the equations include several charactristic times which have different orders of magnitude each other, it is not simple to solve them numerically. In order to make the equations tractable, the reduction of numbers of field quantities will be possible without lossing low frequency physical processes occurring in a strong toroidal field. The procedure will be explained in the next section.

The equation of energy balance is obtained from Eqs.(2.14)–(2.20) as follows

$$\begin{aligned}
&\frac{d}{dt}\int_V d^3x \left\{\frac{1}{2}nm_i\boldsymbol{v}^2 + \frac{B^2}{8\pi} + n\Psi_i(n) + n\Psi_e(n)\right\} \\
&= -\int_S d\boldsymbol{S}\cdot\left\{\frac{1}{2}nm_iv^2\boldsymbol{v} + n\Psi_i(n)\boldsymbol{v} + n\Psi_e(n)\boldsymbol{v}_e + P_i\boldsymbol{v} + \Pi_{gi}\cdot\boldsymbol{v}\right. \\
&\qquad \left. + P_e\boldsymbol{v}_e + \frac{c}{4\pi}\boldsymbol{E}\times\boldsymbol{B}\right\} - \int_V d^3x\{\eta_\parallel J_\parallel^2 + \eta_\perp J_\perp^2\} + \int_V d^3x\Pi_{gi} : \nabla\boldsymbol{v}
\end{aligned} \tag{2.22}$$

where the compression or internal energy per single particle of species α is given by

$$\Psi_\alpha(n) = -\int f_\alpha(n)\, d\left(\frac{1}{n}\right) = \int \frac{f_\alpha(n)}{n^2}dn. \tag{2.23}$$

If we use Eq.(2.21), Eq.(2.23) is rewitten as

$$n\Psi_\alpha = \begin{cases} \dfrac{P_\alpha}{\gamma_\alpha - 1} & (\gamma_\alpha \neq 1) \\ P_\alpha \ln(n/n_0) & (\gamma_\alpha = 1,\ n_0 = \text{const.})\,. \end{cases} \tag{2.24}$$

The left-hand side of Eq.(2.22) expresses the rate of change of the total energy in the volume V, which consists of the kinetic energy of the fluid motion, the

magnetic energy, the ion and electron internal energy. The first and second terms in the right-hand side are interpreted as the energy flows through the surface S and the energy dissipated in the volume as Joule heat, respectiverly. The last term is associated with the change of the internal energy related to the gyromotion and, in the next section, we will discuss that it vanishes in the order of our interest.

2.3 Reduced Two-Fluid Equations

Here we use a coordinate system as shown in Fig.2.1 with the metric

$$ds^2 = dr^2 + r^2 d\theta^2 + (1 + x/R_0)^2 dz^2 \tag{2.25}$$

where $x = r\cos\theta$, $z = -R_0\zeta$ and ζ is the toroidal angle. In order to derive the reduced equations, we employ the ordering[3],[33] in terms of the expansion parmeter λ defined by

$$\lambda \equiv \epsilon^{1/2} \tag{2.26}$$

where $\epsilon \equiv a/R_0 \ll 1$ is the inverse aspect ratio, a and R_0 are the minor and major radii, respectively. We assume that the uniform toroidal magnetic field $B_0\hat{z}$ is of the zeroth-order, the helical field is of the first-order, and the following quantities such as the curvature of the field lines, the pressure gradient, the current and the magnetic field produced by this current are of the second-order. The magnetic field is given by

$$\begin{aligned} \boldsymbol{B} &= \frac{B_0}{1 + x/R_0}\hat{z} + \nabla\Phi + \nabla \times \boldsymbol{A} \\ &= B_0\hat{z} + \nabla\Phi + (B^\beta - B_0 x/R_0)\hat{z} + \nabla A \times \hat{z} \end{aligned} \tag{2.27}$$

where $\hat{z}$ is the toroidal unit vector, Φ is the potential for the helical field, which satisfies

$$\nabla^2\Phi = 0 \tag{2.28}$$

and $\boldsymbol{A}$ is the vector potential for the magnetic fields produced by the plasma currents. In Eq.(2.27) we used

$$\nabla \times \boldsymbol{A} = B^\beta\hat{z} + \nabla A \times \hat{z} \tag{2.29}$$

where $B^\beta = \hat{z} \cdot (\nabla \times \boldsymbol{A})$, $A = \hat{z} \cdot \boldsymbol{A}$ and the derivatives with respect to z are eliminated since $\partial/\partial z = O(\lambda^2)$ for all quantities except the potential Φ, which is discussed in detail later. From the Ampere's law (2.19) and Eq.(2.27), we obtain the current density $\boldsymbol{J}$ in the lowest order

$$\boldsymbol{J} = \frac{c}{4\pi}\nabla \times \boldsymbol{B} = \frac{c}{4\pi}(\nabla B^\beta \times \hat{z} - \nabla_\perp^2 A\hat{z}). \tag{2.30}$$

In the equation of motion (2.15), it is assumed that $\nabla(P_e + P_i)$, $\boldsymbol{v}$ and $\partial/\partial t$ are $O(\epsilon) = O(\lambda^2)$ and that the force due to gyroviscosity $\nabla \cdot \Pi_{gi}$ is $O(\epsilon^2) =$

$O(\lambda^4)$. Then Eq.(2.15) yields the pressure balance for MHD equilibrium in $O(\epsilon)$

$$\nabla_\perp \left(P_e + P_i + \frac{B_0}{4\pi} B^\beta \right) = 0 \tag{2.31}$$

where Eq.(2.30) is used. Taking the inner product of Eq.(2.15) and $\boldsymbol{B}$, we have

$$\boldsymbol{B} \cdot \nabla (P_e + P_i) = -n_0 m_i B_0 \left(\frac{\partial}{\partial t} + \boldsymbol{v}_\perp \cdot \nabla_\perp \right) v_\parallel - B_0 \hat{z} \cdot (\nabla \cdot \Pi_{gi}) \tag{2.32}$$

where $v_\parallel = \boldsymbol{v} \cdot \hat{b}$, $\hat{b} = \boldsymbol{B}/B$ and n_0 denotes the $O(\lambda^0)$ part of the density n. Equation (2.32) is valid to $O(\epsilon^2)$. From the outer product of Eq.(2.15) and $\boldsymbol{B}$, we obtain the perpendicular current density

$$\boldsymbol{J}_\perp = \frac{\boldsymbol{B}}{B^2} \times \boldsymbol{K} \tag{2.33}$$

where

$$\boldsymbol{K} = c \left[\nabla (P_e + P_i) + \nabla \cdot \Pi_{gi} + n m_i \left(\frac{\partial}{\partial t} + \boldsymbol{v} \cdot \nabla \right) \boldsymbol{v} \right] \tag{2.34}$$

The total current density is written as

$$\boldsymbol{J} = \sigma \boldsymbol{B} + \boldsymbol{J}_\perp \tag{2.35}$$

where $\sigma = \boldsymbol{B} \cdot \boldsymbol{J}/B^2$. Substituting Eq.(2.35) into Eq.(2.9) and using Eq.(2.33) yield

$$\boldsymbol{B} \cdot \nabla \sigma = \frac{\nabla B^2 \times \boldsymbol{B}}{B^4} \cdot \boldsymbol{K} + \frac{\boldsymbol{B}}{B^2} \cdot \nabla \times \boldsymbol{K} \tag{2.36}$$

where we used $\boldsymbol{K} \cdot \nabla \times \boldsymbol{B} = 0$ which is derived from Eqs.(2.15) and (2.19).

We can write

$$n = n_0 + \tilde{n} \tag{2.37}$$

$$P_\alpha = P_{\alpha 0} + \tilde{P}_\alpha \qquad (\alpha = e, i) \tag{2.38}$$

where n_0 and $P_{\alpha 0} = n_0 T_{\alpha 0}$ are the lowest order quantities or the volume-averaged values of the density and the pressure respectively. Here we assumed that n_0 and $P_{\alpha 0}$ are $O(\lambda^0)$ and that $\tilde{n}$ and $\tilde{P}_\alpha$ are $O(\lambda^2)$. This ordering is slightly different from the conventional one used in RMHD and should be

treated carefully when it is applied to the equation where density or pressure is contained without being differentiated.

The electric field $\boldsymbol{E}$ is represented in terms of the electrostatic potential ϕ and the vector potential $\boldsymbol{A}$ as

$$\boldsymbol{E} = -\nabla\phi - \frac{1}{c}\frac{\partial \boldsymbol{A}}{\partial t}. \tag{2.39}$$

The parallel component of the generalized Ohm's law (2.16) is

$$\boldsymbol{B}\cdot\nabla\left(\frac{\tilde{P}_e}{n_0 e} - \phi\right) = B_0\left(\frac{1}{c}\frac{\partial A}{\partial t} + \eta_{\parallel} J_{\parallel}\right) \tag{2.40}$$

where higher order terms than $O(\lambda^4)$ are neglected. Here it is assumed that ϕ and η are $O(\lambda^2)$ as well as $\boldsymbol{A}$ and $\boldsymbol{J}$. From Eq.(2.16) we have the perpendicular component of the eletron fluid velocity

$$\boldsymbol{v}_{e\perp} = \frac{\boldsymbol{B}}{B^2}\times\boldsymbol{W} \tag{2.41}$$

where

$$\boldsymbol{W} = c\left(\nabla\phi - \frac{\nabla P_e}{ne} + \frac{1}{c}\frac{\partial \boldsymbol{A}}{\partial t} + \eta_{\perp}\boldsymbol{J}_{\perp}\right). \tag{2.42}$$

In the same way as Eq.(2.35), we can write

$$\boldsymbol{v}_e = \alpha\boldsymbol{B} + \boldsymbol{v}_{e\perp} \tag{2.43}$$

where $\alpha = \boldsymbol{B}\cdot\boldsymbol{v}_e/B^2$. The continuity equation (2.14) gives

$$\nabla\cdot\boldsymbol{v}_e = -\left(\frac{\partial}{\partial t} + \boldsymbol{v}_e\cdot\nabla\right)\ln n. \tag{2.44}$$

From Eqs.(2.41)–(2.44) we obtain

$$\boldsymbol{B}\cdot\nabla\alpha = \frac{\nabla B^2\times\boldsymbol{B}}{B^4}\cdot\boldsymbol{W} + \frac{\boldsymbol{B}}{B^2}\cdot\nabla\times\boldsymbol{W} - \frac{\boldsymbol{W}}{B^2}\cdot\nabla\times\boldsymbol{B} - \left(\frac{\partial}{\partial t} + \boldsymbol{v}_e\cdot\nabla\right)\ln n. \tag{2.45}$$

From Eqs.(2.17), (2.30), (2.31), (2.41) and (2.42) we have

$$\boldsymbol{v}_{e\perp} = \frac{c}{B_0}\hat{z}\times\nabla\left(\phi - \frac{\tilde{P}_e}{n_0 e}\right), \tag{2.46}$$

$$\boldsymbol{v}_\perp = \frac{c}{B_0}\hat{z} \times \nabla \left(\phi + \frac{\tilde{P}_i}{n_0 e} \right), \tag{2.47}$$

in $O(\lambda^2)$. Equations (2.17) and (2.30) yield the parallel components of the electron fluid velocity and the current density of $O(\lambda^2)$

$$v_{e\|} = B_0 \alpha = v_\| - \frac{J_\|}{n_0 e}, \tag{2.48}$$

$$J_\| = B_0 \sigma = -\frac{c}{4\pi} \nabla_\perp^2 A \tag{2.49}$$

In the lowest order of our ordering, the magnetic field becomes uniform and we use the expression for the gyroviscosity obtained by Braginskii,[34]-[36] which is given as

$$\Pi_{gi} = \frac{P_i}{4\omega_{ci}} \{ \hat{b} \times \mathsf{W} \cdot (\mathsf{I} + \hat{b}\hat{b}) + (\mathsf{I} + \hat{b}\hat{b}) \cdot \mathsf{W} \times \hat{b} \} \tag{2.50}$$

where $\omega_{ci} = eB/m_i c$ is the ion cyclotron frequency and W denotes the rate-of-strain tensor defined by

$$W_{\alpha\beta} = \frac{\partial v_\alpha}{\partial x_\beta} + \frac{\partial v_\beta}{\partial x_\alpha} - \frac{2}{3}\delta_{\alpha\beta} \nabla \cdot \boldsymbol{v}. \tag{2.51}$$

It is found that Eq.(2.50) gives $\Pi_{gi} : \nabla \boldsymbol{v} = 0$ and therefore no contribution to dissipation or internal energy. In our ordering Eq.(2.50) is reduced to

$$\Pi_{gi} = \frac{P_i}{2\omega_{ci}} [\nabla_\perp^2 F(\mathsf{I} - \hat{z}\hat{z}) - 2\nabla_\perp \nabla_\perp F + 2\{(\hat{z} \times \nabla_\perp v_\|)\hat{z} + \hat{z}(\hat{z} \times \nabla_\perp v_\|)\}] \tag{2.52}$$

where F is the stream function for the ion fluid velocity which is given as

$$F = \frac{c}{B_0} \left(\phi + \frac{\tilde{P}_i}{n_0 e} \right) \tag{2.53}$$

from Eq.(2.47). Divergerce of (2.52) gives

$$\nabla \cdot \Pi_{gi} = \nabla_\perp \left(\frac{P_i}{2\omega_{ci}} \nabla_\perp^2 F \right) - \nabla_\perp \cdot \left(\frac{P_i}{\omega_{ci}} \nabla_\perp \nabla_\perp F \right) - \hat{z}\hat{z} \times \nabla_\perp \left(\frac{P_i}{\omega_{ci}} \right) \cdot \nabla_\perp v_\| \tag{2.54}$$

where we neglect the inhomogeneity of the magnetic field so that $\omega_{ci} = eB_0/m_i c$.

Equations (2.32), (2.36), (2.40) and (2.45) have the same form as the magnetic differential equation

$$\boldsymbol{B} \cdot \nabla F = G \tag{2.55}$$

where F and G are expanded in powers of λ as follows

$$F = \lambda^2 F^{(2)} + \lambda^3 F^{(3)} + \lambda^4 F^{(4)} + \cdots, \tag{2.56}$$

$$G = \lambda^3 G^{(3)} + \lambda^4 G^{(4)} + \cdots. \tag{2.57}$$

Here $P_{\alpha 0}$ is omitted in Eq.(2.32) because $\nabla P_{\alpha 0} = 0$. Since the helical field $\nabla\Phi$ contains a rapid variation in the z direction, the scale length of which is of the order of the minor radius a. Therefore F and G generally contain this rapid variation and the slowly varying part, the scale length of which is of the order of the major radius R_0. Then we may write

$$\Phi = \Phi(r, \theta, \tilde{z}) \tag{2.58}$$

$$F = F(r, \theta, \tilde{z}, z) \tag{2.59}$$

$$G = G(r, \theta, \tilde{z}, z) \tag{2.60}$$

where $\tilde{z}$ and z are used to represent the rapid and slow variations along the longitudinal direction. Here we assume that the z-derivative is expanded as

$$\frac{\partial}{\partial \tilde{z}} + \lambda^2 \frac{\partial}{\partial z}. \tag{2.61}$$

F and G are assumed to be periodic functions with respect to $\tilde{z}$ over the toroidal pitch length $2\pi R_0/N$ where $N = O(\epsilon^{-1})$ is the toroidal pitch number. From the lowest order of Eq.(2.55) we have

$$B_0 \frac{\partial F^{(2)}}{\partial \tilde{z}} = 0 \tag{2.62}$$

which yields

$$F^{(2)} = F^{(2)}(r, \theta, z) \tag{2.63}$$

Equation (2.55) gives in $O(\lambda^3)$

$$B_0 \frac{\partial F^{(3)}}{\partial \tilde{z}} + \nabla_\perp \Phi \cdot \nabla_\perp F^{(2)} = G^{(3)} \tag{2.64}$$

where we used Eqs.(2.61) and (2.63). Averaging Eq.(2.64) with respect to $\tilde{z}$ over the toroidal pitch length $2\pi R_0/N$, we find

$$\overline{G^{(3)}} = 0 \tag{2.65}$$

where the averaging operator is defined by

$$\overline{f}(r,\theta,z) = \frac{N}{2\pi R_0}\int_0^{2\pi R_0/N} d\tilde{z} f(r,\theta,\tilde{z},z). \tag{2.66}$$

In Eq.(2.65) we have used

$$\overline{\nabla\Phi} = \nabla\overline{\Phi} = 0. \tag{2.67}$$

Equation (2.64) is integrated to give

$$\begin{aligned} F^{(3)}(r,\theta,\tilde{z},z) &= -\frac{1}{B_0}\int_0^{\tilde{z}} d\tilde{z}[\nabla_\perp\Phi(r,\theta,\tilde{z})\cdot\nabla_\perp F^{(2)}(r,\theta,z) - G^{(3)}(r,\theta,\tilde{z},z)] \\ &\quad + H^{(3)}(r,\theta,z) \end{aligned} \tag{2.68}$$

where $H^{(3)}(r,\theta,z)$ is not specified here. From Eq.(2.55), we have in $O(\lambda^4)$

$$B_0\frac{\partial F^{(4)}}{\partial\tilde{z}} + B_0\frac{\partial F^{(2)}}{\partial z} + \nabla\Phi\cdot\nabla F^{(3)} + \nabla A\times\hat{z}\cdot\nabla F^{(2)} = G^{(4)} \tag{2.69}$$

which is averaged with respect to $\tilde{z}$ to yield

$$\begin{aligned} & B_0\frac{\partial F^{(2)}}{\partial z} + \nabla A\times\hat{z}\cdot\nabla F^{(2)} - \overline{G^{(4)}} \\ &= -\overline{\nabla\Phi\cdot\nabla F^{(3)}} \\ &= \frac{1}{B_0}\overline{\nabla\Phi\cdot\nabla\int_0^{\tilde{z}} d\tilde{z}\nabla_\perp\Phi\cdot\nabla_\perp F^{(2)}} - \frac{1}{B_0}\overline{\nabla\Phi\cdot\nabla\int_0^{\tilde{z}} d\tilde{z}G^{(3)}} \end{aligned} \tag{2.70}$$

where Eq.(2.68) is substituted. By using Eqs.(2.28) and (2.67), we can prove the following equation

$$\overline{\nabla\Phi\cdot\nabla\int_0^{\tilde{z}} d\tilde{z}\nabla_\perp\Phi\cdot\nabla_\perp F^{(2)}} = -\frac{1}{2}\nabla\left\{\overline{\left(\nabla\Phi\times\nabla\int_0^{\tilde{z}} d\tilde{z}\Phi\right)\cdot\hat{z}}\right\}\times\hat{z}\cdot\nabla F^{(2)}. \tag{2.71}$$

From Eqs.(2.70) and (2.71), we obtain

$$\overline{\boldsymbol{B}} \cdot \nabla F^{(2)} = \overline{G^{(4)}} - \frac{1}{B_0} \overline{\nabla \Phi \cdot \nabla \int_0^{\tilde{z}} G^{(3)}} \tag{2.72}$$

where

$$\overline{\boldsymbol{B}} \cdot \nabla \equiv B_0 \frac{\partial}{\partial z} + \nabla \psi \times \hat{z} \cdot \nabla \equiv B_0 \nabla_{\parallel} \tag{2.73}$$

$$\psi \equiv A + \frac{1}{2B_0} \overline{\nabla \Phi \times \nabla \int_0^{\tilde{z}} d\tilde{z} \Phi \cdot \hat{z}}. \tag{2.74}$$

Since in Eqs.(2.32) and (2.40) there are no terms corresponding to $G^{(3)}$ in Eq.(2.57), we immediately find from Eq.(2.72)

$$n_0 m_i \left(\frac{\partial}{\partial t} + \frac{c}{B_0} \hat{z} \times \nabla \phi \cdot \nabla \right) v_{\parallel} = -\nabla_{\parallel} (\tilde{P}_e + \tilde{P}_i) \tag{2.75}$$

$$\frac{1}{c} \frac{\partial A}{\partial t} = -\nabla_{\parallel} \left(\phi - \frac{\tilde{P}_e}{n_0 e} \right) - \eta_{\parallel} J_{\parallel} \tag{2.76}$$

where Eqs.(2.47), (2.54) and (2.73) are used. Hereafter the indices for the order of λ-expansion are sometimes omitted.

In Eqs.(2.36) and (2.45) the term corresponding to $G^{(3)}$ come form the first term in the RHS, which has the expression

$$\frac{\nabla B^2 \times \boldsymbol{B}}{B^4} \cdot \boldsymbol{C}. \tag{2.77}$$

Here $\boldsymbol{C}$ also has the common form

$$\boldsymbol{C} = \nabla \chi + O(\lambda^4) \tag{2.78}$$

where χ is $O(\lambda^2)$ and satisfies

$$\boldsymbol{B} \cdot \nabla \chi = O(\lambda^4). \tag{2.79}$$

Since Eq.(2.79) has the form of the magnetic differential equation we obtain from (2.68)

$$\chi^{(3)}(r, \theta, \tilde{z}, z) = -\frac{1}{B_0} \int_0^{\tilde{z}} d\tilde{z} \nabla_{\perp} \Phi(r, \theta, \tilde{z}) \cdot \nabla_{\perp} \chi^{(2)}(r, \theta, z) + \omega^{(3)}(r, \theta, z) \tag{2.80}$$

where $\omega^{(3)}$ denotes an arbitrary function of $O(\lambda^3)$ which is independent of $\tilde{z}$. We find that the contribution of Eq.(2.77) to the right-hand side of Eq.(2.72) is

$$\overline{\left(\frac{\nabla B^2 \times \boldsymbol{B}}{B^4} \cdot \nabla\chi\right)^{(4)}} - \frac{1}{B_0}\overline{\nabla\Phi \cdot \nabla \int_0^{\tilde{z}} d\tilde{z} \left(\frac{\nabla B^2 \times \boldsymbol{B}}{B^4} \cdot \nabla\chi\right)^{(3)}}$$
$$= -\frac{1}{B_0}\hat{z} \cdot \nabla\chi \times \nabla\Omega + \frac{2}{B_0^2}\hat{z} \cdot \nabla\chi \times \nabla B^\beta \tag{2.81}$$

where

$$\Omega = \frac{2x}{R_0} + \frac{\overline{|\nabla\Phi|^2}}{B_0^2}. \tag{2.82}$$

Equations (2.27), (2.28) and (2.80) have been used in the derivation of Eq.(2.81). The contributions from other terms in Eqs.(2.36) and (2.45) are $O(\lambda^4)$ and written as

$$\frac{\boldsymbol{B}}{B^2} \cdot \nabla \times \boldsymbol{K} = \frac{n_0 m_i c}{B_0}\left(\frac{\partial}{\partial t} + \hat{z} \times \nabla F \cdot \nabla\right)\nabla_\perp^2 F - \frac{m_i c^2}{e B_0^2}\nabla_\perp \cdot \left(\hat{z} \times \nabla \tilde{P}_i \cdot \nabla\nabla_\perp F\right) \tag{2.83}$$

$$\frac{\boldsymbol{B}}{B^2} \cdot \nabla \times \boldsymbol{W} = \frac{1}{B_0}\left(\frac{\partial}{\partial t} - \frac{\eta_\perp c^2}{4\pi}\nabla_\perp^2\right) B^\beta \tag{2.84}$$

$$-\frac{\boldsymbol{W}}{B^2} \cdot \nabla \times \boldsymbol{B} = -\frac{c}{B_0^2}\hat{z} \times \nabla\left(\phi - \frac{\tilde{P}_e}{n_0 e}\right) \cdot \nabla B^\beta. \tag{2.85}$$

The last term in the right-hand side of Eq.(2.83) comes from the gyroviscosity term of (2.54). Then using Eqs.(2.81)–(2.85) and applying Eq.(2.72) to Eqs.(2.36) and (2.45), we obtain

$$n_0 m_i \left(\frac{\partial}{\partial t} + \hat{z} \times \nabla F \cdot \nabla\right)\nabla_\perp^2 F - \frac{1}{\omega_{ci}}\nabla_\perp \cdot \left(\hat{z} \times \nabla \tilde{P}_i \cdot \nabla\nabla_\perp F\right)$$
$$= \frac{1}{c} B_0 \nabla_\parallel J_\parallel + \nabla(\tilde{P}_e + \tilde{P}_i) \times \nabla\Omega \cdot \hat{z} \tag{2.86}$$

$$\left[\frac{\partial}{\partial t} + \frac{c}{B_0}\hat{z} \times \nabla\left(\phi - \frac{\tilde{P}_e}{n_0 e}\right) \cdot \nabla\right]\left(\frac{\tilde{n}}{n_0} - \frac{B^\beta}{B_0}\right)$$
$$= -\frac{c}{B_0}\hat{z} \times \nabla\left(\phi - \frac{\tilde{P}_e}{n_0 e}\right) \cdot \nabla\Omega - \nabla_\parallel\left(v_\parallel - \frac{J_\parallel}{n_0 e}\right) - \frac{\eta_\perp c^2}{4\pi}\nabla_\perp^2 \frac{B^\beta}{B_0} \tag{2.87}$$

where we used the relation $\ln n = \ln n_0 + \ln(1 + \tilde{n}/n_0) \simeq \tilde{n}/n_0 + \text{const.}$

According to the equation of state (2.21), the density and the pressure are related by

$$\tilde{P}_\alpha = \gamma_\alpha T_{\alpha 0} \tilde{n} \qquad (\alpha = e, i) \tag{2.88}$$

where $T_{\alpha 0} = P_{\alpha 0}/n_0 = \text{const.}$ Equation (2.88) is required to close the set of equations. Its validity should be examined by experimental results.

Now we have obtained a closed set of the reduced two-fluid equations which consist of

$$n_0 m_i \left(\frac{\partial}{\partial t} + \frac{c}{B_0} \hat{z} \times \nabla \phi \cdot \nabla \right) v_\parallel = -\nabla_\parallel (\tilde{P}_e + \tilde{P}_i) \tag{2.89}$$

$$\begin{aligned} n_0 m_i \left(\frac{\partial}{\partial t} + \hat{z} \times \nabla F \cdot \nabla \right) \nabla_\perp^2 F - \frac{1}{\omega_{ci}} \nabla_\perp \cdot \left(\hat{z} \times \nabla \tilde{P}_i \cdot \nabla \nabla_\perp F \right) \\ = \frac{1}{c} B_0 \nabla_\parallel J_\parallel + \nabla (\tilde{P}_e + \tilde{P}_i) \times \nabla \Omega \cdot \hat{z} \end{aligned} \tag{2.90}$$

$$\frac{1}{c} \frac{\partial A}{\partial t} = -\nabla_\parallel \left(\phi - \frac{\tilde{P}_e}{n_0 e} \right) - \eta_\parallel J_\parallel \tag{2.91}$$

$$\begin{aligned} \left[\frac{\partial}{\partial t} + \frac{c}{B_0} \hat{z} \times \nabla \left(\phi - \frac{\tilde{P}_e}{n_0 e} \right) \cdot \nabla \right] \left(\frac{\tilde{n}}{n_0} - \frac{B^\beta}{B_0} \right) \\ = -\frac{c}{B_0} \hat{z} \times \nabla \left(\phi - \frac{\tilde{P}_e}{n_0 e} \right) \cdot \nabla \Omega - \nabla_\parallel \left(v_\parallel - \frac{J_\parallel}{n_0 e} \right) - \frac{\eta_\perp c^2}{4\pi} \nabla_\perp^2 \frac{B^\beta}{B_0} \end{aligned} \tag{2.92}$$

where

$$\tilde{P}_\alpha = \gamma_\alpha T_{\alpha 0} \tilde{n} \qquad (\alpha = e, i) \tag{2.93}$$

$$F = \frac{c}{B_0} \left(\phi + \frac{\tilde{P}_i}{n_0 e} \right) \tag{2.94}$$

$$\tilde{P}_e + \tilde{P}_i = -\frac{B_0}{4\pi} B^\beta \tag{2.95}$$

$$J_{\parallel} = -\frac{c}{4\pi}\nabla_{\perp}^2 A \tag{2.96}$$

$$\nabla_{\parallel} = \frac{\partial}{\partial z} + \frac{1}{B_0}\nabla\psi \times \hat{z}\cdot\nabla \tag{2.97}$$

$$\psi \equiv A + \frac{1}{2B_0}\overline{\nabla\Phi \times \nabla \int_0^{\tilde{z}} d\tilde{z}\Phi\cdot\hat{z}} \tag{2.98}$$

$$\Omega = \frac{2x}{R_0} + \frac{\overline{|\nabla\Phi|^2}}{B_0^2}. \tag{2.99}$$

From Eqs.(2.89)-(2.99), we find

$$\begin{aligned}
&\frac{\partial}{\partial t}\left\{\frac{n_0 m_i}{2}(v_{\parallel}^2 + |\nabla_{\perp}F|^2) + \frac{1}{8\pi}(B^{\beta 2} + |\nabla_{\perp}A|^2) + \frac{\gamma_e P_{e0} + \gamma_i P_{i0}}{2}\left(\frac{\tilde{n}}{n_0}\right)^2\right\} \\
&= -\eta_{\parallel}J_{\parallel}^2 - \eta_{\perp}\left(\frac{c}{4\pi}|\nabla_{\perp}B^{\beta}|\right)^2 \\
&\quad - \nabla_{\perp}\cdot\left\{\frac{n_0 m_i}{2}(v_{\parallel}^2 + |\nabla_{\perp}F|^2)\boldsymbol{v}_E + \left[\frac{\gamma_e P_{e0} + \gamma_i P_{i0}}{2}\left(\frac{\tilde{n}}{n_0}\right)^2 + \frac{B^{\beta 2}}{8\pi}\right]\boldsymbol{v}_{e\perp}\right\} \\
&\quad - \nabla_{\parallel}\left\{\tilde{P}_i v_{\parallel} + \tilde{P}_e\left(v_{\parallel} - \frac{J_{\parallel}}{n_0 e}\right)\right\} - \nabla_{\parallel}(\phi J_{\parallel}) + \nabla_{\perp}\cdot\left(\frac{1}{4\pi}\frac{\partial A}{\partial t}\nabla_{\perp}A\right) \\
&\quad - \nabla_{\perp}\cdot\left\{\frac{c}{B_0}\phi(\tilde{P}_e + \tilde{P}_i)\nabla\Omega\times\hat{z}\right\} + \nabla_{\perp}\cdot\left\{\frac{c}{2n_0 e B_0}(\tilde{P}_e^2 - \tilde{P}_i^2)\nabla\Omega\times\hat{z}\right\} \\
&\quad + \nabla_{\perp}\cdot\left\{n_0 m_i F\left(\frac{\partial}{\partial t} + \boldsymbol{v}_E\cdot\nabla_{\perp}\right)\nabla_{\perp}F\right\} + \frac{\eta_{\perp}c^2}{(4\pi)^2}\nabla_{\perp}\cdot(B^{\beta}\nabla_{\perp}B^{\beta}),
\end{aligned} \tag{2.100}$$

where $\boldsymbol{v}_{e\perp}$ is given by Eq.(2.46) and

$$\boldsymbol{v}_E = \frac{c}{B_0}\hat{z}\times\nabla\phi. \tag{2.101}$$

Integrating Eq.(2.100) and assuming that there is no contribution from the boudary surface, we have the equation of energy balance

$$\begin{aligned}
&\frac{d}{dt}\int d^3x\left\{\frac{n_0 m_i}{2}(v_{\parallel}^2 + |\nabla_{\perp}F|^2) + \frac{1}{8\pi}(B^{\beta 2} + |\nabla_{\perp}A|^2) + \frac{\gamma_e P_{e0} + \gamma_i P_{i0}}{2}\left(\frac{\tilde{n}}{n_0}\right)^2\right\} \\
&\qquad = -\int d^3x\left\{\eta_{\parallel}J_{\parallel}^2 + \eta_{\perp}\left(\frac{c}{4\pi}|\nabla_{\perp}B^{\beta}|\right)^2\right\},
\end{aligned} \tag{2.102}$$

which corresponds to Eq.(2.22). It is seen that the total energy in the left-hand side consists of the kinetic, magnetic and internal energy and the right-hand side represents the Ohmic dissipation.

We can derive several limiting forms from the reduced two-fluid equations. Here we employ the normalization of quantities usually used in RMHD which is written as

$$\left.\begin{array}{lll} t = (a/\epsilon v_A)t, & r = ar, & z = R_0 z, \\ \boldsymbol{v} = \epsilon v_A \boldsymbol{v}, & \phi = (\epsilon a v_A B_0/c)\phi, & \Phi = \epsilon^{1/2} a B_0 \Phi, \\ \tilde{P}_e + \tilde{P}_i = (\epsilon B_0^2/4\pi)p, & A = \epsilon a B_0 A, & \eta c^2/(4\pi\epsilon a v_A) = \eta, \end{array}\right\} \quad (2.103)$$

where $v_A = B_0/\sqrt{4\pi n_0 m_i}$ is the Alfven velocity and the variables in the right-hand side represent the nondimensional normalized quantities. From this normalization the reduced two-fluid equations are expressed in the following forms

$$\left(\frac{\partial}{\partial t} + \boldsymbol{v}_E \cdot \nabla\right) v_{\parallel} = -\nabla_{\parallel} p \quad (2.104)$$

$$\left(\frac{\partial}{\partial t} + \boldsymbol{v}_\perp \cdot \nabla\right) \nabla_\perp^2 F - \alpha_i \nabla_\perp \cdot (\hat{z} \times \nabla p \cdot \nabla \nabla_\perp F) = \nabla_{\parallel} J_{\parallel} + \nabla p \times \nabla \Omega \cdot \hat{z} \quad (2.105)$$

$$\frac{\partial A}{\partial t} = -\nabla_{\parallel}(\phi - \alpha_e p) - \eta_{\parallel} J_{\parallel} \quad (2.106)$$

$$\frac{1+\beta}{\beta}\left(\frac{\partial}{\partial t} + \boldsymbol{v}_E \cdot \nabla\right) p = -\boldsymbol{v}_{e\perp} \cdot \nabla \Omega - \nabla_{\parallel}(v_{\parallel} - \alpha J_{\parallel}) + \eta_\perp \nabla_\perp^2 p \quad (2.107)$$

where

$$\left.\begin{array}{ll} F = \phi + \alpha_i p, & \boldsymbol{v}_\perp = \hat{z} \times \nabla F, \\ \boldsymbol{v}_E = \hat{z} \times \nabla \phi, & \boldsymbol{v}_{e\perp} = \hat{z} \times \nabla(\phi - \alpha_e p), \\ \nabla_{\parallel} = \dfrac{\partial}{\partial z} + \nabla\psi \times \hat{z} \cdot \nabla, & \psi = A + \dfrac{1}{2}\overline{\nabla\Phi \times \nabla \displaystyle\int_0^{\tilde{z}} d\tilde{z}\Phi} \cdot \hat{z}, \\ J_{\parallel} = -\nabla_\perp^2 A, & \Omega = 2x + \overline{|\nabla\Phi|^2}, \\ \alpha_e = \dfrac{\gamma_e P_{e0}}{\gamma_e P_{e0} + \gamma_i P_{i0}}\alpha, & \alpha_i = \dfrac{\gamma_i P_{i0}}{\gamma_e P_{e0} + \gamma_i P_{i0}}\alpha, \\ \alpha = \dfrac{c}{a\omega_{pi}}, & \beta = \dfrac{4\pi(\gamma_e P_{e0} + \gamma_i P_{i0})}{B_0^2}. \end{array}\right\} \quad (2.108)$$

Here $\omega_{pi} = \sqrt{4\pi n_0 e^2/m_i}$ is the ion plasma frequency. α_e and α_i represent the drift parameters which measure the effects of the electron and ion diamagnetic drift, respectively.

In the limit of $\beta = 0$ the equation of parallel flow, Eq.(2.104), is decoupled from the other equations (2.105)–(2.107) and they construct the closed set of equations for the three field variables ϕ, A and p. Furthermore in the case of $\alpha = 0$, the RMHD equations are obtained as

$$\left(\frac{\partial}{\partial t} + \boldsymbol{v}_\perp \cdot \nabla\right) \nabla_\perp^2 \phi = \nabla_\parallel J_\parallel + \nabla p \times \nabla\Omega \cdot \hat{z} \tag{2.109}$$

$$\frac{\partial A}{\partial t} = -\nabla_\parallel \phi - \eta_\parallel J_\parallel \tag{2.110}$$

$$\left(\frac{\partial}{\partial t} + \boldsymbol{v}_E \cdot \nabla\right) p = 0. \tag{2.111}$$

Next let us consider the electrostatic case where $\partial A/\partial t$ is negligible. The generalized Ohm's law Eq.(2.91) yields

$$J_\parallel = \frac{T_e}{e\eta_\parallel} \nabla_\parallel \left(\frac{\tilde{n}}{n_0} - \frac{e\phi}{T_e}\right). \tag{2.112}$$

Here an isothermal assumption for electrons ($\gamma_e = 1$) is employed. In order to study the drift waves it is convenient to use the following normalization

$$\left.\begin{aligned} &\omega_{ci} t = t, && \boldsymbol{x} = \rho_s \boldsymbol{x}, \\ &\boldsymbol{v} = c_s \boldsymbol{v}, && e\phi/T_e = \phi, \\ &\tilde{n}/n_0 = \overline{n} + n, \end{aligned}\right\} \tag{2.113}$$

where $\rho_s = c_s/\omega_{ci}$, $c_s = \sqrt{T_e/m_i}$ and $\overline{n}$ represents the stationary part which has a gradient in the radial direction. Neglecting the ion temperature and the parallel fluid velocity $v_\parallel$, we obtain from Eqs.(2.90), (2.92), (2.112) and (2.113)

$$\left(\frac{\partial}{\partial t} + \hat{z} \times \nabla\phi \cdot \nabla\right) \nabla_\perp^2 \phi = \frac{\omega_{ce}}{\nu_{e\parallel}} \nabla_\parallel^2 (n - \phi) + \nabla n \times \nabla\Omega \cdot \hat{z} \tag{2.114}$$

$$\left(\frac{\partial}{\partial t} + \hat{z} \times \nabla\phi \cdot \nabla\right) (n + \overline{n}) = \frac{\omega_{ce}}{\nu_{e\parallel}} \nabla_\parallel^2 (n - \phi) + \nabla(n - \phi) \times \nabla\Omega \cdot \hat{z} + \frac{\nu_e}{\beta\omega_{ce}} \nabla_\perp^2 n \tag{2.115}$$

where $\nabla_{\parallel}^2\overline{n}$, $\nabla\overline{n}\times\nabla\Omega\cdot\hat{z}$ and $\nabla_{\perp}^2\overline{n}$ are neglected and $1+\beta\simeq 1$ is used. Here $\omega_{ce}=eB_0/m_ec$, $\nu_{e\parallel}=n_0e^2\eta_{\parallel}/m_e$ and $\nu_e=n_0e^2\eta_{\perp}/m_e$ are the electron cyclotron frequency, the parallel and perpendicular electron collision frequency, respectively. Equations (2.114) and (2.115) are the Hasegawa-Wakatani equations[27] in the case that the curvature of the magnetic field is included.

For small $\eta_{\parallel}$ the Boltzmann distribution $n=\phi$ may be assumed due to Eq.(2.112). Then subtracting Eq.(2.115) from Eq.(2.114) yields

$$\left(\frac{\partial}{\partial t}+\hat{z}\times\nabla\phi\cdot\nabla\right)(\nabla_{\perp}^2\phi-\phi-\overline{n}-\Omega)=-\frac{\nu_e}{\beta\omega_{ce}}\nabla_{\perp}^2\phi. \qquad (2.116)$$

which is similar to the Hasegawa-Mima equation.[28]

So far the reduced equations have been derived for the stellarator/heliotron plasmas. If the magnetic scalar potential Φ is dropped from Eqs.(2.98) and (2.99), we can immediately obtain the expressions for the tokamak plasmas.

2.4 Conclusions

In this chapter, the reduced two-fluid equations have been derived and their properties are discussed. They are suitable to describe large aspect ratio toroidal plasmas in stellarator/heliotron or tokamaks. The reduced two-fluid equatins (2.89)–(2.99) are given by applying the stellarator ordering with the expansion parameter $\lambda = \epsilon^{1/2}$ to the two-fluid plasma equations (2.14)–(2.21). They include four field variables, i.e., the electrostatic potential ϕ, the parallel component of the magnetic vector potential A, the pressure p (or density n) and the parallel fluid velocity $v_{\parallel}$. The time evolutions of them are governed by the vorticity equation, the generalized Ohm's law, the pressure equation and the parallel component of the equation of motion. The reduced two-fluid equations conserve the total energy in the case of no dissipation. Compared with the one-fluid MHD model, the effects of the ion and electron diamagnetic drift due to respective pressure gradient are included in the vorticity equation and the generalized Ohm's law. The parallel ion flow, which is not included in RMHD, appears in the pressure equation through the compressibility, which describes the propagation of the ion accoustic wave along the magnetic field.

In the low beta limit, the parallel ion flow term vanishes in the pressure equation and the equation of the parallel flow is decoupled from the other three equations, which construct the closed set of equations for the three field variables. Furthermore in the case of no diamagnetic drift terms, the three field equations are reduced to RMHD. In the electrostatic case, assuming cold ions and no parallel ion flow, the reduced two-fluid model gives the Hasegawa-Wakatani equations, which consist of the vorticity and density equations for the two field variables ϕ and n. Furthermore assuming the Boltzmann distribution for small $\eta_{\parallel}$, we can also obtain the Hasegawa-Mima type equation with the one field variable ϕ.

Thus we can state that the reduced two-fluid model derived in this chapter is a generalized one which includes the various types of reduced fluid models. In the following chapters, the problems of linear instabilities, nonlinear behaviors and turbulent transport are studied based on this model.

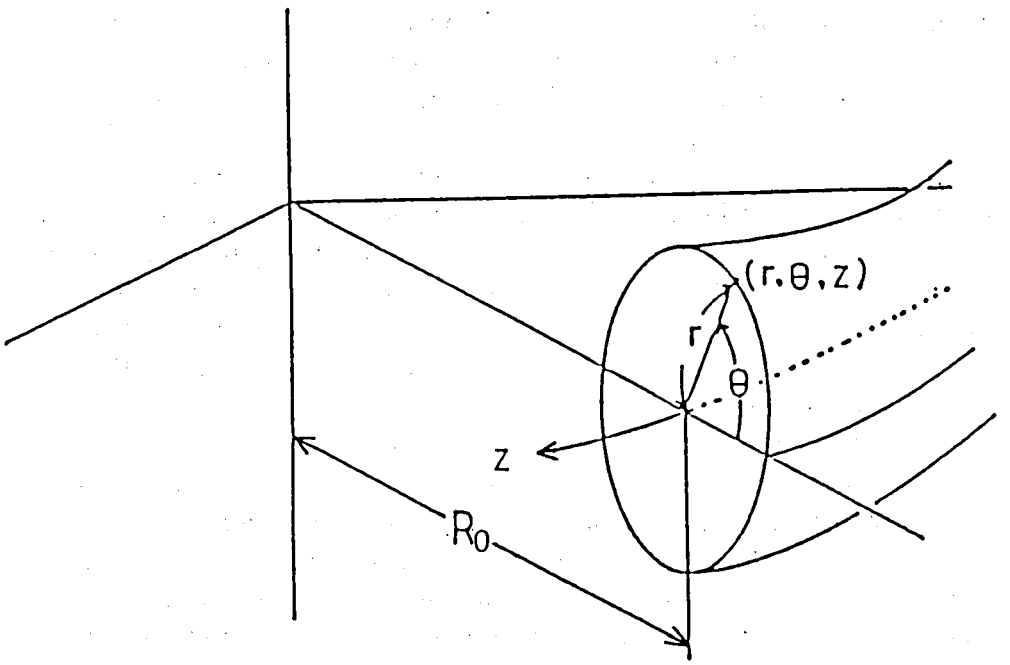

Figure 2.1: Coordinate system for the reduced two-fluid model.

Chapter 3

Ion Diamagnetic Drift Effects on Ideal Interchange Instabilities

3.1 Introduction

In this chapter, effects of ion diamagnetic drift on ideal interchange instabilities are studied based on the model equations derived in Chapter 2. The interchange instability is one of the typical MHD instabilities and it is driven by pressure gradients combined with bad magnetic field curvature. It is important especially in stellarator/heliotron configuration since the average bad curvature or magnetic hill usually appears in the edge region. It is predicted by the numerical studies based on RMHD that the ideal interchange modes with low mode numbers give the beta limit on Heliotron E plasmas. It was shown that the beta limit depends on the pressure profile and $\langle\beta\rangle_{\rm limit} \sim 2\%$ is expected in Heliotron E for $p(r) = p(0)(1-(r/a)^2)^2$, where $\langle\beta\rangle_{\rm limit}$ is the average beta limit obtained by the ideal MHD stability analysis.[37] Here our concern is whether the ideal interchange modes can be stabilized completely or not and how the mode structure is changed by the effects of the ion diamagnetic drift for $\langle\beta\rangle > \langle\beta\rangle_{\rm limit}$.

In Sec.3.2 the condition for the ion diamagnetic drift required to stabilize the interchage modes is estimated. We have interest in plasmas with ion temperature higher than electron temperature and investigate the effects of

the ion diamagnetic drift purely and neglect the electron diamagnetic drift. Also the ion parallel flow in the reduced two-fluid equations may not be important since the interchange mode is localized by the magnetic shear effect in heliotron configuration. In Sec.3.3 the linearized reduced two-fluid equations are numerically solved. The dependence of the linear growth rate and the mode structure on the magnitude of ion diamagnetic drift is given. The numerical results are compared with the analytical expression. Improvement of beta limit due to the ion diamagnetic drift is quantitatively discussed in the case of Heliotron E. Finally conclusions are given in Sec.3.4.

3.2 Model Equations and Linear Theory

Since our concern is in the effect of the ion diamagnetic drift on the ideal interchange instability , we neglect the terms of the electron diamagnetic drift ($\alpha_e = 0$, $\alpha = \alpha_i$) and dissipation ($\eta_\parallel = \eta_\perp = 0$) in the reduced two-fluid equations (2.104)–(2.108). As we assume β to be small, the equation of the ion parallel flow is decoupled from other equations. It is convenient to write the vorticity equation in terms of the electrostatic potential ϕ instead of the stream function F. Thus we obtain the model equations which contain three field variables ϕ,A and p as follows

$$\left(\frac{\partial}{\partial t} + \boldsymbol{v}_E \cdot \nabla\right) \nabla_\perp^2 \phi + \nabla_\perp \cdot (\boldsymbol{v}_{Di} \cdot \nabla \nabla_\perp \phi) = \nabla_\parallel J_\parallel + \nabla p \times \nabla \Omega \cdot \hat{z} \tag{3.1}$$

$$\frac{\partial}{\partial t} A = -\nabla_\parallel \phi \tag{3.2}$$

$$\left(\frac{\partial}{\partial t} + \boldsymbol{v}_E \cdot \nabla\right) p = 0 \tag{3.3}$$

where

$$\left.\begin{aligned} &\boldsymbol{v}_E = \hat{z} \times \nabla \phi && \boldsymbol{v}_{Di} = \alpha \hat{z} \times \nabla p \\ &J_\parallel = -\nabla_\perp^2 A && \alpha = c/a\omega_{pi} \\ &\nabla_\parallel = \frac{\partial}{\partial z} + \nabla \psi \times \hat{z} \cdot \nabla \\ &\psi = A + \frac{1}{2} \overline{\nabla \Phi \times \nabla \int_0^z dz \Phi \cdot \hat{z}} \\ &\Omega = 2x + \overline{|\nabla \Phi|^2}. \end{aligned}\right\} \tag{3.4}$$

Here we have used the normalization given in (2.103). Compared with the RMHD equations the only difference is that the vorticity equation (3.1) contains the term of the ion diamagnetic drift. The magnitude of the additional term is characterized by the drift parameter α. The interchange instability is driven by the term of the pressure gradient ∇p combined with the magnetic curvature $\nabla \Omega$ in the vorticity equation.

Equations (3.1)–(3.3) conserve the same form of energy as RMHD

$$\frac{d}{dt} \int d^3x \left(\frac{|\nabla_\perp \phi|^2}{2} + \frac{|\nabla_\perp A|^2}{2} - \Omega p \right) = 0 \tag{3.5}$$

where we assumed that there is no contribution from the boundary surface.

Let us first consider the equilibrium state where $\phi = 0$ and $\partial/\partial t = \partial/\partial z = 0$. From Eq.(2.104), we find the pressure to be a function of the poloidal flux ψ

$$p = p(\psi) \tag{3.6}$$

Using Eq.(3.6) the vorticity equation in the equilibrium state gives

$$\nabla_\perp^2 A = -\Omega \frac{dp}{d\psi} + G(\psi) \tag{3.7}$$

where G denotes the arbitrary function of ψ. The equilibrium equation (3.7) was first derived by Greene and Johnson and it corresponds to the Grad-Shafranov equation for the axisymmetric system.

Next we consider the linear stability problem. Linearizing Eqs.(3.1)–(3.3), we obtain

$$\frac{\partial}{\partial t}\nabla_\perp^2 \phi_1 + \alpha \nabla_\perp \cdot (\hat{z} \times \nabla p_0 \cdot \nabla \nabla_\perp) \phi_1 = -\nabla_{\|0} \nabla_\perp^2 A_1 + \nabla J_0 \times \nabla A_1 \cdot \hat{z} + \nabla p_1 \times \nabla \Omega \cdot \hat{z} \tag{3.8}$$

$$\frac{\partial}{\partial t} A_1 = -\nabla_{\|0} \phi_1 \tag{3.9}$$

$$\frac{\partial}{\partial t} p_1 = \nabla p_0 \times \nabla \phi_1 \cdot \hat{z} \tag{3.10}$$

where the subscripts 0 and 1 refer to the equilibrium and perturebed quantities respectively. From these equations we have a linear homogeneous equation for ϕ_1,

$$\frac{\partial^2}{\partial t^2} \nabla_\perp^2 \phi + 2\alpha \mathcal{A} \frac{\partial \phi}{\partial t} = \mathcal{S}\phi \tag{3.11}$$

where a subsript 1 for ϕ is omitted and linear operators $\mathcal{S}$ and $\mathcal{A}$ are defined by

$$\mathcal{S}\phi \equiv \nabla_{\|0} \nabla_\perp^2 \nabla_{\|0} \phi - \nabla J_0 \times \nabla (\nabla_{\|0} \phi) \cdot \hat{z} - \nabla \Omega \times \nabla (\nabla p_0 \times \nabla \phi \cdot \hat{z}) \cdot \hat{z} \tag{3.12}$$

$$\mathcal{A}\phi \equiv \frac{1}{2} \nabla_\perp \cdot (\hat{z} \times \nabla p_0 \cdot \nabla \nabla_\perp \phi). \tag{3.13}$$

Here we employ the fixed boundary condition i.e. $\phi = 0$ at the plasma surface $r = 1$. It can be demonstrated that the linear operators $\mathcal{S}$ and $\mathcal{A}$ have the following symmetric and antisymmetric properties

$$\int d^3x \chi \mathcal{S}\phi = \int d^3x \phi \mathcal{S}\chi \tag{3.14}$$

$$\int d^3x \chi \mathcal{A}\phi = -\int d^3x \phi \mathcal{A}\chi \tag{3.15}$$

for any choice of functions ϕ and χ subject to the boundary condition. It can be shown by using these properties that the Lagrangian formulation is possible and the linear equation (3.11) can be derived by using the variational principle

$$\delta \int_{t_0}^{t_1} L dt \equiv \delta \int_{t_0}^{t_1} dt \int d^3x \frac{1}{2} \left\{ \left| \nabla_\perp \frac{\partial \phi}{\partial t} \right|^2 + 2\alpha \phi \mathcal{A} \frac{\partial \phi}{\partial t} - \phi \mathcal{S} \phi \right\} = 0. \tag{3.16}$$

Then the linear equation (3.11) corresponds to the Euler-Lagrange equation for the variational principle. Using the Legendre transformation for the Lagrangian L yields the conjugate field variable π for ϕ

$$\pi = -\nabla_\perp^2 \frac{\partial \phi}{\partial t} - \alpha \mathcal{A}\phi \tag{3.17}$$

Then the Hamiltonian H is written as

$$\begin{aligned} H &= \frac{1}{2} \int d^3x \left\{ \left| \nabla_\perp \frac{\partial \phi}{\partial t} \right|^2 + \phi \mathcal{S} \phi \right\} \\ &= \frac{1}{2} \int d^3x \left\{ \left| \nabla_\perp \nabla_\perp^{-2} (\pi + \alpha \mathcal{A} \phi) \right|^2 + \phi \mathcal{S} \phi \right\} \end{aligned} \tag{3.18}$$

where $\nabla_\perp^{-2}$ denotes the inverse operator for the two dimensional Laplacian $\nabla_\perp^2$. It is easily shown that Eq.(3.11) is expressed by the Hamilton's canonical eqations and that the Hamiltonian H is constant in time.

In the case of $\phi(\boldsymbol{x}, t) = \phi(\boldsymbol{x}) e^{-i\omega t}$, Eq.(3.11) can be written as an eigenvalue equation

$$\omega^2 \nabla_\perp^2 \phi + 2i\omega\alpha \mathcal{A}\phi + \mathcal{S}\phi = 0 \tag{3.19}$$

where an eigenvalue ω and an eigenfunction ϕ are generally complex-valued. Multiplying Eq.(3.19) by ϕ^* and integrating in the plasma region give

$$K\omega^2 - 2\alpha V \omega - W = 0 \tag{3.20}$$

where

$$K = \frac{1}{2} \int d^3x |\nabla_\perp \phi|^2, \quad V = \frac{i}{2} \int d^3x \phi^* \mathcal{A}\phi, \quad W = \frac{1}{2} \int d^3x \phi^* \mathcal{S}\phi. \tag{3.21}$$

Obviously K is a positive real number. Equations (3.14) and (3.15) show that V and W are real. W corresponds to the energy integral in the ordinary linear MHD stability analysis. From Eq.(3.20)

$$\omega = \alpha\frac{V}{K} \pm \sqrt{\alpha^2\left(\frac{V}{K}\right)^2 + \frac{W}{K}}. \tag{3.22}$$

If $\alpha = 0$ or in the case of RMHD, the sign of W determines the stability and this corresponds to the energy principle. However in the case of $\alpha \neq 0$, even when W is negative, the system can be stable if

$$\alpha^2\left(\frac{V}{K}\right)^2 + \frac{W}{K} > 0 \tag{3.23}$$

which is directly related to the finite Larmor radius stabilization of the interchange mode.

Now let us consider the cylindrical configuration where the magnetic curvature due to the toroidicity is neglected but the average magnetic curvature of the helical field described by $d\Omega/dr$ is retained, where Ω is assumed to depend only on the radial coordinate r. Equilibrium quantities such as p_0, J_0, A_0 and ψ_0 are also functions of r alone, which is consistent with the equilibrium equation (3.7). Using a Fourier mode $\phi(\boldsymbol{x}) = \phi(r)\mathrm{e}^{im\theta - inz}$ in Eq.(3.19), we obtain the following linear eigenmode equation

$$\left(\omega^2 - \omega\alpha\frac{m}{r}\frac{dp_0}{dr}\right)\left(\frac{d^2}{dr^2} + \frac{1}{r}\frac{d}{dr} - \frac{m^2}{r^2}\right)\phi - \alpha\frac{m}{r}\left\{r\frac{d}{dr}\left(\frac{1}{r}\frac{dp_0}{dr}\right)\right\}\left\{r\frac{d}{dr}\left(\frac{\phi}{r}\right)\right\}$$
$$= k_\parallel\left(\frac{d^2}{dr^2} + \frac{1}{r}\frac{d}{dr} - \frac{m^2}{r^2}\right)(k_\parallel\phi) - k_\parallel\frac{m}{r}\frac{dJ_0}{dr}\phi - \frac{m^2}{r^2}\frac{dp_0}{dr}\frac{d\Omega}{dr}\phi. \tag{3.24}$$

From Eq.(3.21) we have

$$K = \pi\int_0^1 rdr\left\{\left|\frac{d\phi}{dr}\right|^2 + \frac{m^2}{r^2}|\phi|^2\right\} \tag{3.25}$$

$$V = \frac{\pi}{2}\int_0^1 rdr\frac{m}{r}\frac{dp_0}{dr}\left\{\left|\frac{d\phi}{dr}\right|^2 + \frac{m^2}{r^2}|\phi|^2 - \frac{1}{r}\frac{d}{dr}|\phi|^2\right\} \tag{3.26}$$

$$W = \pi\int_0^1 rdr\left\{\left|\frac{d}{dr}(k_\parallel\phi)\right|^2 + \left(k_\parallel^2\frac{m^2}{r^2} + k_\parallel\frac{m}{r}\frac{dJ_0}{dr} + \frac{m^2}{r^2}\frac{dp_0}{dr}\frac{d\Omega}{dr}\right)|\phi|^2\right\} \tag{3.27}$$

where $k_{\|} = m\iota - n$ and $\iota = -(1/r)(d\psi_0/dr)$ denotes the rotational transform of the equilibrium field. The first term of the integrand in Eq.(3.27) represents the stabilizing effect of the magnetic field line bending.

In order to minimize W, we consider the mode localized only in the neighborhood of the mode resonant surface, $r = r_0$, which is defined by $k_{\|} = 0$ or $\iota = n/m$. If we put $r - r_0 = x$ and $k_{\|} = k'_{\|}x$, we find

$$W \simeq \pi r_0 \int dx \left\{ k_{\|}'^2 \left| \frac{d}{dx}(x\phi) \right|^2 + k_\theta^2 p_0' \Omega' |\phi|^2 \right\} \geq \pi r_0 \left(\frac{k_{\|}'^2}{4} + k_\theta^2 p_0' \Omega' \right) \int dx |\phi|^2 \tag{3.28}$$

where $k_\theta = m/r_0$, $p_0' = dp_0/dr|_{r=r_0}$ and $\Omega' = d\Omega/dr|_{r=r_0}$. In the last part, Schwarz's inequality is used. From the energy principle, (3.28) means that in the case of $\alpha = 0$ or in the ideal MHD the local mode is stable if and only if the following inequality is satisfied

$$\frac{k_{\|}'^2}{4} + k_\theta^2 p_0' \Omega' > 0. \tag{3.29}$$

This condition is equivalent to the Suydam criterion.[38] In terms of the physical parameters (see Eq.(2.103)), the criterion (3.29) gives

$$\frac{1}{4}\left(\frac{d}{dr} \ln \iota \right)^2 + \frac{4\pi}{B_\theta^2} \frac{dp_0}{dr} \frac{d\Omega}{dr} > 0. \tag{3.30}$$

It is noted that the mode number disappears in this expression. Here we are concerned with the case where the Suydam criterion is violated so that the system is MHD unstable. The eigemode equation (3.24) is rewritten for the localized mode as

$$(\gamma_0^2 + k_{\|}'^2 x^2) \frac{d^2\phi}{dx^2} + 2k_{\|}'^2 x \frac{d\phi}{dx} - k_\theta^2 (p_0' \Omega' + k_{\|}'^2 x^2)\phi = 0 \tag{3.31}$$

where

$$\gamma_0^2 = -\omega^2 + \omega_{*i}\omega. \tag{3.32}$$

Here $\omega_{*i} = \alpha k_\theta p_0'$ is the normalized ion diamagnetic drift frequency and γ_0 denotes the growth rate in the MHD limit $\alpha = 0$. In deriving Eq.(3.31), we have neglected the terms of dJ_0/dr and $rd(r^{-1}dp_0/dr)/dr$ in Eq.(3.24) since

equilibrium quantities, such as J_0 and p_0, vary slowly in the radial direction. Equation (3.32) yields

$$\omega = \frac{1}{2}\left[\omega_{*i} \pm \sqrt{\omega_{*i}^2 - 4\gamma_0^2}\right] \tag{3.33}$$

which shows that the interchange mode is stabilized by the effect of the ion diamagnetic drift if

$$\omega_{*i}^2 > 4\gamma_0^2. \tag{3.34}$$

Next let us calculate the eigenvalue γ_0^2. If we put $x=(\gamma_0/k_{\|}')\xi$ in Eq.(3.31), we have

$$(\xi^2+1)\frac{d^2\phi}{d\xi^2} + 2\xi\frac{d\phi}{d\xi} + (\lambda - \mu^2\xi^2)\phi = 0 \tag{3.35}$$

where

$$\lambda = -\frac{k_\theta^2}{k_{\|}'^2}p_0'\Omega' = -\frac{p_0'\Omega'}{(r_0\iota')^2} \tag{3.36}$$

$$\mu = \frac{k_\theta\gamma_0}{k_{\|}'} = \frac{\gamma_0}{(r_0\iota')}. \tag{3.37}$$

The assumption that the Suydam criterion is violated implies $\lambda > 1/4$. This eigenvalue problem is studied by Kulsrud[30] using the method of the asymptotic matching. The boundary conditions that ϕ vanishes at $\xi = \pm\infty$ determine the largest eigenvalue γ_0 which is given by

$$\begin{aligned}\mu &= H(4\lambda) \\ &\equiv 16\exp\left\{\frac{2}{u}\left[3\arg\Gamma\left(1+\frac{1}{2}iu\right) - \arg\Gamma(1+iu) - \tan^{-1}(e^{-\pi u/2}) - \frac{3}{4}\pi\right]\right\}\end{aligned} \tag{3.38}$$

where $u \equiv \sqrt{4\lambda - 1}$ and $\mu \ll 1$ is assumed. Equation (3.38) is derived in Appendix 3.A. Equations (3.36)–(3.38) yield the largest eigenvalue γ_0

$$\gamma_0 = r_0\iota' H\left(4\frac{(-p_0')\Omega'}{(r_0\iota')^2}\right). \tag{3.39}$$

Thus the stability condition (3.34) is rewritten as

$$\left|\frac{\alpha k_\theta p_0'}{r_0\iota'}\right| > 2H\left(4\frac{(-p_0')\Omega'}{(r_0\iota')^2}\right). \tag{3.40}$$

This condition shows that high m modes can be stabilized more easily than low m modes. From Eqs.(3.31) and (3.32), we find that the profile of the eigenfunction is unchanged with increasing α.

Equation (3.10) gives

$$p_1 = -\frac{1}{\omega}\frac{m}{r}\frac{dp_0}{dr}\phi \tag{3.41}$$

which shows that in the MHD limit $\alpha = 0$ the phase difference betweem p_1 and ϕ are $\pi/2$ since $\omega = i\gamma_0$ whereas for large α the eigenfrequency ω approaches ω_{*i} and results in $p_1 \simeq -(1/\alpha)\phi$ which implies the Boltzmann distribution of ions under the isothermal assumption.

3.3 Numerical Results

In this section we solve the linear eigenmode equation (3.24) numerically, which is given below again

$$\left(\omega^2 - \omega\alpha\frac{m}{r}\frac{dp_0}{dr}\right)\left(\frac{d^2}{dr^2} + \frac{1}{r}\frac{d}{dr} - \frac{m^2}{r^2}\right)\phi - \alpha\frac{m}{r}\left\{r\frac{d}{dr}\left(\frac{1}{r}\frac{dp_0}{dr}\right)\right\}\left\{r\frac{d}{dr}\left(\frac{\phi}{r}\right)\right\}$$
$$= k_{\|}\left(\frac{d^2}{dr^2} + \frac{1}{r}\frac{d}{dr} - \frac{m^2}{r^2}\right)(k_{\|}\phi) - k_{\|}\frac{m}{r}\frac{dJ_0}{dr}\phi - \frac{m^2}{r^2}\frac{dp_0}{dr}\frac{d\Omega}{dr}\phi. \quad (3.42)$$

Here the parallel wavenumber is

$$k_{\|} = m\iota - n. \quad (3.43)$$

Since we consider a currentless plasma, we put $A_0 = J_0 = 0$ and the rotational transform ι is determined only by the external helical fields. As is shown in Appendix 3.B, the average magnetic curvature may be written in terms of ι as

$$\frac{d\Omega}{dr} = \frac{N\epsilon}{l}\frac{1}{r^2}\frac{d}{dr}(r^4\iota) \quad (3.44)$$

where l is the pole number, N is the toroidal pitch number and ϵ is the inverse aspect ratio. In the numerical integration of the eigenvalue problem, we used the shooting method to satisfy the boundary condition for an appropriate eigenvalue. Here we employed the fixed boundary condition at $r = 1$ where the eigenfunction ϕ vanishes. Using the fact that the eigenfunction has the form $\phi \propto r^m$ in the neighborhood of $r = 0$ for the poloidal mode numer m, the equation is integrated from $r \simeq 0$ to $r = 1$. The eigenvalue ω is obtained by adjusting the solution to satisfy the boundary condition at $r = 1$ based on a root-finding subroutine called Brent's method. The results of the shooting method were also compared with those obtained by solving the initial value problem of the linearized equations (3.8)–(3.10).

For the Heliotron E plasmas we put $l = 2, N = 19, \epsilon = 0.1$ and the minor radius of the torus $a = 20cm$. The rotational transform due to the external helical fields is assumed as $\iota = 0.51 + 1.69r^{2.5}$. We also assume the equilibrium pressure to take the form

$$p_0(r) = (\beta(0)/2\epsilon)(1 - r^2)^2. \quad (3.45)$$

We studied the stability of this equilibrium against the $m = 1/n = 1$ mode, which is the most dangerous mode in Heliotron E since it has the mode resonant surface at the middle of the plasma minor radius, $r = 0.61$, and low m modes are more unstable than high m modes as seen in Sec.3.2. Figure 3.1 shows the profile of the rotational transform and the location of the $m = 1/n = 1$ mode resonant surface. The stability beta limit determined by the Suydam criterion (3.29) at $r = 0.61$ is $\beta(0) = 1.62\%$.

Figures 3.2 and 3.3 present plots of the numerically obtained linear growth rate $(R_0/v_A)\gamma$ for the $m = 1/n = 1$ mode versus the central beta value $\beta(0)$ and the drift parameter $\alpha = c/a\omega_{pi}$, respectively. The results of the analytical treatments for the slab geometry given in Sec 3.2 are also plotted for comparison in Fig.3.2. We see that the analytical expressions for the localized modes agree with the numerical results for the cylindrical geometry in the dependence of γ on $\beta(0)$ and α though the difference in the magnitude of γ occurs due to the nonlocal properties of the eigenfunction as is seen later in Figs.3.6 and 3.7. It is noted that the analytical treatments become more applicable as the poloidal mode number m increases because the radial width of the eigenmode is inversely proportional to m as is given by Eq.(3.59). When $\beta(0)$ becomes near the Suydam limit, the mode structure in the case of $\alpha = 0$ is localized sharply in the vicinity of the resonant surface and the growth rate becomes close to that given by Eq.(3.39). According to the results of the shooting method we find that the stability beta limit determined by the $m = 1/n = 1$ ideal interchange mode in the ideal MHD case of $\alpha = 0$ is $\beta(0) = 2.2\%$. This value is determined in the numerical calculation using 10,000 meshes equally devided in the radial direction. Its value seems to decrease close to the Suydam limit if we use smaller mesh sizes near the mode resonant surface. Figure 3.4 shows the stability beta limit as a function of the drift parameter α. The beta limit can be improved by including the effect of the ion diamagnetic drift and its value becomes $\beta(0) = 5.1\%$ in the case of $\alpha = 0.5$ which corresponds to the deuterium plasma with the average density $n = 10^{13} cm^{-3}$ and the minor radius $a = 20$ cm.

Figure 3.5 shows the contour of the eigenvalue ω in the complex ω-plane for $0 \leq \alpha \leq 0.6$ and $\beta(0) = 5.5\%$. It is found that, for the unstable region $\gamma \equiv \omega_i > 0$, the eigenvalues obtained by the shooting method also draw a quarter of the circle $\omega_r^2 + \omega_i^2 = \gamma_0^2$ as predicted from Eq.(3.33) where ω_r and ω_i are the real and imaginary parts of ω, respectively. Here γ_0 denotes the linear growth rate in the ideal MHD limit $\alpha = 0$. In Figs.3.6 and 3.7 we have

the contours and the profiles of the eigenfunctions ϕ, p_1 and A_1, respectively, which are numerically obtained for $\alpha = 0$ and $\alpha = 0.5$ at $\beta(0) = 4.5\%$. Here the interchange mode is unstable for $\alpha = 0$ and stable for $\alpha = 0.5$. As expected from Eqs.(3.9) and (3.10), p_1 and A_1 have the same phase and the phase difference between ϕ and p_1 is $\pi/2$ for the MHD unstable case, which goes to π as the ion diamagnetic drift stabilizes the interchange mode. This relation corresponds to the realization of the Boltzmann distribution for ions provided that the temperature is constant. We see from Fig.3.7 that the profiles of the eigenfunctions do not depend much on the drift parameter α compared with the phase differences, which is already explained by the local mode analyses in Sec.3.2. We note that the eigenfunction ϕ has the peak at the mode resonant surface and its radial width is of the same order as the plasma minor radius. In spite of this fact, the local mode analyses given in the previous section are still useful to explain the numerical results obtained for the low mode number.

3.4 Conclusions

We have studied the stabilizing effects of the ion diamagnetic drift on the ideal interchange instabilities in a helical system both analytically and numerically. Our model equations differ from the RMHD for high beta stellarator plasmas with $\beta \sim \epsilon$ in that the vorticity equation has the term corresponding to the ion diamagnetic drift, the magnitude of which is characterized by the drift parameter $\alpha = c/a\omega_{pi}$. The Lagrangian or Hamiltonian formulation is shown for the linearized equations of our model though the energy principle for the linear stability is not available. The local mode analysis gave the stability condition (3.40) which states that the interchange mode is stabilized if the magnitude of the ion diamagnetic drift frequency becomes greater than twice the linear growth rate in the ideal MHD or $\alpha = 0$ case. This result is equivalent to that obtained by Rosenbluth et al.[29] or Kulsrud.[30] The eigenvalue problem was numerically solved for the model configuration of Heliotron E by using the shooting method. The $m = 1/n = 1$ interchange mode, which is the most dangerous one in the Heliotron E configuration, was examined. The eigenfunction ϕ has the peak at the mode resonant surface and its radial width is of the same order as the plasma minor radius when the beta value is much larger than the Suydam limit. However the dispersion relation given by the local mode analysis agree with those obtained numerically in the dependence of the eigenvalue ω on the central beta value $\beta(0)$ and the drift parameter α. The local dispersion relation can be applicable to low poloidal mode number cases with reasonable accuracy especially for smaller beta values close to the Suydam limit. The phase difference between ϕ and p_1 is $\pi/2$ for the ideal MHD unstable mode. When the ion diamagnetic drift is included, the interchange mode is stabilized by the increase of α and the phase difference goes to π at the marginal point, which implies the realization of the Boltzmann distribution for ions under the isothermal assumption. This is an explanation of finite Larmor radius stabilization for the interchange mode. In the Heliotron E model configuration with the equilibrium pressure profile of the form $p(r) = p(0)(1 - (r/a)^2)^2$, then the stability beta limit determined by the $m = 1/n = 1$ ideal interchange mode is $\beta(0) = 2.2\%$ in the ideal MHD case $\alpha = 0$. It is improved up to $\beta(0) = 5.1\%$ in the case of $\alpha = 0.5$ which corresponds to the deuterium plasma with the average density $n = 10^{13} cm^{-3}$ and the minor radius $a = 20cm$.

3.A Derivation of Eq.(3.38)

The method of asymptotic matching is applied to the eigenmode equation

$$(\xi^2+1)\frac{d^2\phi}{d\xi^2}+2\xi\frac{d\phi}{d\xi}+(\lambda-\mu^2\xi^2)\phi=0 \tag{3.46}$$

with the boundary conditions that $\phi = 0$ at $\xi = \pm\infty$. Since Eq.(3.46) is invariant with the transformation $\xi \to -\xi$, both the even and odd modes exist. Multiplying Eq.(3.46) by ϕ^* and integrating over the whole region yield

$$\begin{aligned}
&\int_{-\infty}^{\infty} d\xi \left\{(\xi^2+1)\left|\frac{d\phi}{d\xi}\right|^2-(\lambda-\mu^2\xi^2)|\phi|^2\right\} \\
&= \int_{-\infty}^{\infty} d\xi \left\{\left|\xi\frac{d\phi}{d\xi}+\frac{1}{2}\phi\right|^2+\left(\frac{1}{4}-\lambda\right)|\phi|^2+\left|\frac{d\phi}{d\xi}\right|^2+\mu^2\xi^2|\phi|^2\right\} \\
&= 0.
\end{aligned} \tag{3.47}$$

Here if we use the following inequalities

$$\begin{aligned}
&\int_{-\infty}^{\infty} d\xi \left\{\left|\frac{d\phi}{d\xi}\right|^2+\mu^2\xi^2|\phi|^2\right\} \geq \int_{-\infty}^{\infty} d\xi 2\left|\frac{d\phi}{d\xi}\mu\xi\phi^*\right| \\
&\geq \int_{-\infty}^{\infty} d\xi \left|\mu\xi\frac{d}{d\xi}|\phi|^2\right| \geq \left|\int_{-\infty}^{\infty} d\xi\mu\xi\frac{d}{d\xi}|\phi|^2\right| = \mu\int_{-\infty}^{\infty} d\xi|\phi|^2
\end{aligned} \tag{3.48}$$

then we find

$$\lambda-\frac{1}{4}\geq\mu\geq 0 \tag{3.49}$$

and that $\mu \to +0$ as $\lambda \to 1/4+0$. We assume that λ is close to $1/4$ so that $\mu \ll 1$. In the region $0 \leq \xi \ll 1/\mu$, we have Eq.(3.46) as

$$(\xi^2+1)\frac{d^2\phi}{d\xi^2}+2\xi\frac{d\phi}{d\xi}-\nu(\nu+1)\phi=0 \tag{3.50}$$

where we have used $\lambda = -\nu(\nu+1)$ and defined

$$\nu=-\frac{1}{2}+\frac{1}{2}iu \tag{3.51}$$

$$u = \sqrt{4\lambda - 1}. \tag{3.52}$$

The solution to Eq.(3.50) is given by

$$\phi = AP_\nu(i\xi) + BQ_\nu(i\xi) \tag{3.53}$$

where P_ν and Q_ν are the Legendre functions. For the even mode, the condition $d\phi/d\xi|_{\xi=0} = 0$ yields

$$\frac{A}{B} = \frac{1}{2}\Gamma\left(-\frac{\nu}{2}\right)\Gamma\left(1+\frac{\nu}{2}\right)e^{-i\pi\nu/2} = \frac{\pi}{2}\left\{i - \cot\left(\frac{\pi\nu}{2}\right)\right\}. \tag{3.54}$$

Substituting this into Eq.(3.53) we have the asymptotic form

$$\begin{aligned}\phi \;=\; & \text{const.}\xi^{-1/2}\cos\left[\frac{u}{2}\log\xi + \frac{3}{2}u\log 2 + 2\arg\Gamma\left(1+\frac{1}{2}iu\right) - \arg\Gamma(1+iu)\right. \\ & \left. - \tan^{-1}(e^{-\pi u/2}) - \frac{\pi}{4}\right]\end{aligned} \tag{3.55}$$

for $1 \ll \xi \ll 1/\mu$. Similarly for the odd mode we use $\phi|_{\xi=0} = 0$ to obtain

$$\frac{A}{B} = -\frac{1}{2}\Gamma\left(\frac{1}{2}+\frac{\nu}{2}\right)\Gamma\left(\frac{1}{2}-\frac{\nu}{2}\right)e^{-i\pi(\nu+1)/2} = \frac{\pi}{2}\left\{i + \tan\left(\frac{\pi\nu}{2}\right)\right\} \tag{3.56}$$

and for $1 \ll \xi \ll 1/\mu$

$$\begin{aligned}\phi \;=\; & \text{const.}\xi^{-1/2}\cos\left[\frac{u}{2}\log\xi + \frac{3}{2}u\log 2 + 2\arg\Gamma\left(1+\frac{1}{2}iu\right) - \arg\Gamma(1+iu)\right. \\ & \left. + \tan^{-1}(e^{-\pi u/2}) - \frac{3}{4}\pi\right]\end{aligned} \tag{3.57}$$

In the region of $\xi \gg 1$, Eq.(3.46) is written as

$$\xi^2\frac{d^2\phi}{d\xi^2} + 2\xi\frac{d\phi}{d\xi} - \left[\nu(\nu+1) + \mu^2\xi^2\right]\phi = 0. \tag{3.58}$$

Its solution vanishing at $\xi = +\infty$ is given by

$$\phi = \xi^{-1/2}K_{\nu+1/2}(\mu\xi). \tag{3.59}$$

For $1 \ll \xi \ll 1/\mu$ Eq.(3.59) takes the form

$$\phi = \text{const.}\xi^{-1/2}\cos\left[\frac{u}{2}\log\xi + \frac{u}{2}\log\frac{\mu}{2} - \arg\Gamma\left(1+\frac{1}{2}iu\right) + \frac{\pi}{2}\right]. \tag{3.60}$$

By comparing Eqs.(3.55) with (3.60) for the even modes

$$\mu = 16\exp\left\{\frac{2}{u}\left[3\arg\Gamma\left(1+\frac{1}{2}iu\right)-\arg\Gamma(1+iu)-\tan^{-1}(e^{-\pi u/2})\right.\right.$$
$$\left.\left.-\frac{3}{4}\pi+n\pi\right]\right\} \tag{3.61}$$

is obtained, where $n = 0, -1, -2, \cdots$ since $\mu \to +0$ as $u \to +0$. Similarly by comparing of Eqs.(3.57) with (3.60) for the odd modes

$$\mu = 16\exp\left\{\frac{2}{u}\left[3\arg\Gamma\left(1+\frac{1}{2}iu\right)-\arg\Gamma(1+iu)+\tan^{-1}(e^{-\pi u/2})\right.\right.$$
$$\left.\left.-\frac{5}{4}\pi+n\pi\right]\right\} \tag{3.62}$$

is obtained, where $n = 0, -1, -2, \cdots$ for the same reason as in Eq.(3.61). The largest value of μ is given for $n = 0$ in the even mode as

$$\mu = 16\exp\left\{\frac{2}{u}\left[3\arg\Gamma\left(1+\frac{1}{2}iu\right)-\arg\Gamma(1+iu)-\tan^{-1}(e^{-\pi u/2})-\frac{3}{4}\pi\right]\right\}. \tag{3.63}$$

3.B Magnetic Flux, Curvature and Rotational Transform due to External Helical Fields

The scalar potential for the external helical fields Φ is subject to the Laplace's equation as stated in Sec.2.3

$$\nabla^2\Phi = 0. \tag{3.64}$$

Since the uniform toroidal field and the other fields independent of z are separable from the helical fields, the general solution to Eq.(3.64) is given by

$$\Phi = \sum_{l=-\infty}^{\infty}\sum_{p=1}^{\infty}\Phi_{lp}I_l(phr)\sin(l\theta - phz + \phi_{lp}) \tag{3.65}$$

where I_l is the modified Bessel function and ϕ_{lp} denotes an arbitrary phase angle. In terms of the major radius of the torus R_0 and the toroidal pitch number N, we can write $h = N/R_0$. In this Appendix all quantities are represented by the physical parameters instead of the normalized ones. From Eq.(2.98) we have the magnetic flux due to the helical fields as

$$\begin{aligned}\psi_h &= \frac{1}{2B_0}\overline{\nabla\Phi\times\nabla\int_0^z dz\Phi\cdot\tilde{z}} \\ &= -\frac{1}{2B_0}\sum_{l,m,p}\Phi_{lp}\Phi_{mp}\frac{m}{r}I_l'(phr)I_m(phr)\cos[(l-m)\theta+\phi_{lp}-\phi_{mp}].\end{aligned} \tag{3.66}$$

The scalar potential for the magnetic curvature due to the helical fields is obtained by Eq.(2.99) as

$$\begin{aligned}\Omega_h &= \frac{\overline{|\nabla\Phi|^2}}{B_0^2} \\ &= \frac{1}{2B_0^2}\sum_{l,m,p}\Phi_{lp}\Phi_{mp}p^2h^2\left[I_l'(phr)I_m'(phr)+\left(1+\frac{lm}{p^2h^2r^2}\right)I_l(phr)I_m(phr)\right] \\ &\qquad\times\cos[(l-m)\theta+\phi_{lp}-\phi_{mp}].\end{aligned} \tag{3.67}$$

It is seen from Eqs.(3.66) and (3.67) that both ψ_h and Ω_h depend only on r if we consider the case where, for each p, $\Phi_{lp} \neq 0$ only for a single value of

l such as in a helically symmetric system. Then we can write the rotational transform due to the helical fields as

$$\iota_h(r) = -\frac{R_0}{rB_0}\frac{d\psi_h}{dr}. \tag{3.68}$$

Furthermore if we assume that $\Phi_{lp} \neq 0$ only for $p = 1$ and a single value of l then we find from Eqs.(3.66) and (3.67)

$$\psi_h = -\frac{l\Phi_{l1}^2}{2rB_0} I_l(hr) I_l'(hr) \tag{3.69}$$

$$\Omega_h = \frac{h^2\Phi_{l1}^2}{2B_0^2}\left[I_l'^2(hr) + \left(1 + \frac{l^2}{h^2r^2}\right) I_l^2(hr)\right] = -\frac{h}{lB_0}\frac{1}{r}\frac{d}{dr}(r^2\psi_h). \tag{3.70}$$

Using Eqs.(3.68) and (3.70) we obtain

$$\frac{d\Omega_h}{dr} = \frac{h}{lR_0}\frac{1}{r^2}\frac{d}{dr}(r^4\iota_h). \tag{3.71}$$

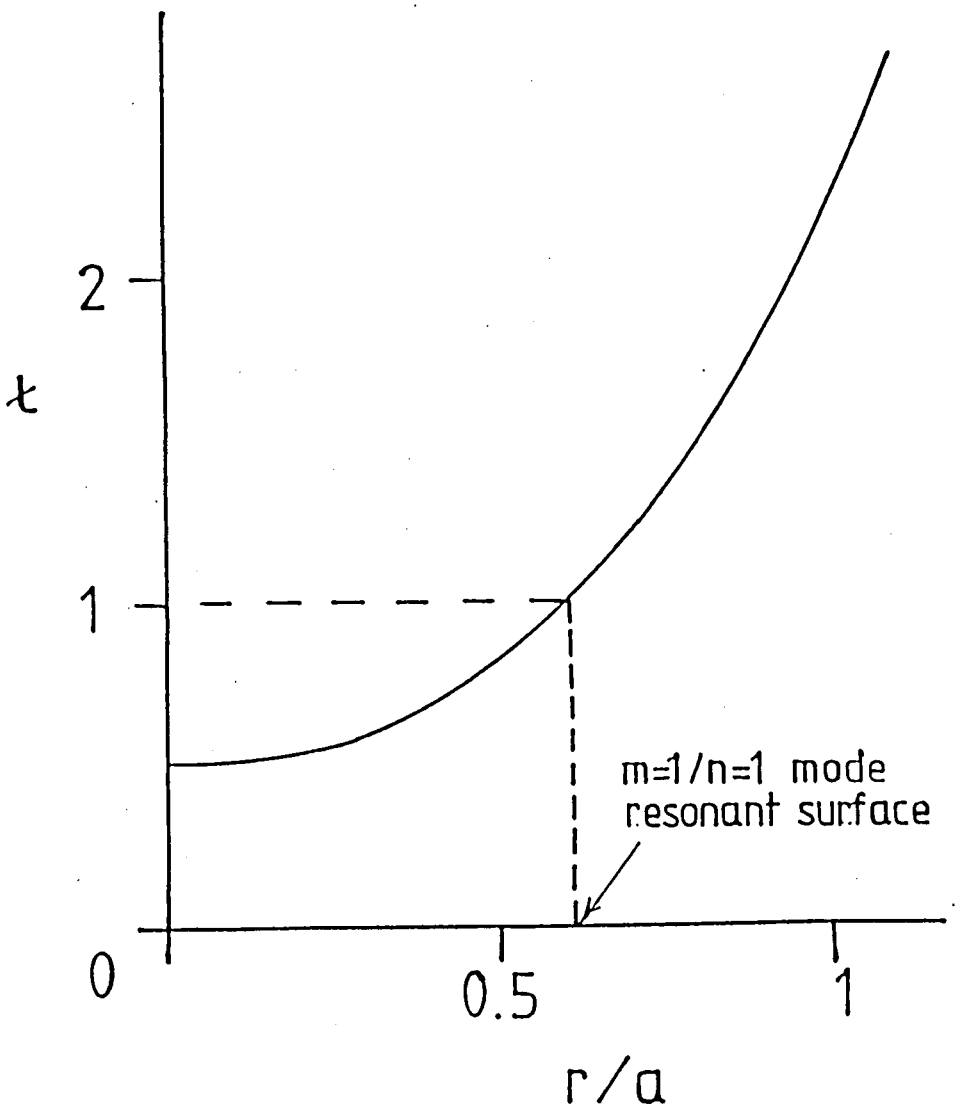

Figure 3.1: The profile of the rotational transform and the location of the $m = 1/n = 1$ mode resonant surface.

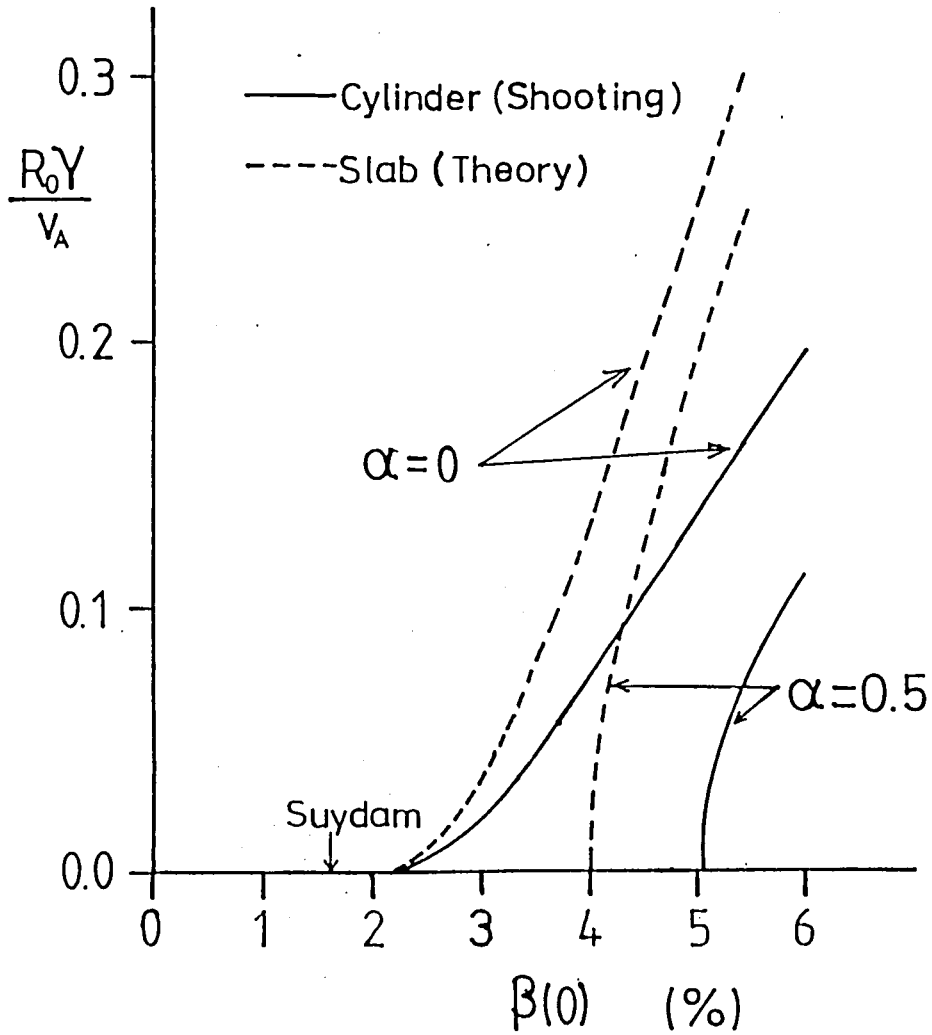

Figure 3.2: Growth rate of the $m = 1/n = 1$ ideal interchange mode as a function of the central beta value $\beta(0)$ for $\alpha = 0$ and $\alpha = 0.5$. Solid lines are obtained by the shooting method for a cylindrical configuration and dashed lines are given by Eqs.(3.33) and (3.39).

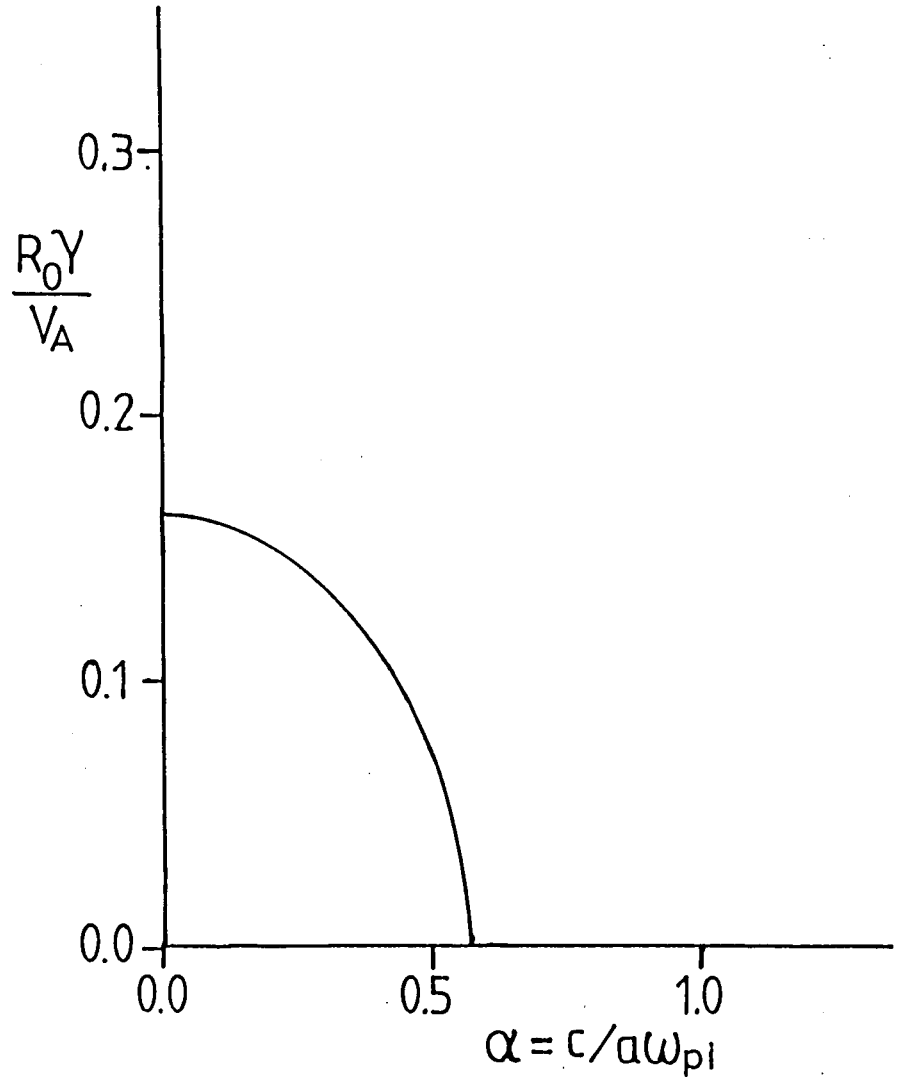

Figure 3.3: Growth rate of the $m = 1/n = 1$ ideal interchange mode at $\beta(0) = 5.5\%$ as a function of the drift parameter $\alpha = c/a\omega_{pi}$.

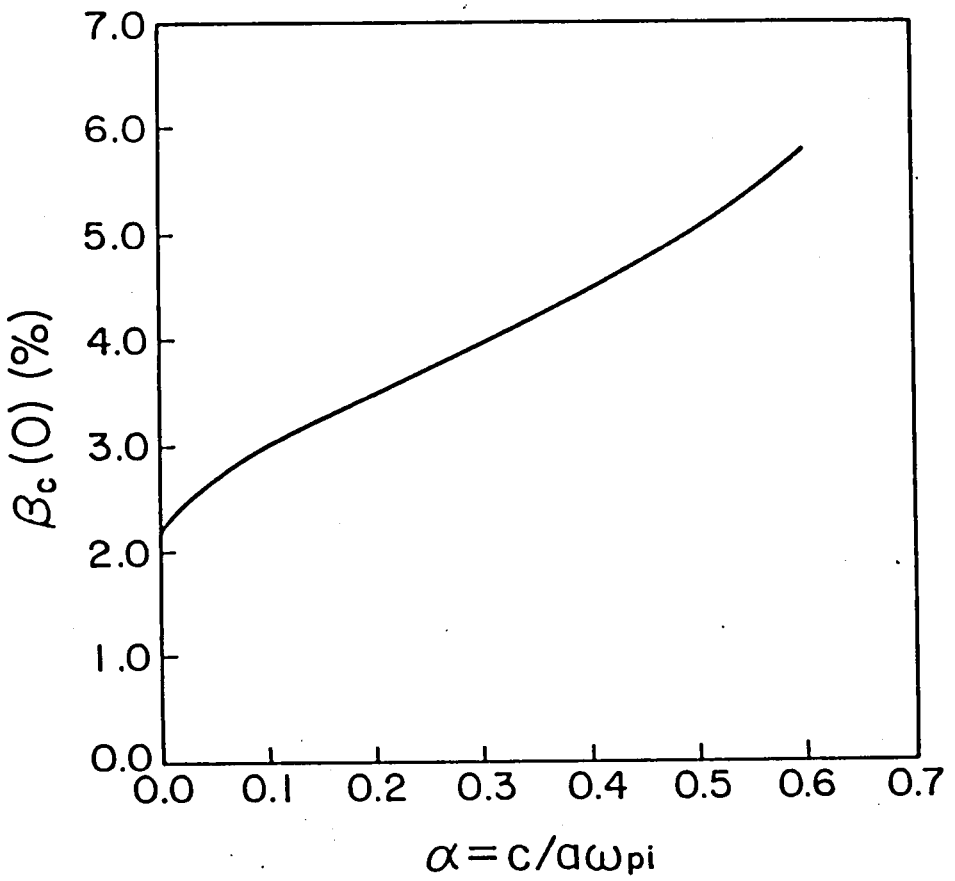

Figure 3.4: Stability beta limit $\beta_c(0)$ determined by the $m = 1/n = 1$ mode as a function of the drift parameter $\alpha = c/a\omega_{pi}$.

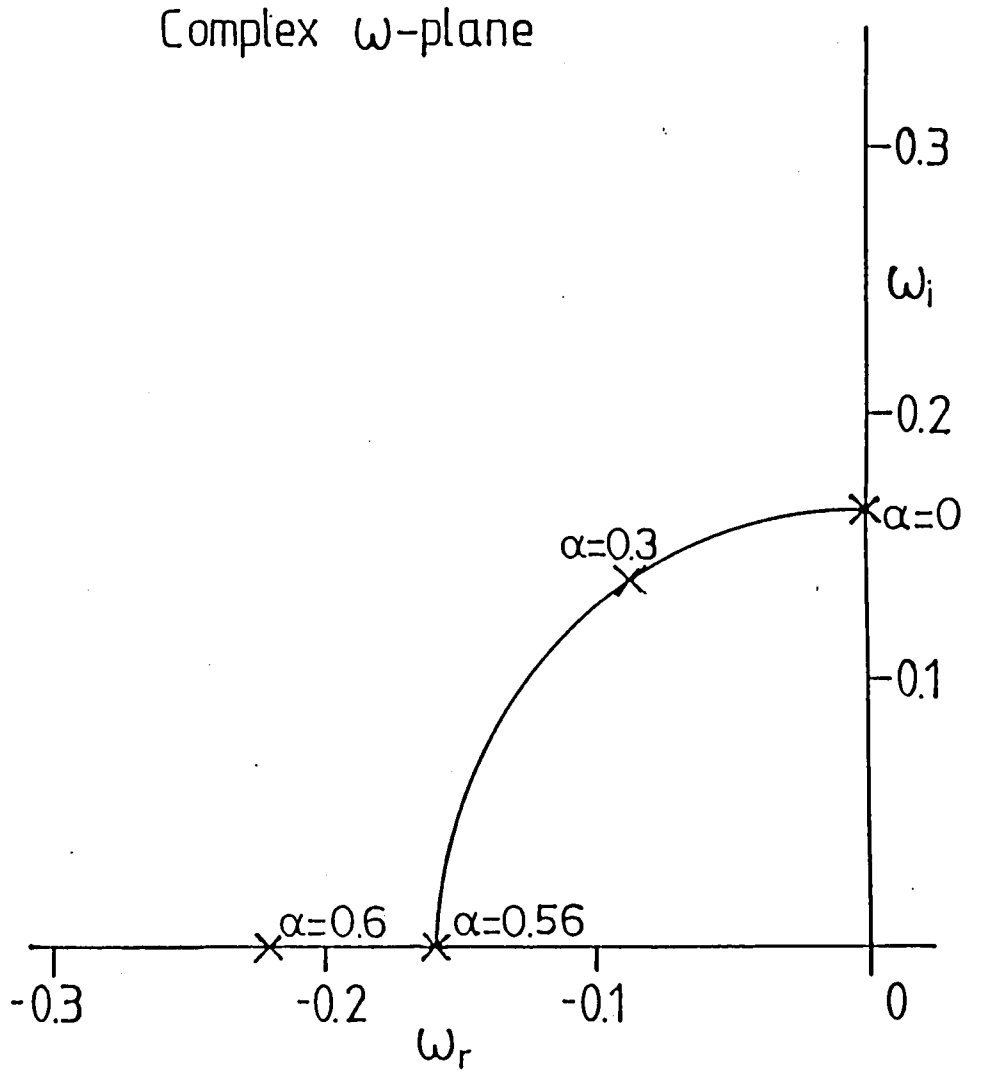

Figure 3.5: Locus of the eigenvalue of the $m = 1/n = 1$ mode at $\beta(0) = 5.5\%$ in the complex ω-plane with increasing α. The eigenvalue is normalized as $R_0\omega/v_A = \omega$.

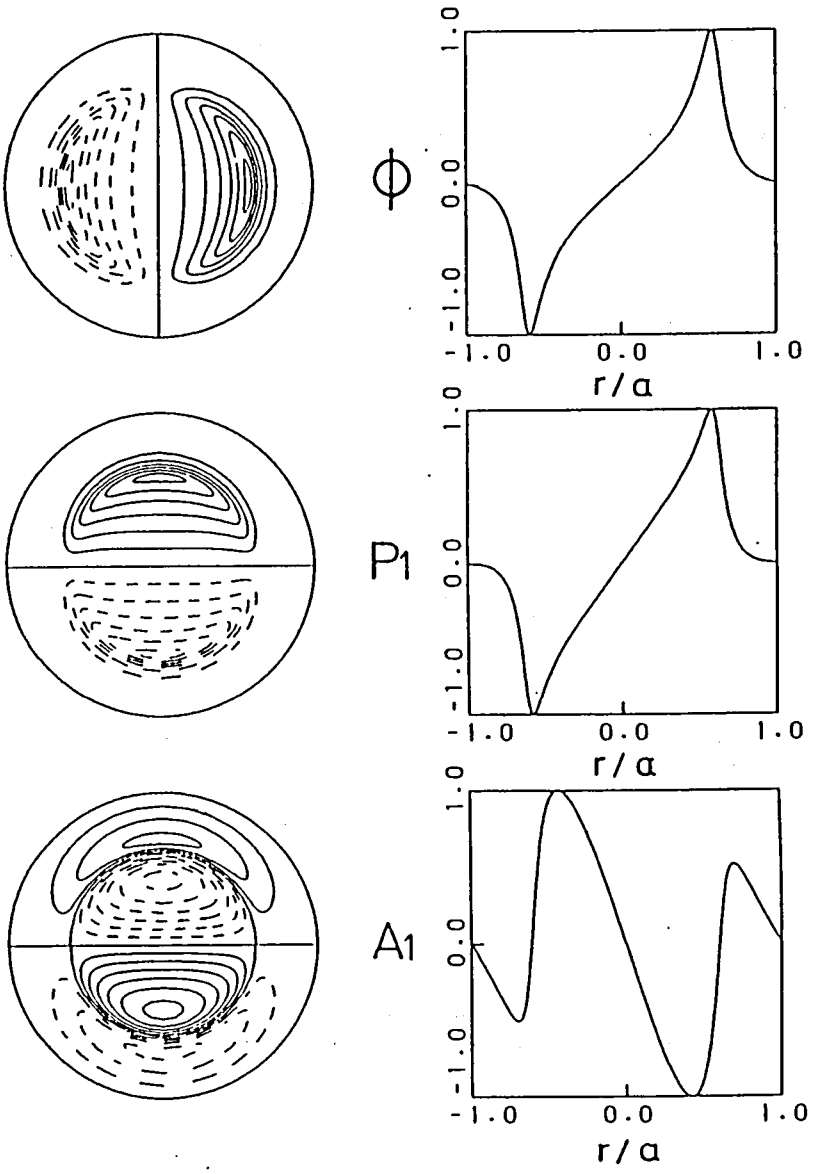

Figure 3.6: Contours and profiles of the eigenfunctions ϕ, p_1 and A_1 of the $m = 1/n = 1$ mode for $\beta(0) = 4.5\%$ and $\alpha = 0$. Dashed lines denote the contours with negative values.

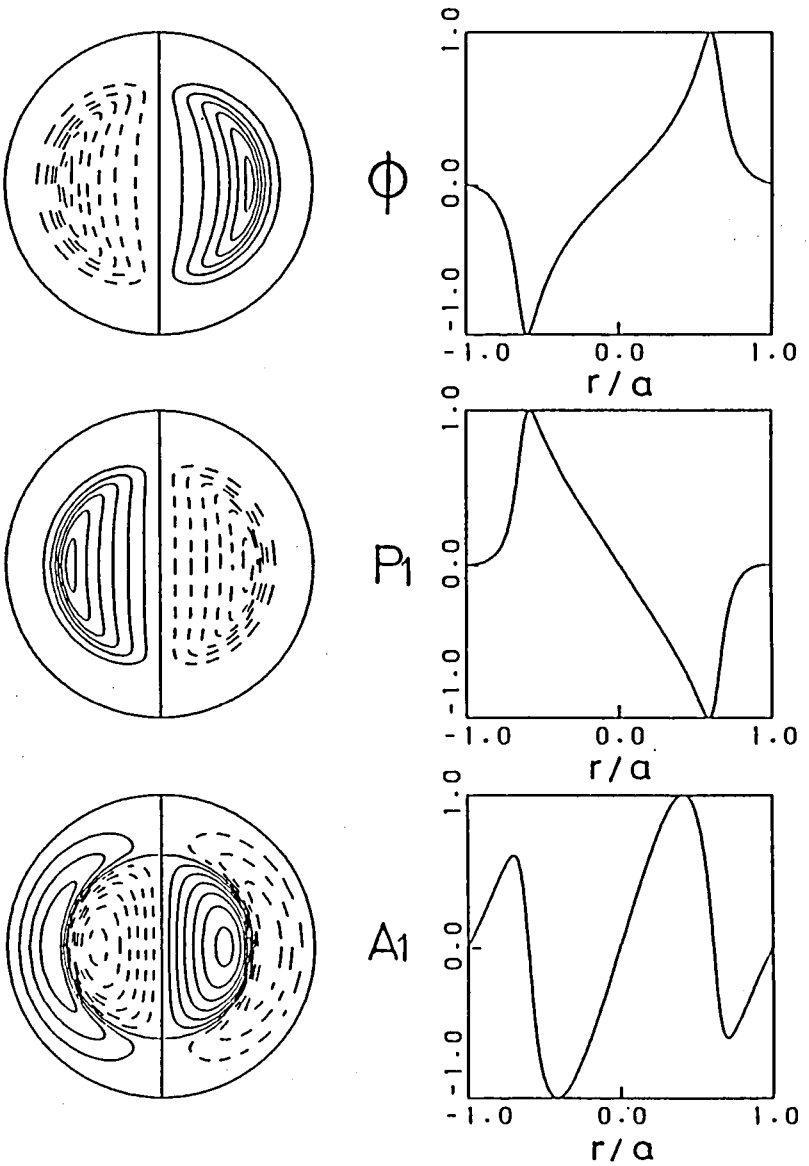

Figure 3.7: Contours and profiles of the eigenfunctions ϕ, p_1 and A_1 of the $m = 1/n = 1$ mode for $\beta(0) = 4.5\%$ and $\alpha = 0.5$. Dashed lines denote the contours with negative values.

Chapter 4

Linear Theory of Resistive Interchange Modes Coupled to Resistive Drift Waves

4.1 Introduction

In the previous chapter we have discussed the stabilizing effect of the ion diamagnetic drift on the ideal interchange instability. Even if the ideal MHD modes are stable, the resistive MHD instabilities[39] such as tearing mode, rippling mode and resistive interchange mode or drift waves destabilized by trapped electrons, toroidal effect and resistivity exist. They have usually smaller growth rates than the ideal modes and play an important role in the relaxation phenomina such as sawtooth oscillations and disruptions or in the anomalous transport observed in magnetically confined systems.

Here our concern is in the resistive interchange mode, which is supposed to be a cause of turbulence and the resultant anomalous transport in the edge region of stellarator/heliotron. In this chapter we study the linear theory of the resistive interchange modes coupled to the resistive drift waves under the electrostatic approximation by using the Hasegawa-Wakatani equations including the average magnetic curvature given in Sec.2.3. This approximation is valid in the edge region where the beta value is low. Chen et al.[40]–[42] showed that the resistive drift waves are stable in slab geometries with magnetic shear, while they become unstable in toroidal geometries. Here it is

found that, if the average magnetic curvature due to the helical fields is included, the radially localized instability occurs even in slab geometries by the coupling of the resistive interchange mode and the resistive drift wave. Parallel ion motion becomes important in the region far from the mode resonant surface and contributes to the localization of the drift wave. However it is shown that in our model the average magnetic curvature causes the localization of the mode around the resonant surface and therefore the ion parallel motion is neglected in our model.

This chapter is organized as follows. In Sec.4.2 we linearize the Hasegawa-Wakatani equations with the average magnetic curvature to obtain the linear eigenmode equation and derive the dispersion relation analytically by using the slab approximation. In Sec.4.3 the eigemode equation is solved numerically and compared with the analytical results. Finally conclusions are given in Sec.4.4.

4.2 Model Equations and Linear Stability Analyses

We consider low frequency electrostatic perturbations in an inhomogeneous collisional plasma in a magnetic field with curvature and a shear. We assume electrons to be isothermal. Ions are treated as a two-dimensional cold fluid where parallel ion motion is neglected. Here we use the Hasegawa-Wakatani equations generalized into helical systems where the average magnetic curvature due to the helical field exists, which are given in Eqs.(2.114) and (2.115) and written again

$$\left(\frac{\partial}{\partial t}+\hat{z}\times\nabla\phi\cdot\nabla\right)\nabla_{\perp}^{2}\phi=\frac{1}{\nu}\nabla_{\parallel}^{2}(n-\phi)+\nabla n\times\nabla\Omega\cdot\hat{z} \tag{4.1}$$

$$\left(\frac{\partial}{\partial t}+\hat{z}\times\nabla\phi\cdot\nabla\right)(n+\overline{n})=\frac{1}{\nu}\nabla_{\parallel}^{2}(n-\phi)+\nabla(n-\phi)\times\nabla\Omega\cdot\hat{z} \tag{4.2}$$

where $\nu=\nu_{e\parallel}/\omega_{ce}$ and the normalizations described in (2.113) are used. Since we have the nonzero average curvature without considering a toroidal geometry, we employ a cylindrical plasma model where all the stationary quantities such as $\overline{n}$, Ω and the magnetic flux ψ depend only on the radial coordinate r. The perpendicular diffusion term in Eq.(2.115) is neglected since $\nu\ll\beta$ is assumed. If there is no stationary electrostatic potential, linearizing Eqs.(4.1) and (4.2) and expressing n and ϕ in terms of the Fourier mode with a frequency ω poloidal and toroidal mode numbers m, n, we obtain the linear response of the density perturbation n to the electrostatic potential ϕ,

$$n=\frac{k_{\parallel}^{2}-i\nu(\omega_{*e}-\omega_{g})}{k_{\parallel}^{2}-i\nu(\omega-\omega_{g})}\phi \tag{4.3}$$

and the linear eigenmode equation

$$\left(\frac{d^{2}}{dr^{2}}+\frac{1}{r}\frac{d}{dr}-\frac{m^{2}}{r^{2}}\right)\phi$$
$$=\frac{1}{k_{\parallel}^{2}-i\nu(\omega-\omega_{g})}\left[\left(1-\frac{\omega_{*e}-\omega_{g}}{\omega}\right)k_{\parallel}^{2}-i\nu\frac{\omega_{g}(\omega_{*e}-\omega_{g})}{\omega}\right]\phi \tag{4.4}$$

where $k_{\parallel}=(\rho_{s}/R_{0})(m\iota-n)$, $\omega_{*e}=(m/r)(-d\overline{n}/dr)$ and $\omega_{g}=(m/r)(d\Omega/dr)$. ω_{*e} is the normalized electron diamagnetic drift frequency and $\omega_{g}/k_{\theta}=d\Omega/dr$

corresponds to the normalized magnetic curvature drift velocity, where $k_\theta = m/r$ is the normalized poloidal wavenumber.

Here we assume a radialy localized mode around the resonant surface $r = r_0$, which enables us to use a slab approximation. We use $x = r - r_0$ and $k_\parallel = k'_\parallel x$ in Eq.(4.4), which yields

$$\frac{d^2}{dx^2}\phi - \frac{\xi x^2 - i x_R^2 \eta}{x^2 - i x_R^2}\phi = 0 \tag{4.5}$$

where

$$x_R^2 = \frac{\nu(\omega - \omega_g)}{k'^2_\parallel} \tag{4.6}$$

$$\xi = 1 - \frac{\omega_{*e} - \omega_g}{\omega} + k_\theta^2 \tag{4.7}$$

$$\eta = \frac{\omega_g(\omega_{*e} - \omega_g)}{\omega(\omega - \omega_g)} + k_\theta^2. \tag{4.8}$$

Since Eq.(4.4) is invariant with the transform $x \to -x$, both even and odd eigenmodes exist. For $x \gg |x_R|$ Eq.(4.5) can be written as

$$\left(\frac{d^2}{dx^2} - \xi + \frac{i x_R^2 \eta}{x^2}\right)\phi = 0 \tag{4.9}$$

Its solution which vanishes at $x = +\infty$ is given by

$$\phi = x^{1/2} H_\lambda^{(1)}(i\xi^{1/2} x) \tag{4.10}$$

where $H_\lambda^{(1)}$ is the Hankel function and λ is defined by

$$\lambda^2 - \frac{1}{4} = -i x_R^2 \eta. \tag{4.11}$$

Here the real parts of $\xi^{1/2}$ and λ are assumed to be positive. In the region $|x_R| \ll x \ll |\xi|^{-1/2}$ Eq.(4.10) takes the form

$$\phi = \mathrm{e}^{-i\lambda\pi/2}\mathrm{cosec}(\lambda\pi)\left\{\frac{2^{-\lambda}\xi^{\lambda/2}}{\Gamma(\lambda+1)}x^{\lambda+1/2} - \frac{2^{\lambda}\xi^{-\lambda/2}}{\Gamma(-\lambda+1)}x^{-\lambda+1/2}\right\}. \tag{4.12}$$

For $0 \leq x < |x_R||\eta/\xi|^{1/2}$ we have Eq.(4.5) as

$$\left(\frac{d^2}{dx^2} + \frac{ix_R^2\eta}{x^2 - ix_R^2}\right)\phi = 0 \tag{4.13}$$

The solution to Eq.(4.13) is

$$\phi = \left(\tau^2 - 1\right)^{1/2}\left\{AP_\mu^1(\tau) + BQ_\mu^1(\tau)\right\} \tag{4.14}$$

where P_μ^1 and Q_μ^1 are the Legendre functions and we defined $\tau = xe^{-i\pi/4}/x_R$ and $\mu(\mu+1) = -ix_R^2\eta$. The last relation gives

$$\mu = \lambda - \frac{1}{2} = \left(\frac{1}{4} - ix_R^2\eta\right)^{1/2} - \frac{1}{2}. \tag{4.15}$$

For the even mode, the condition $d\phi/dx|_{x=0} = 0$ yields

$$\frac{B}{A} = \frac{-2ie^{-i\pi\mu/2}}{\Gamma(-1/2-\mu/2)\,\Gamma(3/2+\mu/2)} = \frac{2i}{\pi}\cos\left(\frac{\pi\mu}{2}\right)e^{-i\pi\mu/2}. \tag{4.16}$$

and for the odd mode, the condition $\phi|_{x=0} = 0$ gives

$$\frac{B}{A} = \frac{2e^{-i\pi\mu/2}}{\Gamma(-\mu/2)\,\Gamma(1+\mu/2)} = -\frac{2}{\pi}\sin\left(\frac{\pi\mu}{2}\right)e^{-i\pi\mu/2}. \tag{4.17}$$

Here we assumed

$$-\frac{\pi}{4} < \arg x_R < \frac{3\pi}{4} \tag{4.18}$$

in deriving Eqs.(4.16) and (4.17). The asymptotic form of Eq.(4.14) in the region $|x_R| \ll x \ll |x_R||\eta/\xi|^{1/2}$ is written as

$$\begin{aligned}\phi \;=\; & \pi^{-1/2}A\left[\frac{\Gamma(\mu+1/2)}{\Gamma(\mu)}2^\mu e^{-i\pi(\mu+1)/4}x_R^{-\mu-1}x^{\mu+1}\right. \\ & \left. + \left\{\frac{\Gamma(-\mu-1/2)}{\Gamma(-\mu-1)} - \pi\frac{B}{A}\frac{\Gamma(\mu+2)}{\Gamma(\mu+3/2)}\right\}2^{-\mu-1}e^{i\pi\mu/4}x_R^\mu x^{-\mu}\right].\end{aligned} \tag{4.19}$$

Since Eqs.(4.12) and (4.19) coincide with each other in the overlapped region where both the equations are valid, we obtain the following equation

$$2^{-4\mu-2}e^{i\pi(\mu/2-3/4)}\xi^{\mu+1/2}x_R^{2\mu+1}\frac{\Gamma(-\mu+1/2)\Gamma(\mu)\Gamma(-\mu-1/2)}{\Gamma(\mu+1/2)\Gamma(-\mu-1)\Gamma(\mu+3/2)}$$
$$\times\left\{1+\pi\frac{B}{A}\cot(\pi\mu)\right\}=1. \tag{4.20}$$

In order to justify the method of asymptotic matching used above, we must require the inequalities, $|\xi|^{1/2} \ll |x_R|^{-1}$ and $|\xi|^{1/2} \ll |\eta|^{1/2}$, to hold. It is difficult to solve Eq.(4.20) analytically. However approximate results may be obtained in the weakly collisional limit $\nu \ll 1$. In this case we may assume $|x_R^2| \ll 1$ and therefore $|\mu| \ll 1$ from Eq.(4.15), which gives

$$\mu \simeq -ix_R^2\eta. \tag{4.21}$$

We focus on the even mode for which we find from Eq.(4.16) and $|\mu| \ll 1$

$$\frac{B}{A} \simeq \frac{2i}{\pi}. \tag{4.22}$$

Substituting this into Eq.(4.20) we obtain approximately the dispersion relation

$$\xi^{1/2} = \frac{\pi}{2}e^{i3\pi/4}x_R\eta \tag{4.23}$$

where x_R, ξ and η were defined in Eqs.(4.6)–(4.8) and we assumed $\mathrm{Real}\xi^{1/2} > 0$ and $-\pi/4 < \arg x_R < 3\pi/4$. We also assumed

$$|\xi| \ll |\eta| \ll |x_R|^{-2}. \tag{4.24}$$

Equation (4.23) reduces to the algebraic equation of the fourth degree in ω. In the limit $\nu \to +0$, the solution to Eq.(4.23) is written as

$$\omega = \omega_g + i\frac{\pi^2}{4}\frac{\nu}{k_\parallel'^2}\frac{\omega_g(\omega_{*e}-\omega_g)^2}{\omega_{*e}-\omega_g(2+k_\theta^2)}. \tag{4.25}$$

It is noted that $\xi \propto \nu^0$, $\eta \propto \nu^{-1}$ and $|x_R|^{-2} \propto \nu^{-2}$ in this limit, which is consistent with Eq.(4.24). Since we may assume $\omega_{*e} > \omega_g(2+k_\theta^2)$ for geometrical parameters and expeimental parameters of Heliotron E[9] under

$k_\theta \leq 1$, localized unstable modes are predicted from Eq.(4.25). We find from Eqs.(4.3) and (4.25) that the ratio of the amplitude of the density perturbation to that of the electrostatic potential is proportional to ν^{-1} and the phase difference between them approaches to $\pi/2$ at the mode resonant surface.

The reason why the localized modes exist is because the average magnetic curvature causes the narrow and deep potential well around the mode resonant surface in Eq.(4.5), which is approximated in the inner region $|x| \ll |x_R||\eta/\xi|^{1/2}$ as

$$U \simeq \frac{-ix_R^2\eta}{x^2 - ix_R^2} \simeq \pi e^{-i\pi/4} x_R \eta \delta(x) \tag{4.26}$$

where $-\pi/4 < \arg x_R < 3\pi/4$ is used. It is shown by Eqs.(4.8) and (4.25) that the absolute value of η can be large for small ν if $\omega_g \neq 0$. Assuming that the eigenfunction ϕ is constant in the inner region we find that the potential well of Eq.(4.26) yields the jump in the logarithmic derivative of the eigenfunction across the inner region and its value is given by $\pi e^{-i\pi/4} x_R \eta$. In the outer region $|x| \gg |x_R||\eta/\xi|^{1/2}$ we have the eigenfunction as $\phi \propto e^{\pm\xi^{1/2}x}$ and the jump of the logarithmic derivative as $-2\xi^{1/2}$ where $\mathrm{Real}\xi^{1/2} > 0$ is assumed. Equating the above two values we obtain the same result as Eq.(4.23).

4.3 Numerical Results

In order to check the analytic expressions for the growth rates obtained in Sec.4.2, the eigenmode equation (4.4) was numerically solved in the cylindrical geometry. We used the shooting method to obtain the eigenvalue $\omega = \omega_r + i\omega_i$ and the eigenfunction ϕ in the same way as in Sec.3.3. The results of the shooting method were also checked with those obtained by solving the time evolution of the linearized versions of Eqs.(4.1) and (4.2). We employed the boundary condition that $\phi = 0$ at the surface of the plasma $r = a$. It was found from the numerical results that in the weakly collisional limit $\nu \ll 1$ the eigenfunction is localized around the mode resonant surface therefore both the eigenvalue and eigenfunction are insensitive to the boundary conditions at $r = 0$ and $r = a$ and the slab model gives a reasonable approximation to derive the dispersion relation. In the numerical calculation the same magnetic configuration as in Sec.3.3 was used. We assumed $\rho_s/a = 1/50$ and the background density of the form $n(0)\exp(-2r^2)$. This density profile is chosen to keep ω_{*e} independent of r, but we found that the profile does not affect the mumerical results for the sharply localized mode in the weakly collisional case. From these parameters we estimate $\omega_g/\omega_{*e} = O(\epsilon)$. Figure 4.1 shows plots of the both numerically and analytically obtained eigenvalues ω/ω_{ci} versus the collision frequency $\nu_{e\|}/\omega_{ce}$ for the $m = 1/n = 1$ mode. It is seen that the analytical results agree with those obtained by the shooting method especially in the dependence of ω_r and ω_i on $\nu_{e\|}$. The magnitude of ω_r is of the same order as that of ω_i and it lies between ω_g and ω_{*e} in the case of $\nu_{e\|}/\omega_{ce} \sim 10^{-4}$ or 10^{-5} which is the typical value for the peripheral plasma of Heliotron E ECRH experiments where the electron density is $n_0 \leq 10^{13}cm^{-3}$, the electron temperature $T_e \sim 10eV$ and the strength of the magnetic field $B \sim 2T$. The contours and the profiles of the electostatic potential ϕ and density perturbation n obtained numerically for the $m = 1/n = 1$ mode at $\nu_{e\|}/\omega_{ce} = 10^{-4}$ are given in Fig.4.2. We find that the eigenfunctions are localized around the mode resonant surface r=0.61a as expected in the analysis in Sec.4.2 and that the phase difference between n and ϕ is about $\pi/4$.

4.4 Conclusions

We have studied the linear stability of an inhomogeneous collisional plasma in a magnetic field with curvature and shear against low frequency electrostatic perturbations. The analysis using the slab approximation predicted the existence of the radially localized instability, which was confirmed by the numerical calculation in the cylindrical geometry. It was found that in the weakly collisional limit $\nu_{e\|}/\omega_{ce} \ll 1$, the linear growth rate $\gamma = \omega_i$ is proportional to the collision frequency $\nu_{e\|}$, the eigenfrequency ω_r is of the order of the curvature drift frequency ω_g which is smaller than the electron diamagnetic drift frequency by a factor of $\epsilon = a/R_0$ and the phase difference between the electrostatic potential ϕ and the density fluctuation n approaches to $\pi/2$ at the mode resonant surface.

For example, if we consider the peripheral plasma in Heliotron E and take $\nu_{e\|}/\omega_{ce} \sim 10^{-4}$ or 10^{-5}, then we have the eigenfrequency in the region $\omega_g < \omega_r \sim \omega_i < \omega_{*e}$ and the phase difference lies around $\pi/4$. These results form a striking contrast to those of the MHD resistive interchange mode with $\omega_r = 0$, $\omega_i \propto \nu_{e\|}^{1/3}$ and the phase difference being constantly $\pi/2$.

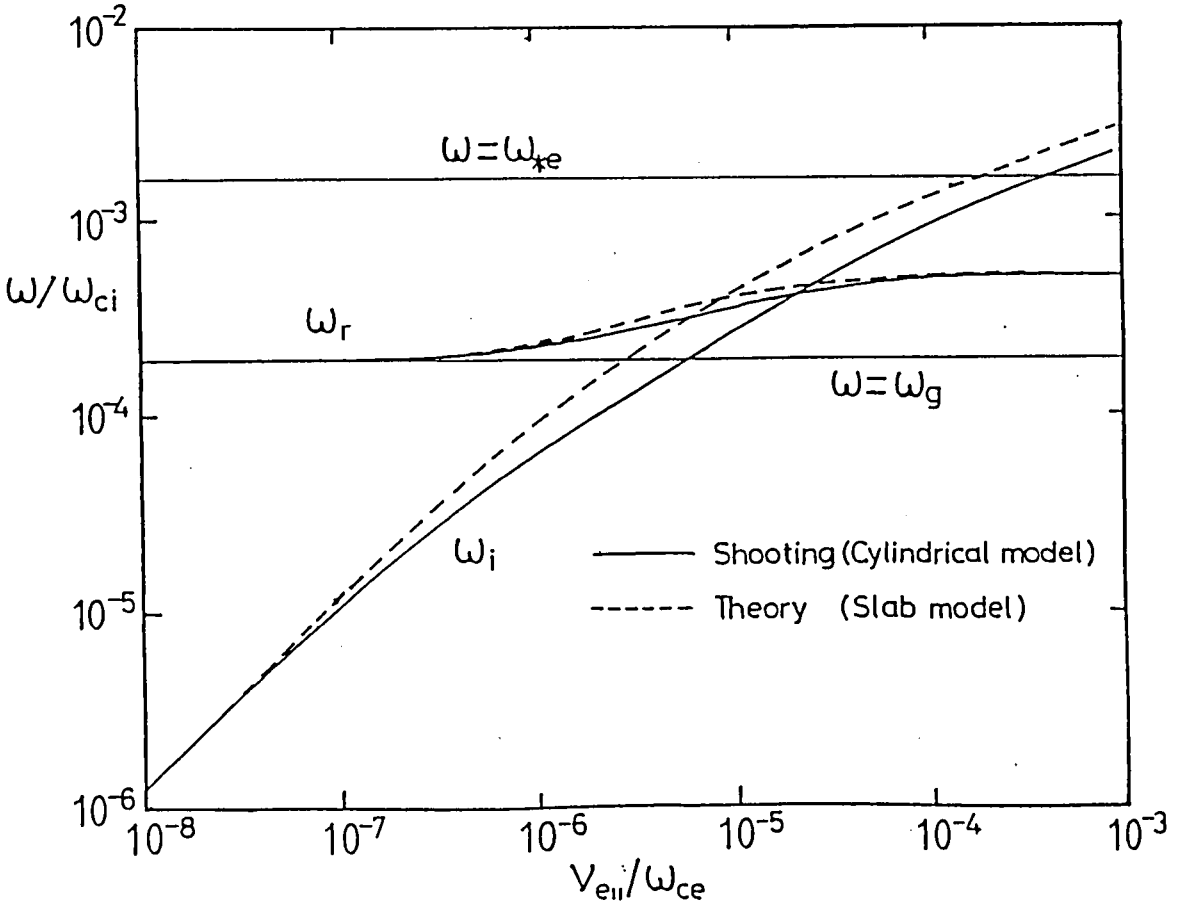

Figure 4.1: Real and imaginary parts of the eigenvalue ω/ω_{ci} versus collisional frequency $\nu_{e\|}/\omega_{ce}$ for the $m = 1/n = 1$ mode. The solid lines are obtained by the shooting method for a cylindrical configuration and dashed lines are given by Eq.(4.23).

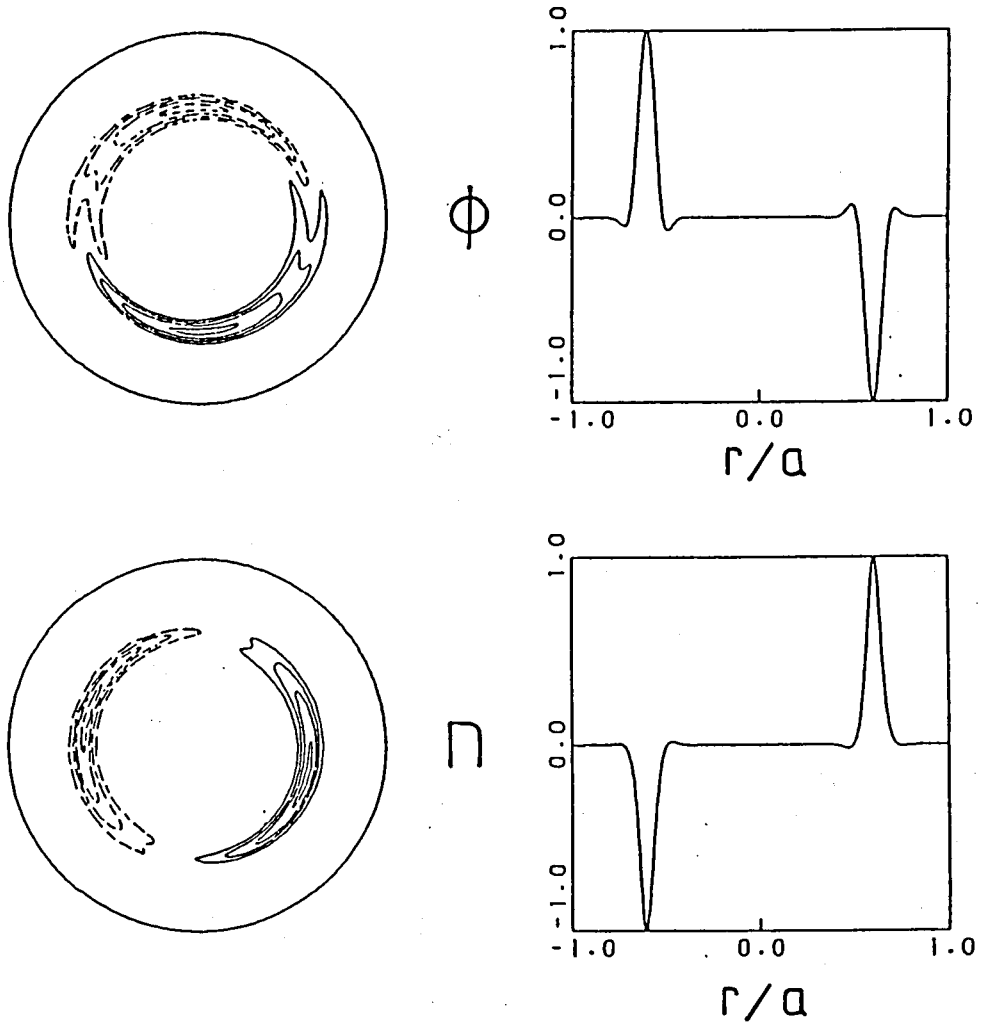

Figure 4.2: Contours and profiles of the eigenfunction ϕ and n of the $m = 1/n = 1$ mode for $\nu_{e\|}/\omega_{ce} = 10^{-4}$. Dashed lines denote the contours with negative values.

Chapter 5

Nonlinear Evolution of Interchange Instabilities

5.1 Introduction

In this chapter we study numerically the nonlinear evolution of the two types of instabilities described in Chapter 3 and Chapter 4, where linear properties are discussed.

In Chapter 3 we explained that the linear growth rate of the ideal interchange mode is reduced by including the ion diamagnetic drift. Here we investigate how the nonlinear evolution of the unstable mode changes by including the ion diamagnetic drift term in Sec.5.2. Especially our concern is in its effects on the saturation level of the fluctuation. We use single-helicity assumption or consider only higher harmonics produced by the mode coupling.

In Sec.5.3 we show the numerical results of the electrostatic turbulence caused by the resistive interchange modes coupled to the resistive drift waves, the linear stability of which is analyzed in Chapter 4. This type of turbulence may occur in stellarator/heliotron plasmas and it might be related to the anomalous transport observed in the edge plasma of Heliotron E.[9] As a model for the electrostatic turbulence, we use the Hasegawa-Wakatani equations including the electron diamagnetic drift and the average magnetic curvature terms.

Finally conclusions are given in Sec.5.4.

5.2 Nonlinear Evolution of the Ideal Interchange Mode

In Chapter 3 linear structures of the ideal interchange modes were investigated. In order to examine nonlinear evolution of the unstable interchange mode, we assume that initially only the $m = 1/n = 1$ mode is excited since the stabilization of the ion diamagnetic drift is the weakest for this mode. We can include only the single helicity modes with helical symmetry in a cylindrical plasma and follow the nonlinear evolution of them consistently. First it grows exponentially with the linear growth rate and the higher harmonics of $(m, n) = (2, 2), (3, 3), \cdots$ will be excited through the nonlinear beating between the modes with finite amplitude. In addition we include $(0, 0)$−mode which corresponds to the quasilinear effect in the real space. Here Eqs.(3.1)-(3.3) are numerically solved by using finite difference scheme and Fourier expansions. The ideal MHD case $\alpha = 0$ and the case of $\alpha = 0.5$ are particularly examined. In the numerical calculation, ϕ, A and p are Fourier-expanded with respect to the variables θ and z such as $\phi = \Sigma_{m,n}\phi_{mn}\exp[i(m\theta - nz/R_0)]$. Finite differences are used in the radial variable r. The potential ϕ_{mn} can be obtained from the vorticity $(\nabla_\perp^2\phi)_{mn}$ by the numerical integration using the recursive procedure. A predictor-corrector method is used in the time evolution of the system. Since we consider a cylindrical plasma surrounded by the perfectly conducting wall, we use the fixed bounary conditions that $\phi = A = p = 0$ at $r = a$. We give initial perturbation only to $m = 1/n = 1$ mode. Fourier modes with $m \leq 7$ are included.

Figures 5.1 and 5.2 show the time evolution of the total kinetic energy and the energy of each mode for $\alpha = 0$ and $\alpha = 0.5$ respectively. Here we used the rotational transform $\iota = 0.51 + 1.69(r/a)^{2.5}$ and the pressure profile $p(r) = p(0)(1 - (r/a)^2)^2$ with $\beta(0) = 5.5\%$ for equilibrium. In the case of Fig.5.2, modes with $m \geq 2$ are linearly stable by the ion diamagnetic drift effect as discussed in Chapter 3. We see that after the linear growth phase, the fundamental mode and the other higher harmonics saturate at $t \sim 40(R_0/v_A)$ for $\alpha = 0$ and at $t \sim 60(R_0/v_A)$ for $\alpha = 0.5$. Fig.5.3 shows the kinetic energy spectrum versus the harmonic mode number in the saturation state. We note that there is no kinetic energy of $m = 0/n = 0$ mode for $\alpha = 0$ because of parity conservation in RMHD model (see Appendix 7.A). It is shown that

by including the ion diamagnetic drift the saturated kinetic energy level is lowered down to about 30% and the contributions from the higher harmonic modes to the total kinetic energy are decreased. This may be explained by the stabilizing effect of the ion diamagnetic drift, which is stronger for higher mode numbers as seen from the linear dispersion relation (3.33) in Chapter 3. Figures 5.4 and 5.5 show the contours and the profiles of the electrostatic potential ϕ and the pressure p in the saturation state for $\alpha = 0$ and $\alpha = 0.5$, respectively. We find from both figures that the saturation occurs when the pressure gradient around the mode resonant surface at $\iota = 1$ almost vanishes, which implies reduction of the source of the interchange instability.

5.3 Nonlinear Evolution of the Resistive Interchange Mode Coupled to the Electron Diamagnetic Drift

Here we study the electrostatic turbulence driven by the resistive interchange modes coupled to the electron diamagnetic drift based on the numerical calculations of the Hasegawa-Wakatani equations (4.1) and (4.2). This may be the model for the turbulence in the peripheral region of a stellarator/heliotron plasma. From Eqs.(4.1) adn (4.2) we have the equation of the energy balance

$$\frac{d}{dt}\int d^3x \left(\frac{|\nabla_\perp \phi|^2}{2} + \frac{n^2}{2}\right) = \int d^3x \left(n\nabla\phi \times \hat{z}\cdot\nabla\bar{n} - \frac{1}{\nu}|\nabla_\parallel(n-\phi)|^2\right) \quad (5.1)$$

where the contributions from the surface integral are neglected by assuming the fixed boundary. The first and second terms of the integrand in the right-hand side denote the energy source from the density gradient and the sink due to the Ohmic dissipation, respectively. In the stationary turbulent state these two terms are balanced on the average.

In the numerical calculation the same methods as in Sec.5.2 are used. Assuming the cylindrical plasma surrounded by the perfectly conducting wall, we employ the fixed boundary conditions that $\phi = n = 0$ at the surface $r = a$. The rotational transform is given by $\iota(r) = 0.51 + 0.39(r/a)^2$ which simulate the inner core of Heliotron E. The mode number is selected within $|m| < 20$ and $|n| < 10$ which has its resonant surface between $\iota = 0.5$ and $\iota = 0.9$. The total mode number is 111 including $m = 0/n = 0$ mode. In order to maintain the constant background density gradient as an energy source and avoid the quasilinear flattening of the density, the $m = 0/n = 0$ component of the density fluctuation n_{00} is kept zero. The viscosity $\mu\nabla_\perp^4\phi$ and the diffusion $D_\perp\nabla_\perp^2 n$ are introduced in the right-handes of Eqs.(4.1) and (4.2), respectively, to assure damping for high m modes, which is required for the realization of the stationary turbulence. The parameters used in the calculations are $\rho_s/a = 1/40$, $\epsilon = a/R_0 = 1/13$, $\nu = \nu_{e\parallel}/\omega_{ce} = 1/(7.5\times 10^3)$, $D_\perp = 5\times 10^{-4}$ and $\mu = 5\times 10^{-4}$. Here $D_\perp$ and μ suppress higher modes of $m \geq 12 \sim 15$. The magnetic flux ψ_0 and the curvature term Ω are calculated in the same way as in Chapter 4. Initial small perturbations are given to

$m = 2/n = 1$ and $m = 3/n = 2$ modes since these two modes are dominant low m mode instabilities in the assumed model configuration.

Figure 5.6 shows the time evolution of the total kinetic energy and the energies of $m = 0/n = 0$, $m = 2/n = 1$ and $m = 3/n = 2$ modes. The latter two modes are shown to demonstrate nonlinear behaviors. The $m = 0/n = 0$ mode also saturates after the nonzero odes do. Figure 5.7 shows the wave energy spectrum versus the poloidal mode number,m, integrated over the toroidal mode number, n for $T = 5$ and $T = 6$. Both spectra show that an almost stationary state is achieved though a small variation still exists. After the saturation the $m = 0$ mode becomes dominant, indicating the condensation of the mode enrgy to $m = 0$. The saturated kinetic energy levels for $m = 1$ to $m \simeq 12 \sim 13$ are comparable while those with higher modes share less energy. Figure 5.8 shows the time evolution of the contours of the electrostatic potential. The most interesting result is that the equi-potential surface is closed around the magnetic axis near the $\phi \simeq 0$ region. This is clearly seen in Fig.5.9, where the radial profile of the dominant mode ϕ_{00} is shown. A positive electric field is obtained in $0.2 \leq r/a \leq 0.8$. The energy transfer to the $m = 0$ mode and the generation of the stationary radial electric field by the $\phi_{00}(r)$ potential observed in our calculations are not seen in those of Carreras et al.[25] based on the RMHD model since the RMHD equations conserve the parity (see Appendix 7.A). The decrease of the energy distributed over the high poloidal mode numbers due to the energy condensation to the $m = 0$ mode is expected to improve the particle confinement.

5.4 Conclusions

We have studied the nonlinear evolution of the ideal and resistive interchange modes, including the effects of the ion and electron diamagnetic drifts, respectively. The single-helicity nonlinear calculations showed that the ion diamagnetic drift lowers the saturation level of the ideal interchange modes and decreases the contributions from the higher harmonic modes to the total kinetic energy. This is consistent with the linear dispersion relation in Chapter 3 which states that the stabilizing effect of the ion diamagnetic drift is stronger for higher mode numbers. We also see that the saturation is related to the flattening of the pressure profile around the mode resonant surface.

By the multi-helicity nonlinear calculations using the Hasegawa-Wakatani equations, we find that in the saturation state the $m = 0$ mode becomes dominant and the stationary electrostatic potential $\phi_{00}(r)$ is generated. This result predicts a zonal flow in the edge plasma region. The decrease of the energy distributed over the high poloidal mode numbers due to the energy condensation to the $m = 0$ mode is expected to improve the particle confinement. These results are not obtained by the RMHD.[25] The generation of the axisymmetric potential $\phi_{00}(r)$ based on the self-organization process has been discussed by Hasegawa and Wakatani.[43] Another implication of our result is that the $\phi_{00}(r)$ potential produces a shear flow predominantly in the poloidal direction. There is a possibility that this shear flow produces the secondary instability and makes the characteristics of the turbulence more complex.

Here we studied global properties of turbulent plasma by using a realistic cylindrical plasma model. There is a microscopic point of view relating to the anomalous transport due to the electrostatic turbulence. We will present the theoretical analyses of the electrostatic turbulence in Chapter 7 based on the renormalized theories formulated in Chapter 6.

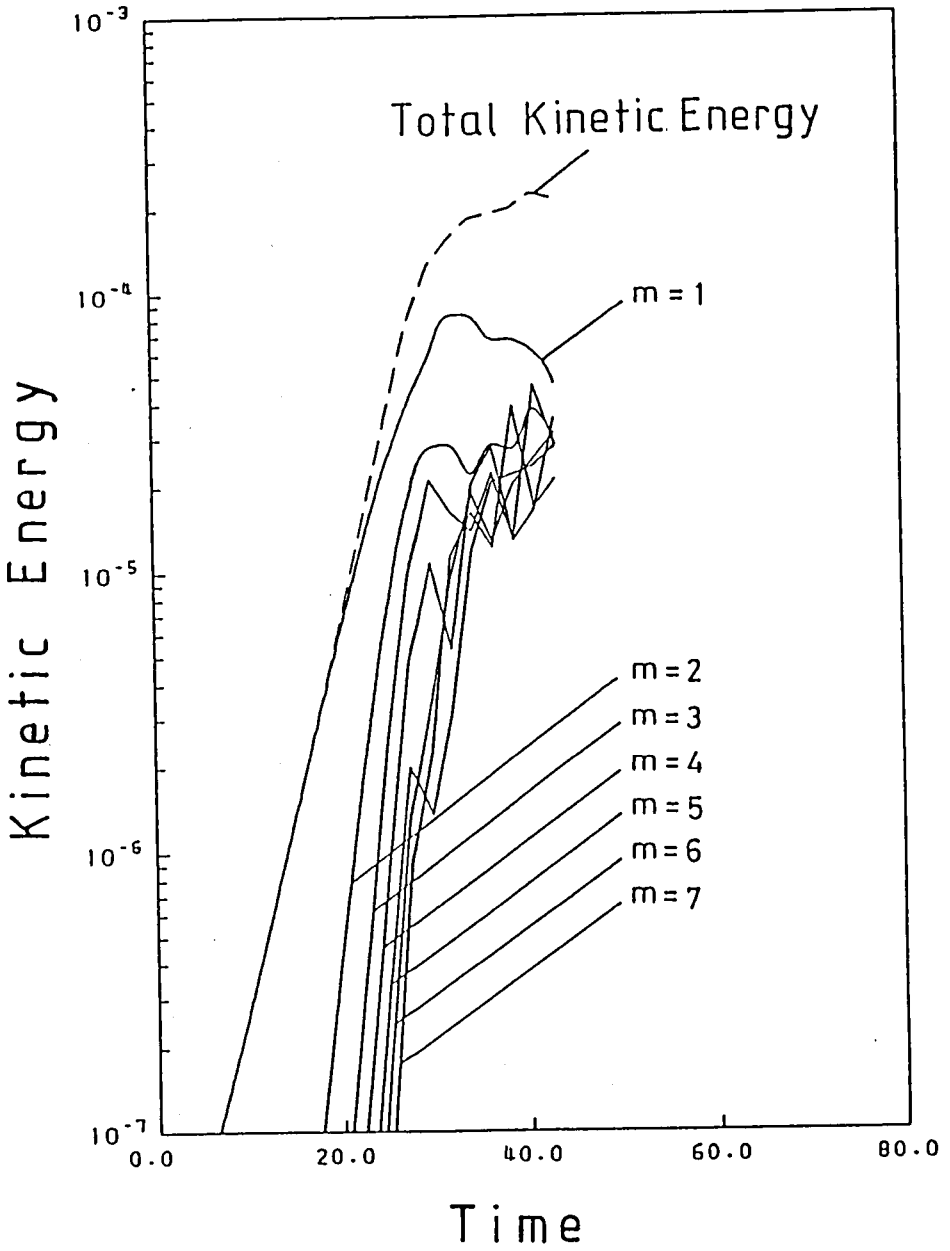

Figure 5.1: Time evolution of kinetic energy of the nonlinear $m = 1/n = 1$ mode in the case of $\alpha = c/a\omega_{pi} = 0$.

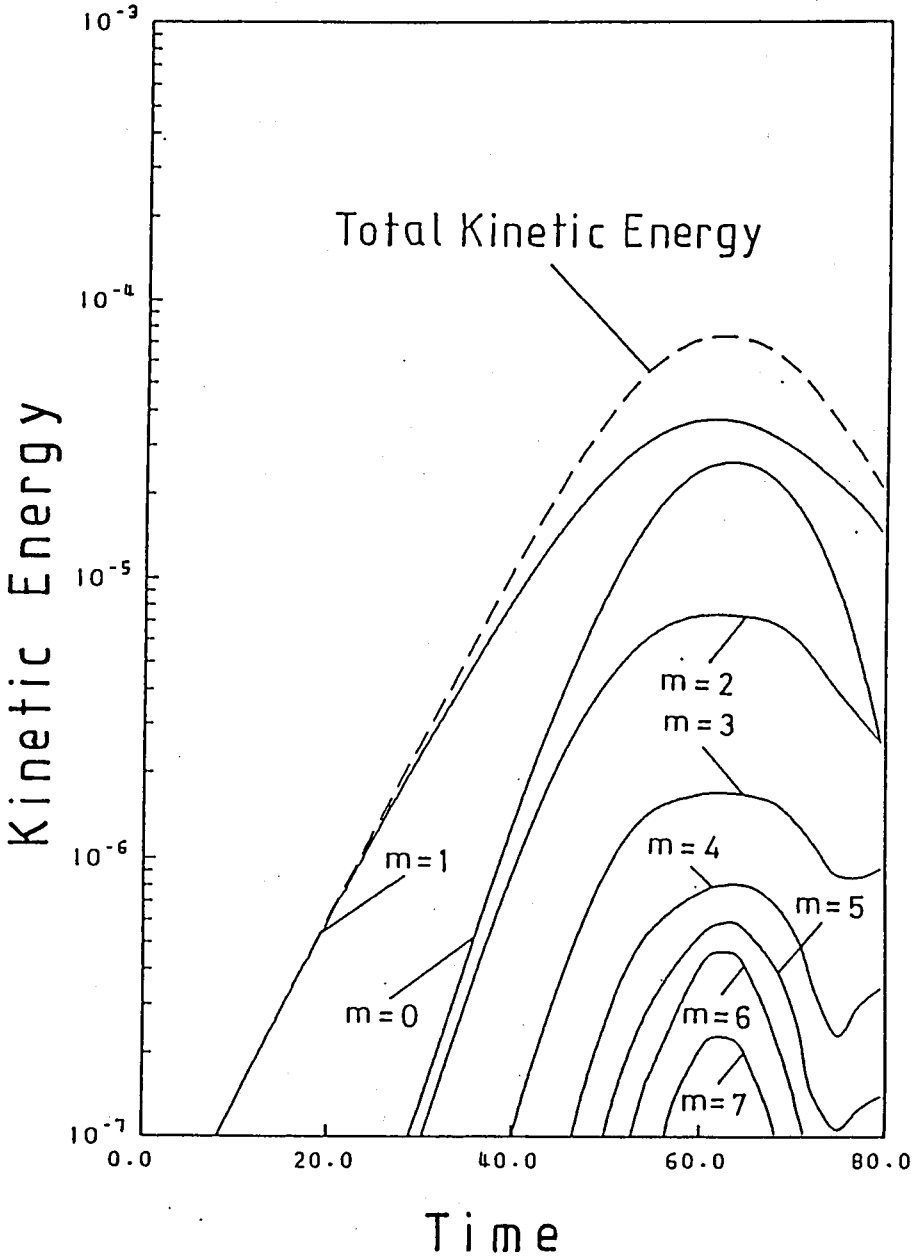

Figure 5.2: Time evolution of kinetic energy of the nonlinear $m = 1/n = 1$ mode in the case of $\alpha = c/a\omega_{pi} = 0.5$.

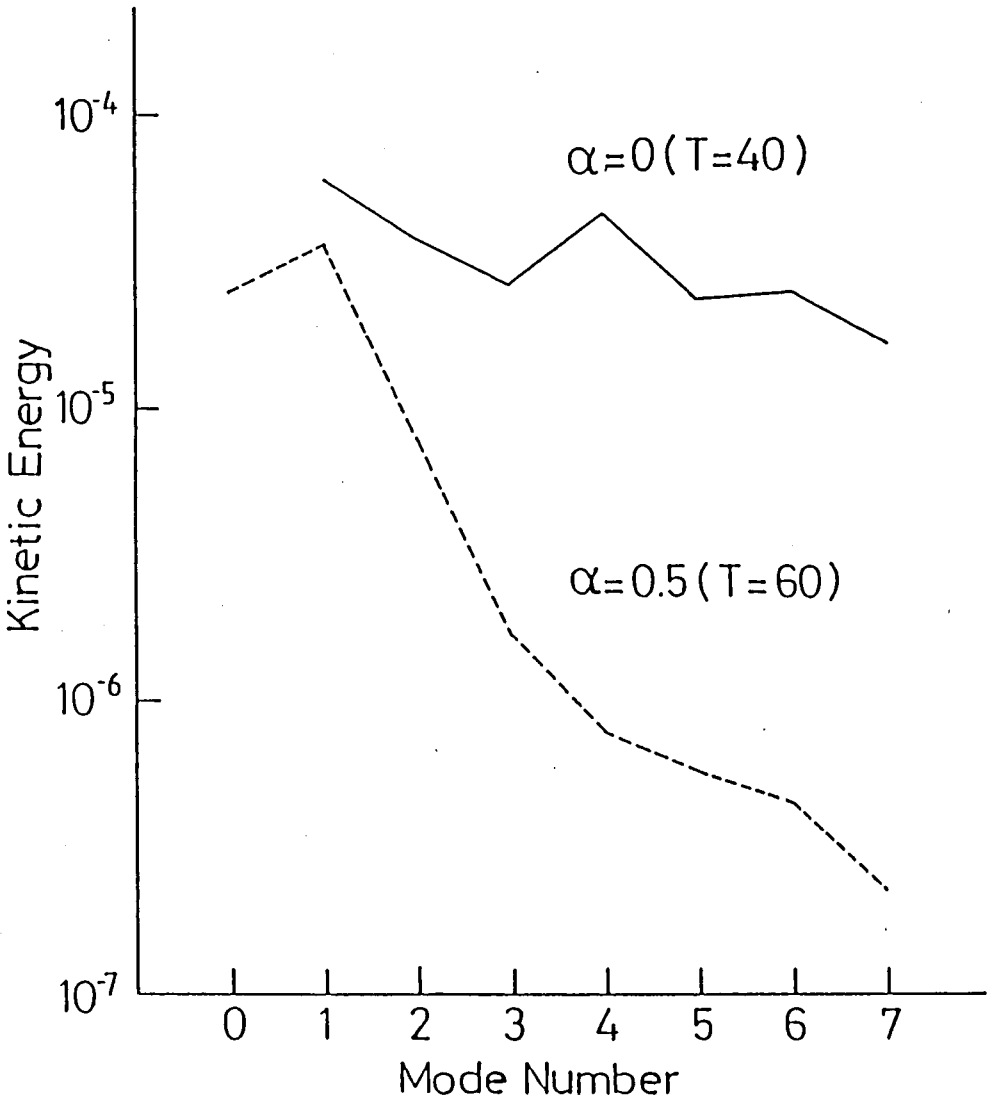

Figure 5.3: Kinetic energy spectrum versus harmonic poloidal mode number at the saturation state.

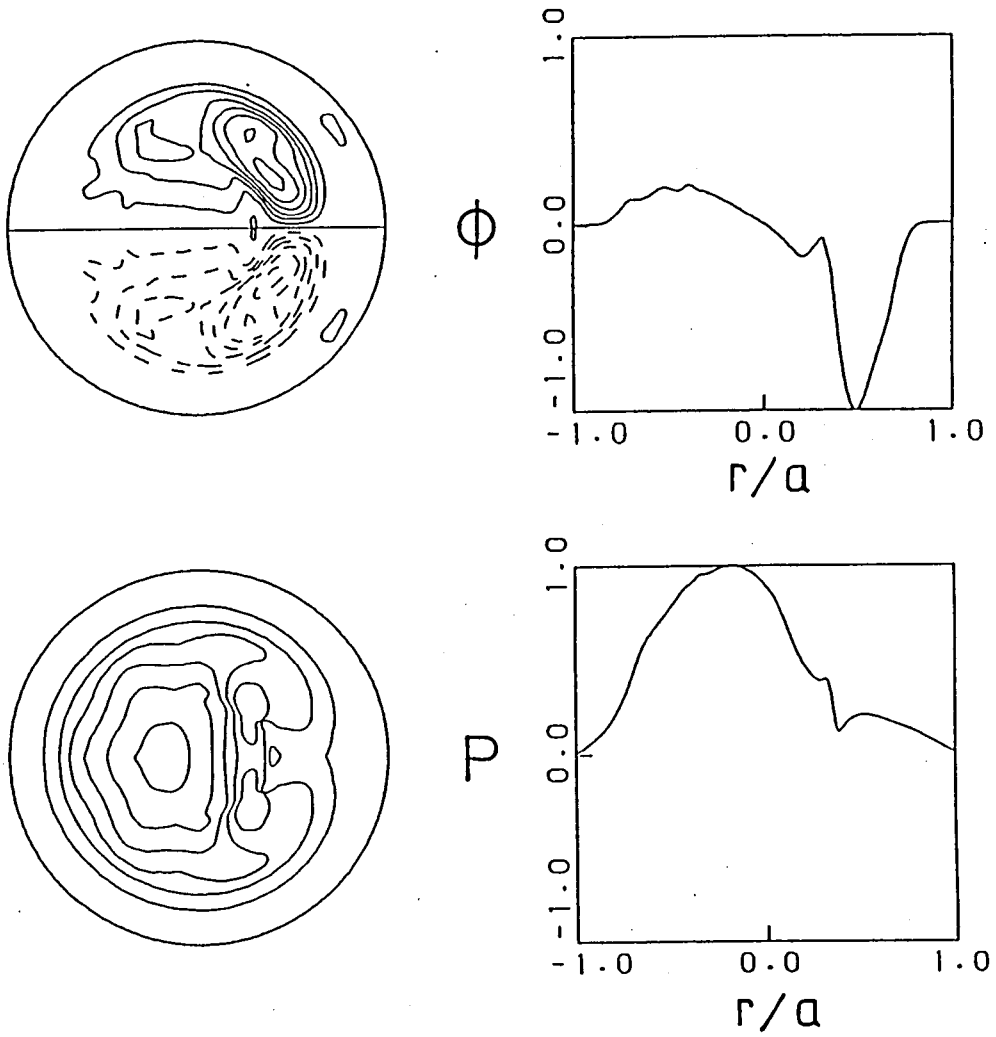

Figure 5.4: Contours and radial profiles of electrostatic potential ϕ and pressure p just after the saturation in the case of $\alpha = 0$. Dashed lines denote the contours with negative values.

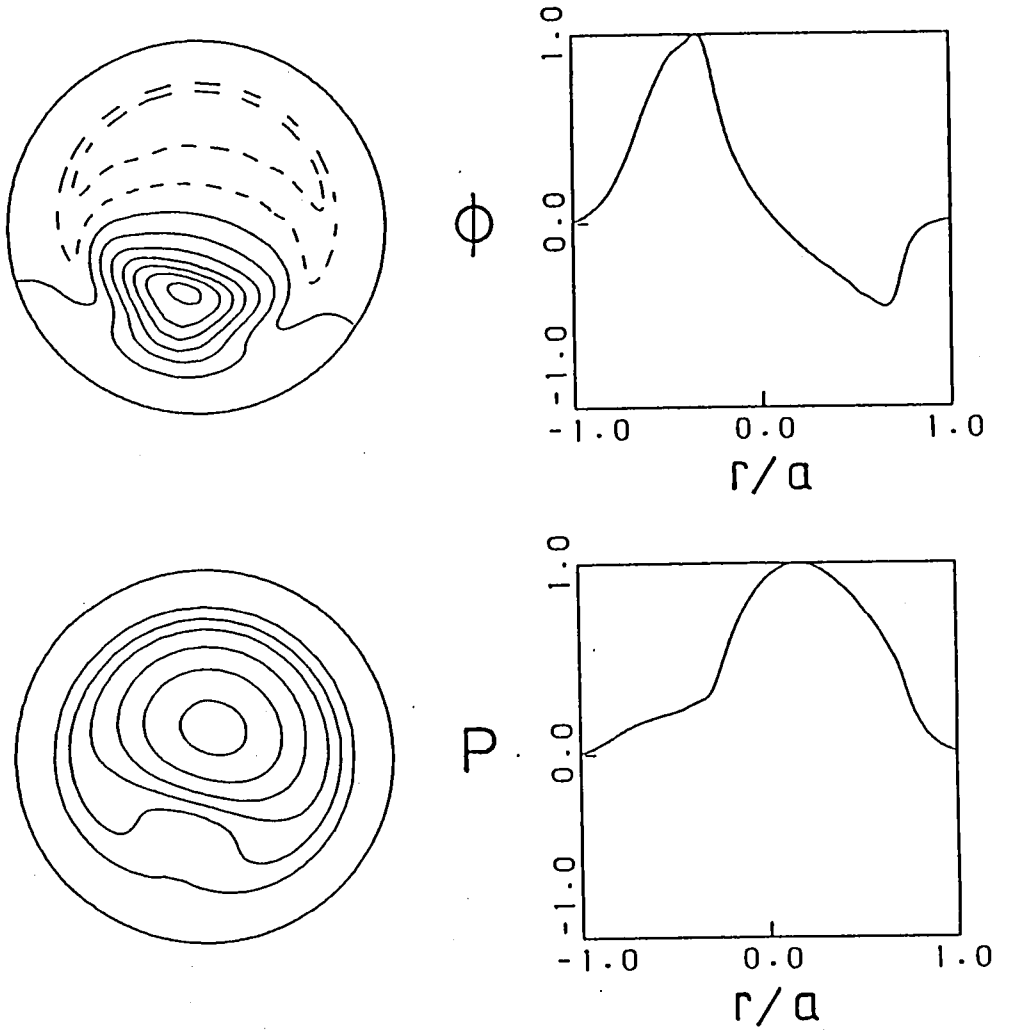

Figure 5.5: Contours and radial profiles of electrostatic potential ϕ and pressure p just after the saturation in the case of $\alpha = 0.5$. Dashed lines denote the contours with negative values.

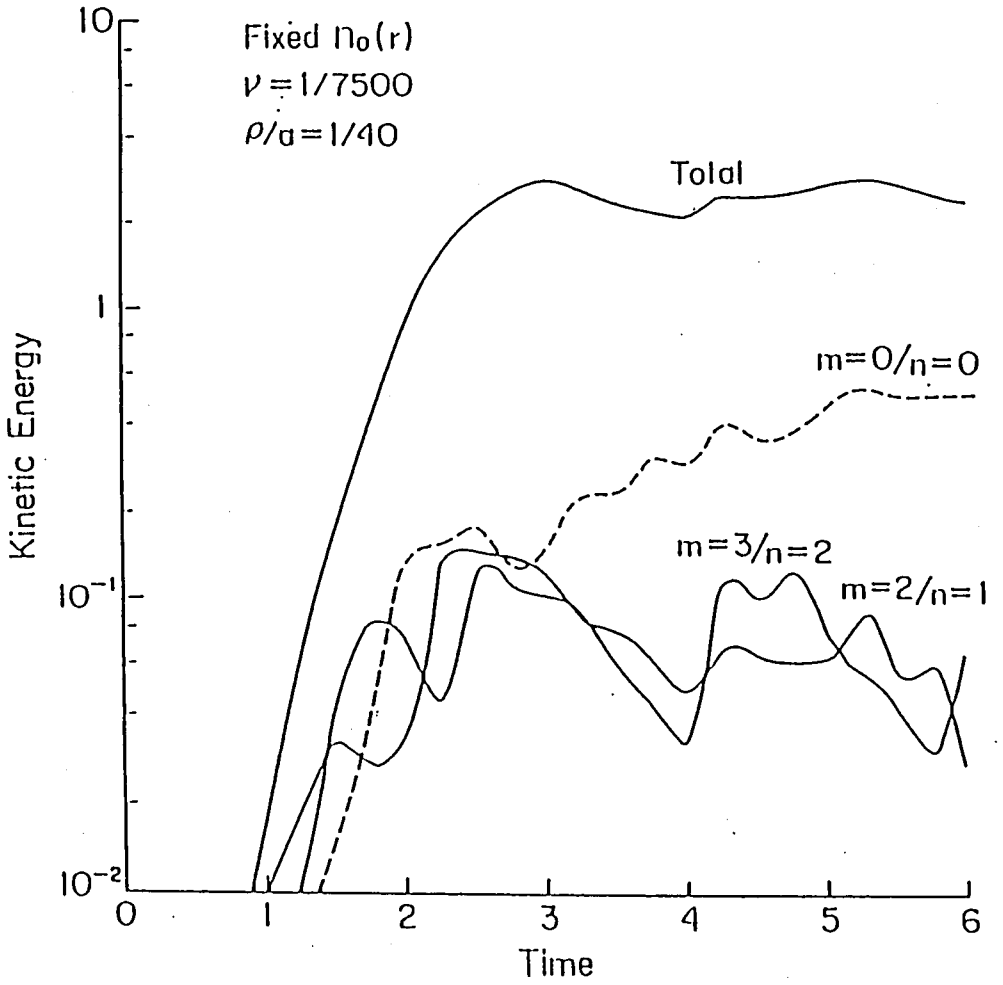

Figure 5.6: Time evolution of total kinetic energy, $m = 2/n = 1$, $m = 3/n = 2$ and $m = 0/n = 0$ modes.

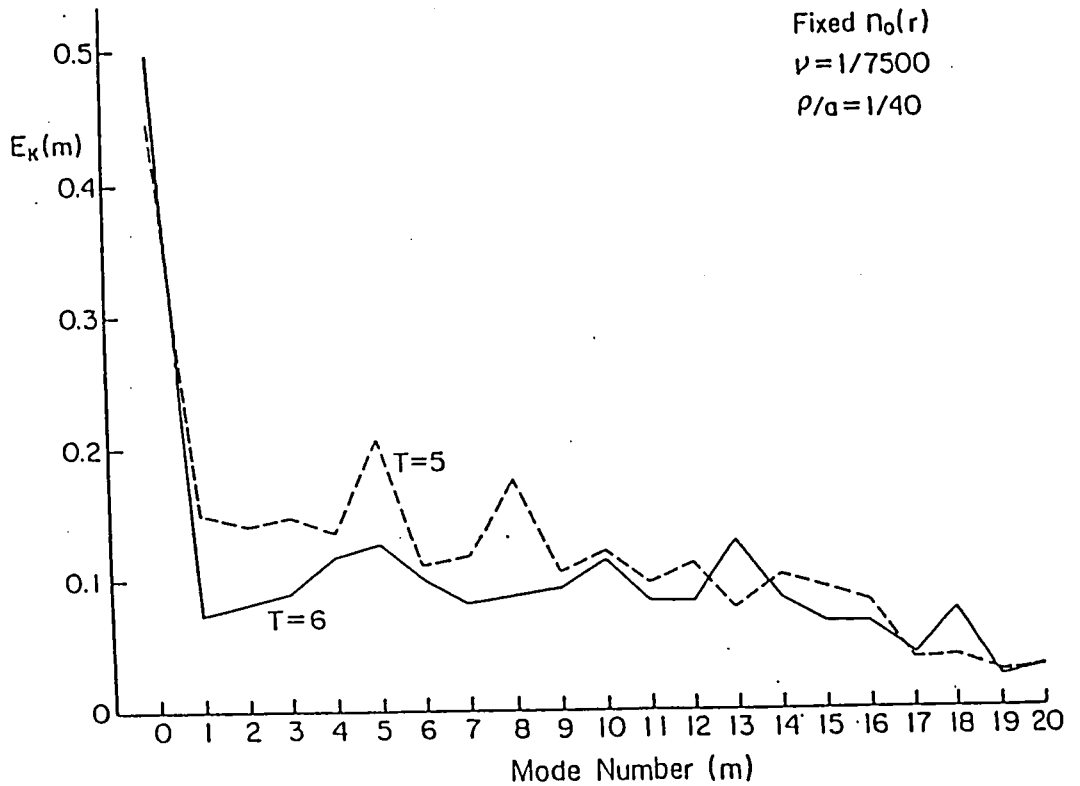

Figure 5.7: Kinetic energy spectrum of $\sum_n \int d^3x |\nabla_\perp \phi_{mn}|^2$ versus poloidal mode number m.

Figure 5.8: Time evolution of electrostatic potential contours. At $T = 4.5$ and $T = 6$, electrostatic potential contours surrounding the axis are seen. In order to clarify $\phi = 0$ contour, intervals between contours at $\phi \sim 0$ are made narrow.

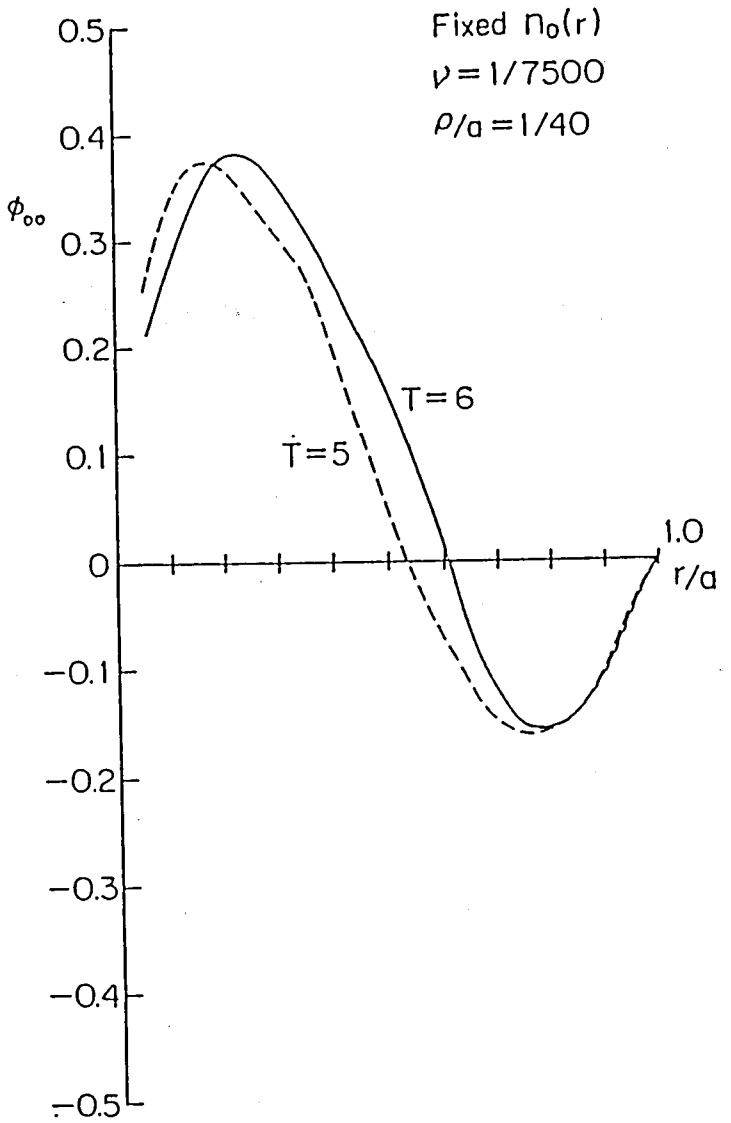

Figure 5.9: Radial profile of ϕ_{00}. Positive electric field region appears for $0.2 < r/a < 0.8$.

Chapter 6

Formulation of Renormalized Theories

6.1 Introduction

In experiments of magnetically confined plasmas, particle and energy transports usually exceed estimations based on Coulomb collisions or the neoclassical transport theory. An typical example is so-called anomalous transport in tokamaks.[6] In order to understand mechanism of anomalous transport, many theoretical efforts were directed to study linear stability of microscopic instabilities, in particular drift waves, and resultant enhanced diffusion based on the quasilinear theory. Recently it is recognized that this approach is not successful to explain the anomalous transport, since characteristics of the obsreved fluctuations are similar to the strong turbulence in neutral fluids.[6]

Several approaches are pursued to develop turbulent transport theory during these ten years. Mixing length argument[23] is used widely to evaluate the magnitude of transport coefficient, which is based on the linear eigenmode analysis of instability. Connor and Taylor[10],[11],[14] introduced scale invariance theory to derive parametric dependence of anomalous transport. Yagi et al.[13] discussed inter-relation between the mixing length argument and the scale invariance theory. However, both theories have a lack of quantitative evaluation or it is difficult to determine absolute magnitude of turbulent transport.

Another approach to overcome this point is renormalized theory, which was developed by Dupree[15]-[18] and Diamond et al.[20]-[25] In this theory, original equations in real space are Fourier transformed into those in wavenumber space and nonlinear terms are renormalized by iteratively substituting the field driven by the direct beating of the test wave ($\boldsymbol{k}$) and background wave ($\boldsymbol{k}'$) into the wave field with $\boldsymbol{k}'' = \boldsymbol{k}+\boldsymbol{k}'$. To make a closure of the nonlinearly driven fields, Diamond et al. have used the semi-quantitative correlation time corresponding to the nonlinear propagator.

In this chapter we present a new formulation of the renormalized theory applicable to both fluid model equation with convective nonlinearity and the Vlasov equation. Our formulation has a similarity to the renormalized theory by Dupree,[15] which treated phase space dynamics described by Vlasov-Poisson equations. It is based on the statistics of random phases between the Fourier modes of the initial electric field, and nonlinear propagator is expanded with respect to the electric field in the form appropriate for strong turbulence. Without using the wavenumber space, we derive a renormalized equation in the real space for a model nonlinear equation with characteristics associated with fluid descripton of plasma dynamics.

This chapter is organized as follows. In Sec.6.2 we formulate the renormalized theories for a general model equation. In Sec.6.2.1 we show the model equation and give the one-point renormalized theory. In Sec.6.2.2 the two-point renormalized theory is presented. In Sec.6.2.3 we discuss the clump lifetime approximation for the solution of the two-point renormalized equation. In Sec.6.3 we apply the renormalized theories to the Vlasov equation and show that the results obtained by Dupree are reproduced by our formulation. Finally conclusions are given in Sec.6.4.

6.2 Formulation of Renormalized Theories

6.2.1 One-point renormalized theory

For explanation of one-point renormalization, we consider the following equation:

$$\left(\frac{\partial}{\partial t} + \boldsymbol{v}(\boldsymbol{x},t)\cdot\nabla + \alpha\right)\tilde{f}(\boldsymbol{x},t) = s(\boldsymbol{x},t). \tag{6.1}$$

Equation having the form (6.1) appears frequently in fluid models for plasma dynamics such as the MHD equations. Here, $\boldsymbol{v}(\boldsymbol{x},t)$ is a given random function which is stationary in time and $\tilde{f}(\boldsymbol{x},t)$ and $s(\boldsymbol{x},t)$ are also random functions. It is assumed that $\nabla\cdot\boldsymbol{v} = \langle\boldsymbol{v}\rangle = \langle\tilde{f}\rangle = 0$, where $\langle\cdot\rangle$ means statistical average. α denotes a time-independent nonrandom differential operator such that $\alpha c = 0$ where c is a constant. Equation (6.1) may also correspond to the Vlasov equation, which is discussed in detail in Sec.6.3. Under the initial condition, $\tilde{f}(t=t_0) = 0$, we obtain the solution to Eq.(6.1)

$$\begin{aligned}\tilde{f}(\boldsymbol{x},t) &= \int_{t_0}^{t} d\tau U(t,\tau)s(\boldsymbol{x},\tau) \\ &= \int_{t_0}^{t} d\tau \int d\boldsymbol{x}' g(t,\tau;\boldsymbol{x},\boldsymbol{x}')s(\boldsymbol{x}',\tau),\end{aligned} \tag{6.2}$$

where g is the Green's function or the kernel of the one-point propagator U defined as a random operator which satisfies the following equation:

$$\left(\frac{\partial}{\partial t} + \boldsymbol{v}(\boldsymbol{x},t)\cdot\nabla + \alpha\right)U(t,t_0) = 0, \tag{6.3}$$

with

$$U(t_0,t_0) = I. \tag{6.4}$$

Here I is an identity operator, which is expressed in terms of the Green's function as $g(t_0,t_0;\boldsymbol{x},\boldsymbol{x}') = \delta(\boldsymbol{x}-\boldsymbol{x}')$. Hereafter the space variable $\boldsymbol{x}$ is sometimes omitted for simplicity. Let us consider a random function, $F(\boldsymbol{x},t)$, which is defined by

$$F(t) = U(t,t_0)F(t_0). \tag{6.5}$$

From the definition of the one-point propagator U,

$$\left(\frac{\partial}{\partial t} + \boldsymbol{v}(t)\cdot\nabla + \alpha\right)F(t) = 0 \tag{6.6}$$

is obtained. Taking the statistical average of this equation yields

$$\left(\frac{\partial}{\partial t}+\alpha\right)\langle F(t)\rangle+\langle \boldsymbol{v}(t)\cdot\nabla F(t)\rangle=0. \tag{6.7}$$

We devide F into an average part, $\langle F\rangle$, and a deviation from it, $\tilde{F}$,

$$F=\langle F\rangle+\tilde{F}. \tag{6.8}$$

Substituting Eq.(6.8) into Eq.(6.6) and using Eq.(6.7), we obtain

$$\left(\frac{\partial}{\partial t}+\boldsymbol{v}(t)\cdot\nabla+\alpha\right)\tilde{F}(t)=-\boldsymbol{v}(t)\cdot\nabla\langle F(t)\rangle+\langle \boldsymbol{v}(t)\cdot\nabla F(t)\rangle. \tag{6.9}$$

The solution is given by

$$\begin{aligned}\tilde{F}(t) &= U(t,t_0)\tilde{F}(t_0)-\int_{t_0}^{t}d\tau U(t,\tau)\left(\boldsymbol{v}(\tau)\cdot\nabla\langle F(\tau)\rangle-\langle \boldsymbol{v}(\tau)\cdot\nabla F(\tau)\rangle\right)\\ &= -\int_{t_0}^{t}d\tau U(t,\tau)\left(\boldsymbol{v}(\tau)\cdot\nabla\langle U(\tau,t_0)\rangle-\langle \boldsymbol{v}(\tau)\cdot\nabla U(\tau,t_0)\rangle\right)F(t_0).\end{aligned} \tag{6.10}$$

Here, it is assumed that $F(t_0)$ is nonrandom and therefore $\tilde{F}(t_0)=0$. Inserting Eqs.(6.5) and (6.10) into Eq.(6.8) and eliminating $F(t_0)$, we obtain the following integral equation for the propagator U:

$$\begin{aligned}U(t,t_0) &= \langle U(t,t_0)\rangle\\ &\quad -\int_{t_0}^{t}d\tau U(t,\tau)\left(\boldsymbol{v}(\tau)\cdot\nabla\langle U(\tau,t_0)\rangle-\langle \boldsymbol{v}(\tau)\cdot\nabla U(\tau,t_0)\rangle\right).\end{aligned} \tag{6.11}$$

In order to solve Eq.(6.11), we use an iterative method which yields the expression of the propagator U appropriate for studying strong turbulence problems:

$$\begin{aligned}&U(t,t_0)\\ &= \langle U(t,t_0)\rangle-\int_{t_0}^{t}d\tau\langle U(t,\tau)\rangle\boldsymbol{v}(\tau)\cdot\nabla\langle U(\tau,t_0)\rangle\\ &\quad+\int_{t_0}^{t}d\tau\int_{\tau}^{t}d\tau'\langle U(t,\tau')\rangle\boldsymbol{v}(\tau')\cdot\nabla\langle U(\tau',\tau)\rangle\boldsymbol{v}(\tau)\cdot\nabla\langle U(\tau,t_0)\rangle\\ &\quad-\int_{t_0}^{t}d\tau\int_{t_0}^{\tau}d\tau'\langle U(t,\tau)\rangle\langle \boldsymbol{v}(\tau)\cdot\nabla\langle U(\tau,\tau')\rangle\boldsymbol{v}(\tau')\rangle\cdot\nabla\langle U(\tau',t_0)\rangle\\ &\quad+\cdots\cdots.\end{aligned} \tag{6.12}$$

When only the first-order term of the expansion series is retained, it is equivalent to the equation given by Dupree.[15] Since the random function $\boldsymbol{v}(t)$ is assumed stationary in time, we can write $\langle U(t,t_0)\rangle = \langle U(t-t_0)\rangle$. By truncating the expansion to the first-order,

$$U(t,t_0) = \langle U(t-t_0)\rangle - \int_0^{t-t_0} d\tau \langle U(\tau)\rangle \boldsymbol{v}(t-\tau)\cdot\nabla\langle U(t-t_0-\tau)\rangle \quad (6.13)$$

is found. If we assume that the integrand is nonzero only in a small time interval, $0 < \tau < \tau_{ac}$, where τ_{ac} denotes the autocorrelation time of $\boldsymbol{v}(t-\tau)$ and that $\nabla\langle U(t-t_0-\tau)\rangle$ does not change significantly during this interval,[15] we can use the following Markovian approximation,

$$U(t,t_0) = \langle U(t-t_0)\rangle - \left[\int_0^{\infty} d\tau \langle U(\tau)\rangle \boldsymbol{v}(t-\tau)\right]\cdot\nabla\langle U(t-t_0)\rangle. \quad (6.14)$$

Substituting this equation into Eq.(6.3) and averaging over the random variables, we obtain

$$\left(\frac{\partial}{\partial t} - \nabla\cdot\mathsf{D}\cdot\nabla + \alpha\right)\langle U(t-t_0)\rangle = 0, \quad (6.15)$$

where D represents turbulent diffusion tensor defined by

$$\mathsf{D} \equiv \int_0^{\infty} d\tau \underline{\langle U(\tau)\rangle}\langle \boldsymbol{v}(t)\underline{\boldsymbol{v}(t-\tau)}\rangle. \quad (6.16)$$

Here an arrow shows the operand of the averaged propagator $\langle U\rangle$. We note that D has the form of quasilinear diffusion tensor generalized into the case of strong turbulence. Equation (6.16) reduces to the quasilinear diffusion tensor if we replace the averaged propagator $\langle U\rangle$ by the linear propagator $U^{(l)}$ which is defined by

$$\left(\frac{\partial}{\partial t} + \alpha\right) U^{(l)}(t) = 0, \quad (6.17)$$

with

$$U^{(l)}(t=0) = I. \quad (6.18)$$

If we replace the propagator U by the averaged propagator $\langle U\rangle$ in Eq.(6.2) and set $t - t_0 \to \infty$, we have

$$\begin{aligned}\tilde{f}^c(t) &= \int_{t_0}^{t} d\tau \langle U(t-\tau)\rangle s(\tau) = \int_0^{t-t_0} d\tau \langle U(\tau)\rangle s(t-\tau) \\ &\simeq \int_0^{\infty} d\tau \langle U(\tau)\rangle s(t-\tau) \end{aligned} \quad (6.19)$$

which denotes the coherent part of $\tilde{f}$ and it is called the nonlinear coherent response to s. When $\langle U \rangle$ is replaced by $U^{(t)}$, $\tilde{f}^c$ reduces to a linear response. From Eqs.(6.15) and (6.19), we obtain

$$\left(\frac{\partial}{\partial t} - \nabla \cdot \mathsf{D} \cdot \nabla + \alpha\right) \tilde{f}^c(t) = s(t). \tag{6.20}$$

This is the one-point renormalized equation for Eq.(6.1).

Nonlinear convection term is renormalized in the turbulent diffusion term. Turbulent diffusion tensor D is given by Eqs.(6.15) and (6.16), which are represented in the real space.

In the one-point renormalized theory, a nonlinear dispersion relation[6],[15]–[17] is derivable by substituting the coherent response of (6.19) into other equations, e.g., Poisson equation, which is needed to close the system with Eq.(6.1). This dispersion relation shows that the frequency spectrum for a given wavenumber has the form of a delta function and only the mode having the largest growth rate survives damping due to the turbulent diffusion.

6.2.2 Two-point renormalized theory

We now consider the evolution of the two-point function, $\tilde{f}(1)\tilde{f}(2) \equiv \tilde{f}(\boldsymbol{x}_1, t)\tilde{f}(\boldsymbol{x}_2, t)$. Using Eq.(6.1), we obtain

$$\left(\frac{\partial}{\partial t} + \boldsymbol{v}(1) \cdot \nabla_1 + \boldsymbol{v}(2) \cdot \nabla_2 + \alpha(1) + \alpha(2)\right) \tilde{f}(1)\tilde{f}(2)$$
$$= \tilde{f}(1)s(2) + \tilde{f}(2)s(1) \equiv S(1,2) \tag{6.21}$$

With the initial condition, $\tilde{f}(t_0) = 0$, the solution to this equation is given by

$$\tilde{f}(1,t)\tilde{f}(2,t) = \int_{t_0}^{t} d\tau U(1,t,\tau)U(2,t,\tau)S(1,2,\tau), \tag{6.22}$$

where $U(1)$ and $U(2)$ are the one-point propagators already defined by Eqs.(6.3) and (6.4) and $U(1)U(2)$ represents the two-point propagator which satisfies

$$\left(\frac{\partial}{\partial t} + \boldsymbol{v}(1) \cdot \nabla_1 + \boldsymbol{v}(2) \cdot \nabla_2 + \alpha(1) + \alpha(2)\right) U(1,t,t_0)U(2,t,t_0) = 0, \tag{6.23}$$

with

$$U(1,t_0,t_0)U(2,t_0,t_0)=I. \tag{6.24}$$

Comparing Eqs.(6.23) and (6.24) with Eqs.(6.3) and (6.4), we find that they have similarities except the dimension of the space variables. Thus the formulation in Sec.2.1 is usable provided that the following relations are taken into accout:

$$\left.\begin{aligned}
&\boldsymbol{x}\to(\boldsymbol{x}_1,\boldsymbol{x}_2)\equiv(1,2),\\
&\nabla\to(\nabla_1,\nabla_2),\\
&\boldsymbol{v}(\boldsymbol{x})\to(\boldsymbol{v}(1),\boldsymbol{v}(2)),\\
&U\to U(1)U(2),\\
&\alpha(\boldsymbol{x})\to\alpha(1)+\alpha(2).
\end{aligned}\right\} \tag{6.25}$$

We obtain the integral equation for the two-point propagator $U(1)U(2)$ corresponding to Eqs.(6.11),

$$\begin{aligned}
&U(1,t,t_0)U(2,t,t_0)\\
&=\langle U(1,t,t_0)U(2,t,t_0)\rangle\\
&\quad-\int_{t_0}^{t}d\tau U(1,t,\tau)U(2,t,\tau)\\
&\qquad\times[(\boldsymbol{v}(1,\tau)\cdot\nabla_1+\boldsymbol{v}(2,\tau)\cdot\nabla_2)\langle U(1,\tau,t_0)U(2,\tau,t_0)\rangle\\
&\qquad-\langle(\boldsymbol{v}(1,\tau)\cdot\nabla_1+\boldsymbol{v}(2,\tau)\cdot\nabla_2)U(1,\tau,t_0)U(2,\tau,t_0)\rangle],
\end{aligned} \tag{6.26}$$

and the iterative scheme gives:

$$\begin{aligned}
&U(1,t,t_0)U(2,t,t_0)\\
&=\langle U(1,t,t_0)U(2,t,t_0)\rangle\\
&\quad-\int_{t_0}^{t}d\tau\langle U(1,t,\tau)U(2,t,\tau)\rangle\\
&\qquad\times(\boldsymbol{v}(1,\tau)\cdot\nabla_1+\boldsymbol{v}(2,\tau)\cdot\nabla_2)\langle U(1,\tau,t_0)U(2,\tau,t_0)\rangle\\
&\quad+\int_{t_0}^{t}d\tau\int_{\tau}^{t}d\tau'\langle U(1,t,\tau')U(2,t,\tau')\rangle\\
&\qquad\times(\boldsymbol{v}(1,\tau')\cdot\nabla_1+\boldsymbol{v}(2,\tau')\cdot\nabla_2)\langle U(1,\tau',\tau)U(2,\tau',\tau)\rangle\\
&\qquad\times(\boldsymbol{v}(1,\tau)\cdot\nabla_1+\boldsymbol{v}(2,\tau)\cdot\nabla_2)\langle U(1,\tau,t_0)U(2,\tau,t_0)\rangle\\
&\quad-\int_{t_0}^{t}d\tau\int_{t_0}^{\tau}d\tau'\langle U(1,t,\tau)U(2,t,\tau)\rangle\\
&\qquad\times\langle(\boldsymbol{v}(1,\tau)\cdot\nabla_1+\boldsymbol{v}(2,\tau)\cdot\nabla_2)\langle U(1,\tau,\tau')U(2,\tau,\tau')\rangle
\end{aligned}$$

$$\times (\boldsymbol{v}(1,\tau')\cdot\nabla_1 + \boldsymbol{v}(2,\tau')\cdot\nabla_2)\rangle\langle U(1,\tau',t_0)U(2,\tau',t_0)\rangle$$
$$+\cdots\cdots. \tag{6.27}$$

We can use an expression $\langle U(1,t,t_0)U(2,t,t_0)\rangle = \langle UU\rangle(1,2,t-t_0)$ by assuming a stationary turbulence. Keeping only the first-order of Eq.(6.27) and using the Markovian approximation, we obtain

$$\begin{aligned} & U(1,t,t_0)U(2,t,t_0) \\ &= \langle UU\rangle(1,2,t-t_0) \\ &\quad - \int_0^\infty d\tau[(\langle U(1,\tau)\rangle \boldsymbol{v}(1,t-\tau))\cdot\nabla_1 + (\langle U(2,\tau)\rangle \boldsymbol{v}(2,t-\tau))\cdot\nabla_2] \\ &\quad \times \langle UU\rangle(1,2,t-t_0). \end{aligned} \tag{6.28}$$

Here we used the relation $U(t)c = c$, where c is a constant. Substituting the above equation into Eq.(6.23) and averaging it, we obtain

$$\left(\frac{\partial}{\partial t} - \sum_{i,j=1,2} \nabla_i \cdot \mathsf{D}(i,j)\cdot\nabla_j + \alpha(1) + \alpha(2)\right)\langle UU\rangle(1,2,t-t_0) = 0, \tag{6.29}$$

where

$$\mathsf{D}(i,j) \equiv \int_0^\infty d\tau \langle U(j,\tau)\rangle\langle \boldsymbol{v}(i,t)\boldsymbol{v}(j,t-\tau)\rangle. \tag{6.30}$$

Averaging Eq.(6.22), we have

$$\begin{aligned} \langle \tilde{f}(1,t)\tilde{f}(2,t)\rangle &= \int_{t_0}^t d\tau \langle UU\rangle(1,2,t-\tau)\langle S(1,2,\tau)\rangle \\ &= \int_0^{t-t_0} d\tau \langle UU\rangle(1,2,\tau)\langle S(1,2,t-\tau)\rangle \\ &\simeq \int_0^\infty d\tau \langle UU\rangle(1,2,\tau)\langle S(1,2,t-\tau)\rangle. \end{aligned} \tag{6.31}$$

From Eqs.(6.29) and (6.31), we obtain

$$\left(\frac{\partial}{\partial t} - \sum_{i,j=1,2} \nabla_i \cdot \mathsf{D}(i,j)\cdot\nabla_j + \alpha(1) + \alpha(2)\right)\langle \tilde{f}(1,t)\tilde{f}(2,t)\rangle = \langle S(1,2,t)\rangle, \tag{6.32}$$

which is called the two-point renormalized equation. Here, we note that Eqs.(6.15) and (6.20) give

$$\left(\frac{\partial}{\partial t} - \nabla_1 \cdot \mathsf{D}(1,1) \cdot \nabla_1 - \nabla_2 \cdot \mathsf{D}(2,2) \cdot \nabla_2 + \alpha(1) + \alpha(2)\right) \langle U(1,t)\rangle\langle U(2,t)\rangle = 0 \tag{6.33}$$

and

$$\left(\frac{\partial}{\partial t} - \nabla_1 \cdot \mathsf{D}(1,1) \cdot \nabla_1 - \nabla_2 \cdot \mathsf{D}(2,2) \cdot \nabla_2 + \alpha(1) + \alpha(2)\right) \langle \tilde{f}^c(1,t)\tilde{f}^c(2,t)\rangle = \langle \tilde{f}^c(1,t)s(2,t) + \tilde{f}^c(2,t)s(1,t)\rangle \equiv \langle S^c(1,2,t)\rangle. \tag{6.34}$$

These equations yield

$$\begin{aligned}\langle \tilde{f}^c(1,t)\tilde{f}^c(2,t)\rangle &= \int_0^{t-t_0} d\tau \langle U(1,\tau)\rangle\langle U(2,\tau)\rangle\langle S^c(1,2,t-\tau)\rangle \\ &\simeq \int_0^{\infty} d\tau \langle U(1,\tau)\rangle\langle U(2,\tau)\rangle\langle S^c(1,2,t-\tau)\rangle.\end{aligned} \tag{6.35}$$

We note that $\langle \tilde{f}\tilde{f}\rangle$ is propagated by the averaged two-point propagator $\langle UU\rangle$ while $\langle \tilde{f}^c\tilde{f}^c\rangle$ by the product of the averaged one-point propagator $\langle U\rangle\langle U\rangle$. This difference comes from the cross diffusion terms of $\mathsf{D}(1,2)$ and $\mathsf{D}(2,1)$ which depend on the relative separation between two points and take into account of the incoherent property in the two-point renormalized theory. Dupree[18] defined the incoherent (clump) correlation function by $\langle \tilde{f}\tilde{f}\rangle_{\text{incoherent}} \equiv \langle \tilde{f}\tilde{f}\rangle - \langle \tilde{f}^c\tilde{f}^c\rangle$.

6.2.3 Clump lifetime approximation

We will describe an approximation for the two-point function (6.31), which is the solution to the two-point renormalized equation (6.32), based on the clump lifetime. This expression was given by Dupree [18] and has been frequently used by Diamond et al.[21]–[24]

It is convenient to introduce centric and relative coordinates [19] $(\boldsymbol{x}_+, \boldsymbol{x}_-)$

in place of two-point coordinates $(\boldsymbol{x}_1, \boldsymbol{x}_2)$:

$$\left.\begin{aligned} \boldsymbol{x}_+ &= \frac{1}{2}(\boldsymbol{x}_1 + \boldsymbol{x}_2), \quad \boldsymbol{x}_- = \boldsymbol{x}_1 - \boldsymbol{x}_2 \\ \boldsymbol{x}_1 &= \boldsymbol{x}_+ + \frac{1}{2}\boldsymbol{x}_-, \quad \boldsymbol{x}_2 = \boldsymbol{x}_+ - \frac{1}{2}\boldsymbol{x}_-. \end{aligned}\right\} \tag{6.36}$$

Using the above transformation of the coordinates yields

$$\sum_{i,j=1,2} \nabla_i \cdot \mathsf{D}(i,j) \cdot \nabla_j = \sum_{\mu,\nu=+,-} \frac{\partial}{\partial \boldsymbol{x}_\mu} \cdot \mathsf{D}_{\mu,\nu} \cdot \frac{\partial}{\partial \boldsymbol{x}_\nu}, \tag{6.37}$$

where

$$\left.\begin{aligned} \mathsf{D}_+ &\equiv \mathsf{D}_{++} \equiv \frac{1}{4}[\mathsf{D}(1,1) + \mathsf{D}(1,2) + \mathsf{D}(2,1) + \mathsf{D}(2,2)], \\ \mathsf{D}_{\pm\mp} &\equiv \frac{1}{2}[\mathsf{D}(1,1) - \mathsf{D}(2,2) \mp (\mathsf{D}(1,2) - \mathsf{D}(2,1))], \\ \mathsf{D}_- &\equiv \mathsf{D}_{--} \equiv \mathsf{D}(1,1) + \mathsf{D}(2,2) - \mathsf{D}(1,2) - \mathsf{D}(2,1). \end{aligned}\right\} \tag{6.38}$$

We define a reciprocal of the correlation length for $\langle \boldsymbol{v}(1)\boldsymbol{v}(2)\rangle$, k_0, which is interpreted as a representative wavenumber of the turbulence. From Eq.(6.30), D(1,2) and D(2,1) vanish when $k_0|\boldsymbol{x}_-| \gg 1$, and $\langle UU\rangle$ is approximated by $\langle U\rangle\langle U\rangle$. When $k_0|\boldsymbol{x}_-| \ll 1$, we find

$$\left.\begin{aligned} &\mathsf{D}(i,j) \to \mathsf{D}(\boldsymbol{x}_+), \quad \mathsf{D}_{+-}, \mathsf{D}_{-+} \to 0, \\ &\mathsf{D}_+ \to \mathsf{D}(\boldsymbol{x}_+), \qquad \mathsf{D}_- \to 0, \end{aligned}\right\} \tag{6.39}$$

where $\mathsf{D}(\boldsymbol{x}_+)$ corresponds to the value of Eq.(6.16) at $\boldsymbol{x} = \boldsymbol{x}_+$. In the limit of $k_0|\boldsymbol{x}_-| \ll 1$, we assume that D_{+-}, D_{-+} are negligibly small, $\boldsymbol{x}_+$ dependence of D_- is negligible, and $\alpha(1) + \alpha(2) \simeq \alpha_+(\boldsymbol{x}_+) + \alpha_-(\boldsymbol{x}_-)$. Based on these assumptions, we find from Eqs.(6.29) and (6.37) that $\langle UU\rangle$ is approximated by the product of $\langle U_+\rangle$ and $\langle U_-\rangle$:

$$\langle U(1)U(2)\rangle \simeq \langle U_+\rangle\langle U_-\rangle, \tag{6.40}$$

where $\langle U_+\rangle$ and $\langle U_-\rangle$ are the propagators which describe the centric and relative motion of the two points respectively and satisfy the following equations:

$$\left(\frac{\partial}{\partial t} - \frac{\partial}{\partial \boldsymbol{x}_+} \cdot \mathsf{D}_+ \cdot \frac{\partial}{\partial \boldsymbol{x}_+} + \alpha_+\right) \langle U_+(t)\rangle = 0, \tag{6.41}$$

$$\left(\frac{\partial}{\partial t} - \frac{\partial}{\partial \boldsymbol{x}_-} \cdot \mathsf{D}_- \cdot \frac{\partial}{\partial \boldsymbol{x}_-} + \alpha_-\right) \langle U_-(t) \rangle = 0, \tag{6.42}$$

$$\langle U_+(t=0) \rangle = I, \ \langle U_-(t=0) \rangle = I. \tag{6.43}$$

Here, the turbulent diffusivity, $\mathsf{D}_+ = \mathsf{D}(\boldsymbol{x}_+)$, is the same as that for the one-point propagator, but the turbulent diffusivity, D_-, vanishes as $k_0|\boldsymbol{x}_-| \to 0$ and this describes the correlation of two points at small distance.

Clump lifetime $\tau_{cl}(\boldsymbol{x}_-)$ is defined as follows.[18],[21]-[24] First we follow the orbits of two points backward in time with the initial distance $|\boldsymbol{x}_-| \ll k_0^{-1}$. Usually, the orbits diverge and the average distance between the two points becomes the order of the correlation length k_0^{-1} at $t = -\tau_{cl}$. For convenience, we introduce the kernel of the propagator $\langle U_- \rangle$ or the Green's function $g_t(\boldsymbol{x}_-|\boldsymbol{x}'_-)$ which satisfies

$$\left(\frac{\partial}{\partial t} - \frac{\partial}{\partial \boldsymbol{x}_-} \cdot \mathsf{D}_- \cdot \frac{\partial}{\partial \boldsymbol{x}_-} + \alpha_-\right) g_t(\boldsymbol{x}_-|\boldsymbol{x}'_-) = 0, \tag{6.44}$$

with an initial condition

$$g_{t=0}(\boldsymbol{x}_-|\boldsymbol{x}'_-) = \delta(\boldsymbol{x}_- - \boldsymbol{x}'_-). \tag{6.45}$$

Assuming that $g_t(\boldsymbol{x}_-|\boldsymbol{x}'_-) = g_t(\boldsymbol{x}'_-|\boldsymbol{x}_-)$ based on the time reversibility of the statistics for $\boldsymbol{v}(t)$, we can write the mean square relative separation as

$$\begin{aligned} \langle \boldsymbol{x}_-^2(-t) \rangle &\equiv \langle U_-(t) \rangle \boldsymbol{x}_-^2 \equiv \int d\boldsymbol{x}'_- g_t(\boldsymbol{x}_-|\boldsymbol{x}'_-) \boldsymbol{x}'^2_- \\ &= \int d\boldsymbol{x}'_- \boldsymbol{x}'^2_- g_t(\boldsymbol{x}'_-|\boldsymbol{x}_-) \equiv \langle \boldsymbol{x}_-^2(t) \rangle, \end{aligned} \tag{6.46}$$

where $\boldsymbol{x}_-(t)$ is the relative separation at $t = t$ with the initial condition that $\boldsymbol{x}_-(t=0) = \boldsymbol{x}_-$. By using the above relations, the clump lifetime $\tau_{cl}(\boldsymbol{x}_-)$ is defined by

$$k_0^2 \langle \boldsymbol{x}_-^2(t = \tau_{cl}) \rangle = 1. \tag{6.47}$$

Dupree and Diamond et al. have used the clump lifetime $\tau_{cl}(\boldsymbol{x}_-)$ to describe the solution (6.31) approximately as

$$\langle \tilde{f}(1)\tilde{f}(2) \rangle = \tau_{cl}(\boldsymbol{x}_-) \langle S(1,2) \rangle \tag{6.48}$$

where $\langle \tilde{f}(1)\tilde{f}(2) \rangle$ and $\langle S(1,2) \rangle$ are independent of time, since a stationary turbulence is considered.

6.3 An Application of the Renormalized Theories to the Vlasov Equation

In this section we discuss the application of the renormalized theories presented in Sec.6.2 to the Vlasov equation as an example. For convenience we take the plasma as a gas of electrons, while ions are considered as a homogeneous positive background with charge density ne. We consider the strongly turbulent plasma that the behavior of the electric field $\boldsymbol{E}(\boldsymbol{x},t)$ is turbulent and treated as a random function. The distribution function $f(\boldsymbol{x},\boldsymbol{v},t)$ is devided into the average part $f_0 \equiv \langle f \rangle$ and the fluctuating part $\tilde{f}$

$$f(\boldsymbol{x},\boldsymbol{v},t) = f_0(\boldsymbol{v}) + \tilde{f}(\boldsymbol{x},\boldsymbol{v},t) \tag{6.49}$$

where f_0 is independent of the position $\boldsymbol{x}$ and the time t since we assume the turbulence to be homogeneous in space and statiorary in time. The dynamics of the system may be described by the Vlasov equation

$$\left[\frac{\partial}{\partial t} + \boldsymbol{v}\cdot\frac{\partial}{\partial \boldsymbol{x}} - \frac{e}{m}\boldsymbol{E}(\boldsymbol{x},t)\cdot\frac{\partial}{\partial \boldsymbol{v}}\right] f(\boldsymbol{x},\boldsymbol{v},t) = 0 \tag{6.50}$$

and the Poisson's equation

$$\frac{\partial}{\partial \boldsymbol{x}}\cdot\boldsymbol{E}(\boldsymbol{x},t) = 4\pi ne\int d^3v\tilde{f}(\boldsymbol{x},\boldsymbol{v},t) \tag{6.51}$$

where the electrostatic approximation is taken and the average distribution function f_0 cancels the background positive charge due to ions. The Vlasov equation (6.50) can be rewritten by Eq.(6.49) as

$$\left[\frac{\partial}{\partial t} + \boldsymbol{v}\cdot\frac{\partial}{\partial \boldsymbol{x}} - \frac{e}{m}\boldsymbol{E}(\boldsymbol{x},t)\cdot\frac{\partial}{\partial \boldsymbol{v}}\right]\tilde{f}(\boldsymbol{x},\boldsymbol{v},t) = \frac{e}{m}\boldsymbol{E}(\boldsymbol{x},t)\cdot\frac{\partial f_0(\boldsymbol{v})}{\partial \boldsymbol{v}}. \tag{6.52}$$

It is found that the above equation has the same form as Eq.(6.1) by taking the following relation into account

$$\left.\begin{aligned}
&\boldsymbol{x} \to (\boldsymbol{x},\boldsymbol{v}),\\
&\nabla \to (\partial/\partial\boldsymbol{x}, \partial/\partial\boldsymbol{v}),\\
&\boldsymbol{v}(\boldsymbol{x},t) \to (0, -(e/m)\boldsymbol{E}(\boldsymbol{x},t)),\\
&\alpha \to \boldsymbol{v}\cdot\partial/\partial\boldsymbol{x},\\
&\tilde{f}(\boldsymbol{x},t) \to \tilde{f}(\boldsymbol{x},\boldsymbol{v},t),\\
&s(\boldsymbol{x},t) \to (e/m)\boldsymbol{E}(\boldsymbol{x},t)\cdot\partial f_0(\boldsymbol{v})/\partial\boldsymbol{v}
\end{aligned}\right\} \tag{6.53}$$

where the electric field $\boldsymbol{E}(\boldsymbol{x},t)$ is a random function with the statistical average $\langle \boldsymbol{E} \rangle = 0$. According to Eqs.(6.3) and (6.4) the one-point propagator U is defined by

$$\left[\frac{\partial}{\partial t} + \boldsymbol{v}\cdot\frac{\partial}{\partial \boldsymbol{x}} - \frac{e}{m}\boldsymbol{E}(\boldsymbol{x},t)\cdot\frac{\partial}{\partial \boldsymbol{v}}\right] U(t,t_0) = 0 \tag{6.54}$$

with

$$U(t_0,t_0) = I. \tag{6.55}$$

The kernel of the propagator U or the Green's function g is given by

$$\begin{aligned} & g(t,t_0;\boldsymbol{x},\boldsymbol{v},\boldsymbol{x}',\boldsymbol{v}') \\ &= \delta[\boldsymbol{x} - \overline{\boldsymbol{x}}(t,t_0;\boldsymbol{x}',\boldsymbol{v}')]\delta[\boldsymbol{v} - \overline{\boldsymbol{v}}(t,t_0;\boldsymbol{x}',\boldsymbol{v}')] \\ &= \delta[\boldsymbol{x}' - \overline{\boldsymbol{x}}(t_0,t;\boldsymbol{x},\boldsymbol{v})]\delta[\boldsymbol{v}' - \overline{\boldsymbol{v}}(t_0,t;\boldsymbol{x},\boldsymbol{v})] \end{aligned} \tag{6.56}$$

where $\overline{\boldsymbol{x}}(t,t_0;\boldsymbol{x}',\boldsymbol{v}')$ and $\overline{\boldsymbol{v}}(t,t_0;\boldsymbol{x}',\boldsymbol{v}')$ are the solutions to the following differential equations

$$\frac{d\overline{\boldsymbol{x}}}{dt} = \overline{\boldsymbol{v}}, \qquad \frac{d\overline{\boldsymbol{v}}}{dt} = -\frac{e}{m}\boldsymbol{E}(\overline{\boldsymbol{x}},t) \tag{6.57}$$

with the initial conditions

$$\overline{\boldsymbol{x}}(t=t_0) = \boldsymbol{x}', \qquad \overline{\boldsymbol{v}}(t=t_0) = \boldsymbol{v}'. \tag{6.58}$$

In Eq.(6.56) we used the fact that the motion given by Eq.(6.57) conserves the volume in the phase space, which is found from

$$\frac{\partial}{\partial \boldsymbol{x}}\cdot\left(\frac{d\overline{\boldsymbol{x}}}{dt}\right) + \frac{\partial}{\partial \boldsymbol{v}}\cdot\left(\frac{d\overline{\boldsymbol{v}}}{dt}\right) = \frac{\partial}{\partial \boldsymbol{x}}\cdot\boldsymbol{v} + \frac{\partial}{\partial \boldsymbol{v}}\cdot\left(-\frac{e}{m}\boldsymbol{E}(\overline{\boldsymbol{x}},t)\right) = 0. \tag{6.59}$$

The integral equation and its expansion for the propogator U are immediately obtained from Eqs.(6.11) and (6.12)

$$\begin{aligned} & U(t,t_0) \\ &= \langle U(t,t_0)\rangle \\ &\quad + \frac{e}{m}\int_{t_0}^{t} d\tau U(t,\tau)\left(\boldsymbol{E}(\boldsymbol{x},\tau)\cdot\frac{\partial}{\partial \boldsymbol{v}}\langle U(\tau,t_0)\rangle - \left\langle \boldsymbol{E}(\boldsymbol{x},\tau)\cdot\frac{\partial}{\partial \boldsymbol{v}}U(\tau,t_0)\right\rangle\right) \end{aligned}$$

$$
\begin{aligned}
&= \langle U(t,t_0)\rangle + \frac{e}{m}\int_{t_0}^{t} d\tau \langle U(t,\tau)\rangle \boldsymbol{E}(\boldsymbol{x},\tau)\cdot\frac{\partial}{\partial \boldsymbol{v}}\langle U(\tau,t_0)\rangle \\
&+\left(\frac{e}{m}\right)^2\int_{t_0}^{t} d\tau\int_{\tau}^{t} d\tau' \langle U(t,\tau')\rangle \boldsymbol{E}(\boldsymbol{x},\tau')\cdot\frac{\partial}{\partial \boldsymbol{v}}\langle U(\tau',\tau)\rangle \boldsymbol{E}(\boldsymbol{x},\tau)\cdot\frac{\partial}{\partial \boldsymbol{v}}\langle U(\tau,t_0)\rangle \\
&-\left(\frac{e}{m}\right)^2\int_{t_0}^{t} d\tau\int_{t_0}^{\tau} d\tau' \langle U(t,\tau)\rangle \left\langle \boldsymbol{E}(\boldsymbol{x},\tau)\cdot\frac{\partial}{\partial \boldsymbol{v}}\langle U(\tau,\tau')\rangle \boldsymbol{E}(\boldsymbol{x},\tau')\right\rangle\cdot\frac{\partial}{\partial \boldsymbol{v}}\langle U(\tau',t_0)\rangle \\
&+\cdots\cdots. \qquad (6.60)
\end{aligned}
$$

The expansion in Eq.(6.60) coincides exactly with that given by Dupree (see Eq.(4.1) in Ref.[15]) up to the first-order with respect to the electric field. Dupree obtained this result by considering the interaction between test and background waves in the Fourier space by assuming the random phases among intial Fourier modes. On the other hand, Eq.(6.60) is derived systematically by applying the iterative scheme to the integral equation for the propagor U in the phase space representation.

Truncating the expansion to the first-order and using the Markovian approximation yield

$$
\left(\frac{\partial}{\partial t}+\boldsymbol{v}\cdot\frac{\partial}{\partial \boldsymbol{x}}-\frac{\partial}{\partial \boldsymbol{v}}\cdot \mathsf{D}\cdot\frac{\partial}{\partial \boldsymbol{v}}\right)\langle U(t-t_0)\rangle = 0 \qquad (6.61)
$$

and

$$
\mathsf{D}\equiv\left(\frac{e}{m}\right)^2\int_0^{\infty} d\tau \underbrace{\langle U(\tau)\rangle}\langle \boldsymbol{E}(t)\underbrace{\boldsymbol{E}(t-\tau)}\rangle \qquad (6.62)
$$

which correspond to Eqs.(6.15) and (6.16), respectively. Here the homogeneous and stationary turbulence is considered and also in order to reproduce the Dupree's results it is convenient to take the Fourier transform as follows

$$
\langle \boldsymbol{E}(\boldsymbol{x},t)\boldsymbol{E}(\boldsymbol{x}',t')\rangle = \int\frac{d^3k}{(2\pi)^3}\int\frac{d\omega}{2\pi}\mathrm{e}^{i\boldsymbol{k}\cdot(\boldsymbol{x}-\boldsymbol{x}')-i\omega(t-t')}\langle \boldsymbol{E}\boldsymbol{E}\rangle(\boldsymbol{k},\omega). \qquad (6.63)
$$

Sustituting Eq.(6.63) into Eq.(6.62) gives

$$
\mathsf{D}=\left(\frac{e}{m}\right)^2\int\frac{d^3k}{(2\pi)^3}\int\frac{d\omega}{2\pi}\langle \boldsymbol{E}\boldsymbol{E}\rangle(\boldsymbol{k},\omega)\Re g(\boldsymbol{k},\omega,\boldsymbol{v}) \qquad (6.64)
$$

where $\Re$ denotes the real part of the complex variable and $g(\boldsymbol{k},\omega,\boldsymbol{v})$ is defined by

$$
g(\boldsymbol{k},\omega,\boldsymbol{v}) = \mathrm{e}^{-i\boldsymbol{k}\cdot\boldsymbol{x}}\int_0^{\infty} d\tau \mathrm{e}^{i\omega\tau}\langle U(\tau)\rangle \mathrm{e}^{i\boldsymbol{k}\cdot\boldsymbol{x}}. \qquad (6.65)
$$

From Eq.(6.19) the coherent part of the distribution function $\tilde{f}^c$ is obtained as

$$\tilde{f}^c(\boldsymbol{x},\boldsymbol{v},t) = \frac{e}{m}\int_0^\infty d\tau \langle U(\tau)\rangle \boldsymbol{E}(\boldsymbol{x},t-\tau)\cdot\frac{\partial f_0(\boldsymbol{v})}{\partial \boldsymbol{v}}. \tag{6.66}$$

Replace $\tilde{f}$ in the Poisson's equation (6.51) with the nonlinear coherent response $\tilde{f}^c$ given by Eq.(6.66), and use $\boldsymbol{E} = -\nabla\phi$ and $\langle U(\tau)\rangle \boldsymbol{E}(\boldsymbol{x},t-\tau)\cdot \partial f_0(\boldsymbol{v})/\partial \boldsymbol{v} \simeq (\langle U(\tau)\rangle \boldsymbol{E}(\boldsymbol{x},t-\tau))\cdot \partial f_0(\boldsymbol{v})/\partial \boldsymbol{v}$. By using Fourier transformation with respect to $\boldsymbol{x}$ and t, we get the nonlinear dispersion relation

$$1 - i\frac{\omega_{pe}^2}{k^2}\int d^3v g(\boldsymbol{k},\omega,\boldsymbol{v})\boldsymbol{k}\cdot\frac{\partial f_0(\boldsymbol{v})}{\partial \boldsymbol{v}} = 0 \tag{6.67}$$

where $\omega_{pe} \equiv \sqrt{4\pi n e^2/m}$ is the electron plasma frequency. The nonlinear dispersion relation determines the frequency $\omega = \omega(\boldsymbol{k})$ and thus the one-point or coherent renormalized theory gives the discrete frequency spectrum at fixed $\boldsymbol{k}$ represented by

$$\langle \boldsymbol{E}\boldsymbol{E}\rangle(\boldsymbol{k},\omega) = 2\pi\langle \boldsymbol{E}\boldsymbol{E}\rangle(\boldsymbol{k})\delta[\omega-\omega(\boldsymbol{k})]. \tag{6.68}$$

By eliminating the nonlinear term Eq.(6.54) gives the linear propagator $U^{(l)}$, which is defined by

$$\left(\frac{\partial}{\partial t} + \boldsymbol{v}\cdot\frac{\partial}{\partial \boldsymbol{x}}\right)U^{(l)}(t) = 0 \tag{6.69}$$

with the initial condition $U^{(l)}(t=0) = I$. Then we find

$$U^{(l)}(t)\mathrm{e}^{i\boldsymbol{k}\cdot\boldsymbol{x}} = \mathrm{e}^{i\boldsymbol{k}\cdot(\boldsymbol{x}-\boldsymbol{v}t)}. \tag{6.70}$$

If we use $U^{(l)}$ instead of $\langle U\rangle$, we obtain the linear response from Eq.(6.66) and the linear dispersion relation from Eq.(6.67), where $g(\boldsymbol{k},\omega,\boldsymbol{v})$ is replaced by

$$\begin{aligned} g^{(l)}(\boldsymbol{k},\omega,\boldsymbol{v}) &= \mathrm{e}^{-i\boldsymbol{k}\cdot\boldsymbol{x}}\int_0^\infty d\tau \mathrm{e}^{i\omega\tau}U^{(l)}(\tau)\mathrm{e}^{i\boldsymbol{k}\cdot\boldsymbol{x}} \\ &= \frac{1}{-i(\omega-\boldsymbol{k}\cdot\boldsymbol{v}+i\epsilon)} \qquad (\epsilon\to+0). \end{aligned} \tag{6.71}$$

Similarly Eq.(6.64) reduces to the quasilinear diffusion tensor

$$\mathrm{D}^{QL} = \pi\left(\frac{e}{m}\right)^2\int\frac{d^3k}{(2\pi)^3}\langle \boldsymbol{E}\boldsymbol{E}\rangle(\boldsymbol{k})\delta[\omega(\boldsymbol{k})-\boldsymbol{k}\cdot\boldsymbol{v}], \tag{6.72}$$

where Eqs.(6.68) and (6.71) are used.

Dupree described the resonance broadening by using the following approximation.[15] Neglecting $\boldsymbol{v}$ dependence of D in Eq.(6.61) we find

$$\langle U(t)\rangle \mathrm{e}^{i\boldsymbol{k}\cdot\boldsymbol{x}} = \mathrm{e}^{i\boldsymbol{k}\cdot(\boldsymbol{x}-\boldsymbol{v}t)-\frac{1}{3}\boldsymbol{k}\boldsymbol{k}:\mathrm{D}t^3}. \tag{6.73}$$

By substituting this into Eq.(6.65) we obtain

$$\Re g(\boldsymbol{k},\omega,\boldsymbol{v}) = \int_0^\infty dt \cos[(\omega-\boldsymbol{k}\cdot\boldsymbol{v})t] \exp\left[-\frac{1}{3}\boldsymbol{k}\boldsymbol{k}:\mathrm{D}t^3\right]. \tag{6.74}$$

This function has a peak at $\omega - \boldsymbol{k}\cdot\boldsymbol{v} = 0$ and goes to zero for $|\omega - \boldsymbol{k}\cdot\boldsymbol{v}| \gg kw \equiv (\boldsymbol{k}\boldsymbol{k} : \mathrm{D}/3)^{1/3}$, where w is the width of the velocity along $\boldsymbol{k}$ at which particles interact with waves. The finiteness of w corresponds to the resonance broadening.

Now let us apply the two-point renormalized theory to the Vlasov equation. The two-point renormalized equation is given from Eq.(6.32) as

$$\left(\frac{\partial}{\partial t} + \boldsymbol{v}_1\cdot\frac{\partial}{\partial \boldsymbol{x}_1} + \boldsymbol{v}_2\cdot\frac{\partial}{\partial \boldsymbol{x}_2} - \sum_{i,j=1,2}\frac{\partial}{\partial \boldsymbol{v}_i}\cdot\mathrm{D}_{i,j}\cdot\frac{\partial}{\partial \boldsymbol{v}_j}\right)\langle\tilde{f}(1,t)\tilde{f}(2,t)\rangle = \langle S(1,2)\rangle \tag{6.75}$$

where $1 = (\boldsymbol{x}_1, \boldsymbol{v}_1)$, $2 = (\boldsymbol{x}_2, \boldsymbol{v}_2)$ and

$$\begin{aligned}\langle S(1,2)\rangle &= \frac{e}{m}\langle\tilde{f}(1)\boldsymbol{E}(2)\rangle\cdot\frac{\partial f_0(\boldsymbol{v}_2)}{\partial \boldsymbol{v}_2} + (1\leftrightarrow 2)\\ &\simeq (\mathrm{D}_{12}+\mathrm{D}_{21}) : \frac{\partial f_0(\boldsymbol{v}_1)}{\partial \boldsymbol{v}_1}\frac{\partial f_0(\boldsymbol{v}_2)}{\partial \boldsymbol{v}_2}\end{aligned} \tag{6.76}$$

$$\begin{aligned}\mathrm{D}_{ij} &= \left(\frac{e}{m}\right)^2\int_0^\infty d\tau\langle U(j,\tau)\rangle\langle\boldsymbol{E}(\boldsymbol{x}_i,t)\boldsymbol{E}(\boldsymbol{x}_j,t-\tau)\rangle\\ &= \left(\frac{e}{m}\right)^2\int\frac{d^3k}{(2\pi)^3}\int\frac{d\omega}{2\pi}\langle\boldsymbol{E}\boldsymbol{E}\rangle(\boldsymbol{k},\omega)\mathrm{e}^{i\boldsymbol{k}\cdot(\boldsymbol{x}_i-\boldsymbol{x}_j)}g(-\boldsymbol{k},-\omega,\boldsymbol{v}_j).\end{aligned} \tag{6.77}$$

From Eq.(6.31) and the clump lifetime approximation (6.48), the stationary solution of Eq.(6.75) is written as

$$\begin{aligned}\langle\tilde{f}(1)\tilde{f}(2)\rangle &= \int_0^\infty d\tau\langle UU\rangle(1,2,\tau)\langle S(1,2)\rangle\\ &\simeq \tau_{cl}(\boldsymbol{x}_-,\boldsymbol{v}_-)\langle S(1,2)\rangle\end{aligned} \tag{6.78}$$

where the averaged two-point propagator $\langle UU \rangle$ is defined by

$$\left(\frac{\partial}{\partial t} + \boldsymbol{v}_1 \cdot \frac{\partial}{\partial \boldsymbol{x}_1} + \boldsymbol{v}_2 \cdot \frac{\partial}{\partial \boldsymbol{x}_2} - \sum_{i,j=1,2} \frac{\partial}{\partial \boldsymbol{v}_i} \cdot \mathsf{D}_{i,j} \cdot \frac{\partial}{\partial \boldsymbol{v}_j} \right) \langle UU \rangle (1,2,t) = 0. \tag{6.79}$$

Then the centric and relative coordinates are introduced as in Eq.(6.36)

$$\left. \begin{aligned} \boldsymbol{x}_+ &= \frac{1}{2}(\boldsymbol{x}_1 + \boldsymbol{x}_2), \quad \boldsymbol{v}_+ = \frac{1}{2}(\boldsymbol{v}_1 + \boldsymbol{v}_2) \\ \boldsymbol{x}_- &= \boldsymbol{x}_1 - \boldsymbol{x}_2, \qquad \boldsymbol{v}_- = \boldsymbol{v}_1 - \boldsymbol{v}_2. \end{aligned} \right\} \tag{6.80}$$

According to Eq.(6.40) for small $\boldsymbol{x}_-$, $\boldsymbol{v}_-$, $\langle UU \rangle$ is factorized into the product of $\langle U_+ \rangle$ and $\langle U_- \rangle$, which satisfy

$$\left(\frac{\partial}{\partial t} + \boldsymbol{v}_+ \cdot \frac{\partial}{\partial \boldsymbol{x}_+} - \frac{\partial}{\partial \boldsymbol{v}_+} \cdot \mathsf{D}_+ \cdot \frac{\partial}{\partial \boldsymbol{v}_+} \right) \langle U_+(t) \rangle = 0 \tag{6.81}$$

$$\left(\frac{\partial}{\partial t} + \boldsymbol{v}_- \cdot \frac{\partial}{\partial \boldsymbol{x}_-} - \frac{\partial}{\partial \boldsymbol{v}_-} \cdot \mathsf{D}_- \cdot \frac{\partial}{\partial \boldsymbol{v}_-} \right) \langle U_-(t) \rangle = 0 \tag{6.82}$$

where $\mathsf{D}_+ = \mathsf{D}(\boldsymbol{v}_+)$ and

$$\begin{aligned} \mathsf{D}_- &= \mathsf{D}_{11} + \mathsf{D}_{22} - \mathsf{D}_{12} - \mathsf{D}_{21} \\ &\simeq \left(\frac{e}{m} \right)^2 \int \frac{d^3k}{(2\pi)^3} \int \frac{d\omega}{2\pi} \langle \boldsymbol{E}\boldsymbol{E} \rangle (\boldsymbol{k}, \omega) 2\Re g(\boldsymbol{k}, \omega, \boldsymbol{v}_+)[1 - \cos(\boldsymbol{k} \cdot \boldsymbol{x}_-)]. \end{aligned} \tag{6.83}$$

The clump lifetime τ_{cl} can be calculated in the following way. For simplicity we consider a one-dimensional plasma turbulence. The kernel of $\langle U_- \rangle$ or the Green's function $g_t(x_-, v_- | x'_-, v'_-)$ satisfies

$$\left(\frac{\partial}{\partial t} + v_- \frac{\partial}{\partial x_-} - \frac{\partial}{\partial v_-} D_- \frac{\partial}{\partial v_-} \right) g_t(x_-, v_- | x'_-, v'_-) = 0 \tag{6.84}$$

with the initial condition

$$g_{t=0}(x_-, v_- | x'_-, v'_-) = \delta(x_- - x'_-)\delta(v_- - v'_-). \tag{6.85}$$

Assuming the time reversibility of the statistics of the electric field yields

$$g_t(x_-, v_- | x'_-, v'_-) = g_{-t}(x'_-, -v'_- | x_-, -v_-). \tag{6.86}$$

Using Eq.(6.83) the relative diffusivity D_- is approximated by

$$D_- \simeq k_0^2 x_-^2 D \qquad (k_0|x_-| \ll 1) \tag{6.87}$$

where k_0 represents the typical wavenumber of the turbulence. The clump lifetime τ_{cl} is defined by

$$\langle \overline{x}_-^2(-\tau_{cl}, x_-, v_-)\rangle = \langle \overline{x}_-^2(\tau_{cl}, x_-, -v_-)\rangle = k_0^{-2} \tag{6.88}$$

where $\overline{x}_-(t, x_-, v_-)$ is the relative distance in the x_- direction at $t = t$ between the two points in the phase space which have a relative separation (x_-, v_-) at $t = 0$. Equation (6.86) is also used in Eq.(6.88) to obtain the first equality. Taking the following second moments of Eq.(6.84) we find

$$\left.\begin{aligned} &\frac{\partial}{\partial t}\langle \overline{x}_-^2(t)\rangle = 2\langle \overline{x}_-(t)\overline{v}_-(t)\rangle \\ &\frac{\partial}{\partial t}\langle \overline{x}_-(t)\overline{v}_-(t)\rangle = \langle \overline{v}_-^2(t)\rangle \\ &\frac{\partial}{\partial t}\langle \overline{v}_-^2(t)\rangle = 2\langle D_-\rangle. \end{aligned}\right\} \tag{6.89}$$

By using Eq.(6.87), Eq.(6.89) is solved to give the solution for $k_0^2\langle \overline{x}_-^2\rangle \ll 1$ and $t \gg \tau_0$

$$\langle \overline{x}_-^2(t)\rangle = \frac{1}{3}[\overline{x}_-^2(0) + 2\overline{x}_-(0)\overline{v}_-(0)\tau_0 + 2\overline{v}_-^2(0)\tau_0^2]\exp(t/\tau_0) \tag{6.90}$$

where $\tau_0 \equiv (4k_0^2 D)^{-1/3}$. From Eqs.(6.88) and (6.90) we obtain

$$\tau_{cl}(x_-, v_-) = \begin{cases} \tau_0 \ln\left[\dfrac{3}{k_0^2(x_-^2 - 2x_- v_- \tau_0 + 2v_-^2\tau_0^2)}\right] \\ \qquad (\text{ for arg of ln} > 1\ ) \\ 0 \qquad\qquad (\text{ otherwise }). \end{cases} \tag{6.91}$$

This clump lifetime plays a key role in the two-point renormalized theory presented in this chapter and its applications will be shown in Chapter 7.

6.4 Conclusions

The exact integral equation (6.11) to determine time evolution of the nonlinear propagator has been derived for the general model equation (6.1) with convective nonlinearity. The iterative scheme has been applied to the integral equation to obtain the approximate expression (6.12) of the propagator which is appropriate for studying the strong turbulence. The first order of this expasion is exactly equivalent to Eq.(4.1) in Ref.[15]. Dupree treated the Vlasov equation and derived the expansion form of the propagator by considering interaction between test and background waves in the Fourier space based on the random phases among initial Fourier modes. We have considered the model equation (6.1) in the real space and obtained the integral equation with respect to time. A systematic derivation of the expansion form for the propagator, which is more straightforward than that in Ref.[15], has been given. Using this expression, we have developed the one-point (coherent) and two-point (incoherent) renormalized theories represented with the real space coordinates. The clump lifetime approximation for the solution of the two-point renormalized equation was also described. In this approximation the correlation function of the fluctuation is given by the product of the clump lifetime and the source term in the two-point equation.

The renormalized theories have been applied to the Vlasov equation and it is found that Dupree's results[15],[18] are reproduced. The one-point (coherent) theory has shown the generalization of the quasilinear diffusion theory into the case of the strong turbulence by including the resonance broadening. However, it is remarked that in the one-point theory the frequency spectrum at fixed wavenumber takes the form of delta function, which is the same as in the linear and weak turbulence theories. In the application of the two-point theory, the expression of the clump lifetime is given in the relative phase space coordinates.

In the next chapter the renormalized theories will be applied to the reduced fluid equations in order to obtain the wavenumber spectrum and the turbulent diffusivity for estimating the edge turbulence and the related anomalous transport in toroidally confined plasmas.

Chapter 7

Anormalous Transport Driven by Resistive Interchange Mode Turbulence

7.1 Introduction

In this chapter we apply the renormalized theories developed in Chapter 6 to the reduced fluid models in order to study the edge turbulence and the anomalous transport such as observed in Heliotron E. We consider turbulence driven by the resistive interchange modes which are destabilized by pressure gradients and bad magnetic curvature. We treat two types of reduced fluid equations to describe low frequency electrostatic perturbations in an inhomogeneous collisional plasma confined by a magnetic field with curvature and shear. One is the RMHD equations in the electrostatic limit and the other is the Hasegawa-Wakatani equations which include the effect of the electron diamagnetic drift. By using the two-point renormalized theory and the clump lifetime approximation, wave number spectra and turbulent diffusivities are obtained. This approach has been taken by Diamond et al. in the analyses for the resistivity-gradient-driven turbulence[22] and the ion temperature-gradient-driven turbulence.[24]

This chapter is organized as follows. In Sec.7.2 and Sec.7.3, the wavenumber spectra and the turbulent diffusivities are calculated by applying the two-point renormalized theory and the clump lifetime approximation to the

RMHD equations and the Hasegawa-Wakatani equations, respectively. Finally problems of this approach are discussed and conclusions are given in Sec.7.4.

7.2 Resistive Interchange Mode Turbulence by Reduced MHD Model

We will apply the renormalized theories and the clump lifetime approximation in Sec.6.2 to the resistive interchange or g mode turbulence based on the reduced MHD model and obtain the wavenumber spectrum and the turbulent diffusivity.

The reduced MHD model in the electrostatic limit consists of the pressure convection equation:

$$\left(\frac{\partial}{\partial t}+\boldsymbol{v}\cdot\nabla\right)\tilde{p}=-v_x\frac{dp_0}{dx}, \tag{7.1}$$

and the vorticity equation:

$$\frac{\rho_m c}{B_0}\left(\frac{\partial}{\partial t}+\boldsymbol{v}\cdot\nabla\right)\nabla_\perp^2\phi=-\frac{B_0}{c\eta}\nabla_{||}^2\phi+\nabla\tilde{p}\times\nabla\Omega\cdot\hat{z}. \tag{7.2}$$

Here ϕ is the electrostatic potential and $p=p_0+\tilde{p}$ the total pressure, where $p_0=\langle p\rangle$ and $\tilde{p}$ are the average and fluctuating parts, respectively. The velocity $\boldsymbol{v}$ is approximated by the $\boldsymbol{E}\times\boldsymbol{B}$ drift velocity:

$$\boldsymbol{v}=-\frac{c}{B_0}\nabla\phi\times\hat{z}, \tag{7.3}$$

and $\nabla_{||}\equiv(\boldsymbol{B}_0/B_0)\cdot\nabla$ where $\boldsymbol{B}_0$ is the static sheared magnetic field and $B_0\equiv|\boldsymbol{B}_0|$. In Eq.(7.2), $\nabla\Omega$ represents the average curvature of the magnetic field line[3],[33], ρ_m is the average mass density, c the light velocity in the vacuum and η the resistivity. The pressure p_0 and Ω are assumed to depend only on the local radial coordinate x. We apply the renormalized theory to the pressure equation (7.1) since Eq.(7.1) has the same form as Eq.(6.1). From Eq.(6.20), we obtain the one-point renormalized equation:

$$\left(\frac{\partial}{\partial t}-\nabla\cdot\mathsf{D}\cdot\nabla\right)\tilde{p}^c=-v_x\frac{dp_0}{dx}, \tag{7.4}$$

where $\tilde{p}^c$ represents the coherent part of $\tilde{p}$ and the turbulent diffusion tensor D is given by Eq.(6.16). The two-point renormalized equaiton is obtained

from Eq.(6.32) as follows:

$$\left(\frac{\partial}{\partial t} - \sum_{i,j=1,2} \nabla_i \cdot \mathsf{D}(i,j) \cdot \nabla_j\right) \langle \tilde{p}(1)\tilde{p}(2)\rangle = S(1,2), \tag{7.5}$$

where the source term in the right-hand side is defined as

$$S(1,2) \equiv \frac{c}{B_0}\frac{dp_0}{dx}\frac{\partial}{\partial y_1}\langle \phi(1)\tilde{p}(2)\rangle + (1 \leftrightarrow 2). \tag{7.6}$$

Hereafter we assume dp_0/dx to be negative and constant for simplicity since our concern is in the localized turbulence. From Eq.(6.48), the approximate solution to the two-point renormalized equation (7.5) can be expressed by using the clump lifetime as

$$\langle \tilde{p}(1)\tilde{p}(2)\rangle = \tau_{cl}(\boldsymbol{x}_-)S(1,2). \tag{7.7}$$

As discussed in Sec.6.2.3, we introduce the Green's function $g_t(\boldsymbol{x}_-|\boldsymbol{x}'_-)$ which is defined by

$$\left(\frac{\partial}{\partial t} - \frac{\partial}{\partial x_-}D_-\frac{\partial}{\partial x_-}\right) g_t(\boldsymbol{x}_-|\boldsymbol{x}'_-) = 0, \tag{7.8}$$

with the same initial condition as Eq.(6.45), where the only (x,x)-component of the relative diffusion tensor, $D_- \equiv (\mathsf{D}_-)_{xx}$, is retained and the other components are assumed to be negligible. From Eq.(6.38), we find that D_- is an even function with respect to x_- and vanishes at $x_- = 0$. We approximate D_- in the limit of small $|x_-|$ as

$$D_- \simeq D\left(\frac{1}{3}k_{0x}^2 x_-^2 + k_{0y}^2 y_-^2 + k_{0z}^2 z_-^2\right), \tag{7.9}$$

where k_{0x}, k_{0y} and k_{0z} are the representative wavenumber in the x, y and z directions respectively and D is the (x,x)-component of Eq.(6.16). We define the relative separation between two points normalized with the correlation scale $|\boldsymbol{k}_0|^{-1}$ by[24]

$$R_-^2(t) \equiv k_{0x}^2 x_-^2(t) + k_{0y}^2 y_-^2(t) + k_{0z}^2 z_-^2(t). \tag{7.10}$$

Using Eqs.(6.46) and (7.9) and taking the second moments of Eq.(7.8), we have

$$\frac{\partial}{\partial t}\langle R_-^2(t)\rangle = 2k_{0x}^2 D\langle R_-^2(t)\rangle. \tag{7.11}$$

Solving the above equation with the initial condition $R_-^2(t=0) = k_{0x}^2 x_-^2 + k_{0y}^2 y_-^2 + k_{0z}^2 z_-^2$, we obtain

$$\langle R_-^2(t)\rangle = (k_{0x}^2 x_-^2 + k_{0y}^2 y_-^2 + k_{0z}^2 z_-^2)\exp(2k_{0x}^2 Dt). \tag{7.12}$$

The clump lifetime τ_{cl} is defined by $\langle R_-^2(t=\tau_{cl})\rangle = 1$ and the resulting expression of τ_{cl} is

$$\tau_{cl}(\boldsymbol{x}_-) = \begin{cases} \dfrac{1}{2k_{0x}^2 D}\ln\left(\dfrac{1}{k_{0x}^2 x_-^2 + k_{0y}^2 y_-^2 + k_{0z}^2 z_-^2}\right) & (k_{0x}^2 x_-^2 + k_{0y}^2 y_-^2 + k_{0z}^2 z_-^2 < 1) \\ 0 & (k_{0x}^2 x_-^2 + k_{0y}^2 y_-^2 + k_{0z}^2 z_-^2 > 1). \end{cases} \tag{7.13}$$

Except the small region denoted by $k_{0x}^2 x_-^2 + k_{0y}^2 y_-^2 + k_{0z}^2 z_-^2 < 1$, the clump lifetime vanishes and it is assumed that the source term in the right-hand side of Eq.(7.7) varies slowly in this region. Thus we can approximate Eq.(7.7) with

$$\langle \tilde{p}(1)\tilde{p}(2)\rangle \simeq \tau_{cl}(\boldsymbol{x}_-)S^0, \tag{7.14}$$

where S^0 is the value of source term $S(1,2)$ at $\boldsymbol{x}_- = 0$. Thus the two-point correlation function of the pressure fluctuation, $\langle \tilde{p}(1)\tilde{p}(2)\rangle$, depends on the relative coordinate $\boldsymbol{x}_-$ only through the clump lifetime τ_{cl} given by Eq.(7.13). By integrating Eq.(7.14) over $\boldsymbol{x}_-$ and performing Fourier transform with respect to y_- and z_-, the wavenumber spectrum is given by

$$\begin{aligned} \langle \tilde{p}\tilde{p}\rangle_{\boldsymbol{k}} &\equiv \int k_{0x}dx_- \int dy_- \int dz_- \mathrm{e}^{-ik_y y_- - ik_z z_-}\langle \tilde{p}(1)\tilde{p}(2)\rangle \\ &= S^0 \int k_{0x}dx_- \int dy_- \int dz_- \mathrm{e}^{-ik_y y_- - ik_z z_-}\tau_{cl}(\boldsymbol{x}_-) \\ &= \frac{4\pi S^0}{k_{0x}^2 D k_{0y} k_{0z}} I(\boldsymbol{k}), \end{aligned} \tag{7.15}$$

where $\boldsymbol{k} \equiv (k_y, k_z)$,

$$I(\boldsymbol{k}) = \int_0^1 \rho d\rho J_0(\beta\rho)\left(\sqrt{1-\rho^2} - \rho\cos^{-1}\rho\right), \tag{7.16}$$

and

$$\beta = \sqrt{(k_y/k_{0y})^2 + (k_z/k_{0z})^2}. \tag{7.17}$$

Further integration over k_z yields the k_y-spectrum,

$$\langle\tilde{p}\tilde{p}\rangle_{k_y} \equiv \int \frac{dk_z}{2\pi}\langle\tilde{p}\tilde{p}\rangle_{\boldsymbol{k}} = \frac{2\pi S^0}{k_{0x}^2 D k_{0y}}\left(\frac{k_y}{k_{0y}}\right)^{-2}\left[1 - J_0\left(\frac{k_y}{k_{0y}}\right)\right]. \tag{7.18}$$

These results are the same as those given by Sydora et al.[23] The essential point in these approximations is that the $\boldsymbol{x}_-$ dependence of the two-point correlation function and the $\boldsymbol{k}$ dependence of the wavenumber spectrum are determined only by the clump lifetime. It is directly related to the propagator describing the evolution of the fluctuation and therefore the same propagator gives the same form of the wavenumber spectrum independent of the form of the function $s(\boldsymbol{x}, t)$ in Eq.(6.1).

Next we calculate the turbulent diffusivity D. Up to now, we treated the pressure equation (7.1) only, but hereafter we need to consider the vorticity equation (7.2). The time evolution of the kinetic energy defined by

$$E_K \equiv \frac{1}{2}\int d^3x \rho_m \left(\frac{c}{B_0}\nabla_\perp\phi\right)^2, \tag{7.19}$$

is obtained from Eq.(7.2):

$$\begin{aligned}\frac{d}{dt}E_K &= \int d^3x \left[\tilde{p}v_x\frac{d\Omega}{dx} - \frac{1}{\eta}(\nabla_\parallel\phi)^2\right] \\ &= \int dx \int \frac{d^2k}{(2\pi)^2}\left[i\frac{c}{B_0}\frac{d\Omega}{dx}k_y\tilde{p}_{\boldsymbol{k}}\phi_{-\boldsymbol{k}} - \frac{1}{\eta}k_\parallel^2|\phi_{\boldsymbol{k}}|^2\right],\end{aligned} \tag{7.20}$$

where $\tilde{p}_{\boldsymbol{k}}$ and $\tilde{\phi}_{\boldsymbol{k}}$ stand for the Fourier components with the wavenumber $\boldsymbol{k} = (k_y, k_z)$ and $k_\parallel = \boldsymbol{k}\cdot\boldsymbol{B}_0/B_0$. The first term in the right-hand side represents the change of the energy caused by the convective motion in the presence of the effective gravity corresponding to the average curvature due to the helical magnetic field and the second term the sink of energy by the Ohmic dissipation. We consider the stationary state, $d\langle E_k\rangle/dt = 0$. Hence we balance the first term with the second term in the right-hand side of Eq.(7.20) as

$$i\frac{c}{B_0}\frac{d\Omega}{dx}k_y\tilde{p}_{\boldsymbol{k}} \simeq \frac{1}{\eta}\frac{k_y^2}{L_s^2 k_{0x}^2}\phi_{\boldsymbol{k}}. \tag{7.21}$$

Here we used $k_\parallel \simeq k_y(x - x_2(\boldsymbol{k}))/L_s \simeq k_y/(L_s k_{0x})$, where $x_s(\boldsymbol{k})$ is the position of the mode resonant surface defined by $k_\parallel(x = x_s(\boldsymbol{k})) = 0$. The relation

(7.21) shows that the phase difference between $\phi_{\boldsymbol{k}}$ and $p_{\boldsymbol{k}}$ is $\pi/2$. It is related to the parity conservation in the reduced MHD model Eqs.(7.1) and (7.2) with respect to the (y,z)-space (see Appendix 7.A). From Eqs.(7.6) and (7.21), we obtain

$$\begin{aligned} S^0 &= 2\frac{c}{B_0}\left(-\frac{dp_0}{dx}\right)\int \frac{d^2k}{(2\pi)^2} k_y \Im\langle\phi\tilde{p}\rangle_{\boldsymbol{k}} \\ &\simeq 2\left(\frac{c}{B_0}\right)^2\left(-\frac{dp_0}{dx}\right)\left(\frac{d\Omega}{dx}\right)\eta L_s^2 k_{0x}^2 \int \frac{d^2k}{(2\pi)^2}\langle\tilde{p}\tilde{p}\rangle_{\boldsymbol{k}}. \end{aligned} \tag{7.22}$$

where $\Im$ denotes the imaginary part of the complex valuable. Substituting this into Eq.(7.15) yields

$$\langle\tilde{p}\tilde{p}\rangle_{\boldsymbol{k}} = \frac{8\pi I(\boldsymbol{k})}{D k_{0y} k_{0z}}\left(\frac{c}{B_0}\right)^2\left(-\frac{dp_0}{dx}\right)\left(\frac{d\Omega}{dx}\right)\eta L_s^2 \int \frac{d^2k'}{(2\pi)^2}\langle\tilde{p}\tilde{p}\rangle_{\boldsymbol{k}'}. \tag{7.23}$$

Integrating both sides of this equation over $\boldsymbol{k}$, we obtain the turbulent diffusivity

$$\begin{aligned} D &= \left(\frac{c}{B_0}\right)^2 \eta\left(-\frac{dp_0}{dx}\right)\left(\frac{d\Omega}{dx}\right) L_s^2 \left(\frac{2}{\pi}\int\frac{dk_y}{k_{0y}}\int\frac{dk_z}{k_{0z}} I(\boldsymbol{k})\right) \\ &= 4\left(\frac{c}{B_0}\right)^2 \eta\left(-\frac{dp_0}{dx}\right)\left(\frac{d\Omega}{dx}\right) L_s^2. \end{aligned} \tag{7.24}$$

In the case of toroidal configuration, x-axis corresponds to the minor radial direction, y-axis the poloidal direction and z-axis the toroidal direction, respectively. In this case, $L_s = Rq/s$, where R is a major radius, q a safety factor, $s \equiv (r/q)(dq/dr)$ a shear parameter of the magnetic field and r a minor radius. Thus Eq.(7.24) is expressed as

$$D = 4D_{cl}\frac{q^2}{\epsilon^2}\left(\frac{r}{q}\frac{dq}{dr}\right)^{-2}\left(\frac{-r}{p_0}\frac{dp_0}{dr}\right)\left(r\frac{d\Omega}{dr}\right), \tag{7.25}$$

where $D_{cl} = (c^2 p_0/B_0^2)\eta$ is a classical diffusion coefficient, $\epsilon = r/R$ an inverse aspect ratio. Eqs.(7.24) and (7.25) agree with the result of the scale invariance method [12] or $D = \gamma/k_\perp^2$-type mixing length argument.[23] The constant factor 4 obtained by the two-point renormalized theory is not as large as that obtained by Carreras et al.[25] by combining the one-point renormalized theory with the marginal stability analysis including dissipations to suppress high mode number instabilities.

7.3 Resistive Interchange Mode Turbulence Coupled to Resistive Drift Waves

Here we apply the renormalized theory given in Chapter 6 to the Hasegawa-Wakatani equations which describe the resistive interchange mode coupled to the resistive drift wave. The model consists of the electron continuity equation:

$$\left(\frac{\partial}{\partial t}+\boldsymbol{v}\cdot\nabla\right)n^*=\kappa_{\|}\nabla_{\|}^2(n^*-\phi^*)+\rho_s c_s\nabla\ln n_0\times\nabla\phi^*\cdot\hat{z}+\rho_s c_s\nabla(n^*-\phi^*)\times\nabla\Omega\cdot\hat{z}, \tag{7.26}$$

and the vorticity equation:

$$\rho_s^2\left(\frac{\partial}{\partial t}+\boldsymbol{v}\cdot\nabla\right)\nabla_{\perp}^2\phi=\kappa_{\|}\nabla_{\|}^2(n^*-\phi^*)+\rho_s c_s\nabla n^*\times\nabla\Omega\cdot\hat{z}. \tag{7.27}$$

Here n^* and ϕ^* are normalized density fluctuation and normalized electrostatic potential defined by

$$n^*\equiv\ln(n/n_0)=\ln(1+\tilde{n}/n_0)\simeq\tilde{n}/n_0 \tag{7.28}$$

and

$$\phi^*\equiv e\phi/T_e, \tag{7.29}$$

where $n\equiv n_0+\tilde{n}$ is the total density, $n_0\equiv\langle n\rangle$ the average part and $\tilde{n}$ the fluctuating part. The velocity $\boldsymbol{v}$ is the same as Eq.(7.3) and is written as

$$\boldsymbol{v}=-\rho_s c_s\nabla\phi^*\times\hat{z}, \tag{7.30}$$

$\kappa_{\|}\equiv T_e/(m_e\nu_{e\|})$ is a diffusion coefficient along the magnetic field line, $\nu_{e\|}$ a parallel electron collision frequency, $\rho_s\equiv c_s/\omega_{ci}$ an effective ion Larmor radius, $c_s\equiv(T_e/m_i)^{1/2}$ an ion sound velocity, ω_{ci} an ion cyclotron frequency and $\rho_s c_s\equiv cT_e/(eB_0)$. In our model, the generalized Ohm's law in the electrostatic limit is employed and the electron motion along the field line is included; however, the ion parallel motion is assumed negligible.

The one-point and two-point renormalized theories in Chapter 6 are applicable to the density equation (7.26), which can be written in the form of Eq.(6.1):

$$\left(\frac{\partial}{\partial t}+\boldsymbol{v}\cdot\nabla-\kappa_{\|}\nabla_{\|}^2+\rho_s c_s\frac{d\Omega}{dx}\frac{\partial}{\partial y}\right)n^*=\left(\rho_s c_s\left(\frac{d\Omega}{dx}+\frac{d\ln n_0}{dx}\right)\frac{\partial}{\partial y}-\kappa_{\|}\nabla_{\|}^2\right)\phi^*. \tag{7.31}$$

The one-point renormalized equation for Eq.(7.31) is obtained from Eq.(6.20) as

$$\left(\frac{\partial}{\partial t} - \nabla \cdot \mathsf{D} \cdot \nabla - \kappa_{\|}\nabla_{\|}^2 - \rho_s c_s \frac{d\Omega}{dx}\frac{\partial}{\partial y}\right) n^{*c} = \left(\rho_s c_s \left(\frac{d\Omega}{dx} + \frac{d\ln n_0}{dx}\right)\frac{\partial}{\partial y} - \kappa_{\|}\nabla_{\|}^2\right)\phi^*, \tag{7.32}$$

where n^{*c} is the coherent part of n^* and D has the same form as that defined by Eq.(6.16). It is useful to define Raynolds number as the ratio of the nonlinear perpendicular diffusion term to the parallel diffusion term[21],[22],[24]:

$$\mathrm{Re} \equiv \frac{D k_{0x}^4 L_s^2}{k_{0y}^2 \kappa_{\|}} = \frac{\tau_d}{\tau_c}, \tag{7.33}$$

where $\tau_c \equiv (k_{0x}^2 D)^{-1}$ is the nonlinear coherent time, $\tau_d \equiv (k_{0y}^2 \kappa_{\|}/k_{0x}^2 L_s^2)^{-1}$ the parallel diffusion time and k_{0x}, k_{0y}, L_s and D are the same as those in Sec.7.2 (see Eq.(7.9)). By using Eq.(6.32), the two-point renormalized equaiton becomes

$$\left[\frac{\partial}{\partial t} - \sum_{i,j=1,2} \nabla_i \cdot \mathsf{D}(i,j) \cdot \nabla_j - \kappa_{\|}(\nabla_{\|1}^2 + \nabla_{\|2}^2)\right] \langle n^*(1) n^*(2)\rangle = S(1,2), \tag{7.34}$$

where the source term in the right-hand side is

$$S(1,2) \equiv \left[\rho_s c_s \left(\frac{d\Omega}{dx} + \frac{d\ln n_0}{dx}\right)\frac{\partial}{\partial y_1} - \kappa_{\|}\nabla_{\|1}^2\right] \langle \phi^*(1) n^*(2)\rangle + (1 \leftrightarrow 2). \tag{7.35}$$

Here we assumed that $d\Omega/dx$ and $d\ln n_0/dx$ are constants and that correlation function such as $\langle n^*(1)n^*(2)\rangle$ and $\langle \phi^*(1)\phi^*(2)\rangle$ are independent of the centric coordinates $y_+ \equiv (y_1 + y_2)/2$ and $z_+ \equiv (z_1 + z_2)/2$ because of translational symmetry in the y and z directions. It is noted that the operator in the left-hand side of Eq.(7.34) is the same as that studied by Diamond et al. in the analyses for the resistivity-gradient-driven turbulence [22] and the ion temperature-gradient-driven turbulence.[24] In Eq.(7.34), the parallel diffusion operator can be written as

$$\begin{aligned} \kappa_{\|}(\nabla_{\|1}^2 + \nabla_{\|2}^2) &= -\kappa_{\|} \sum_{\boldsymbol{k}} (k_{\|1}^2 + k_{\|2}^2) \\ &= -\kappa_{\|} \sum_{\boldsymbol{k}} \frac{k_y^2}{L_s^2}[(x_1 - x_s(\boldsymbol{k}))^2 + (x_2 - x_s(\boldsymbol{k}))^2] \end{aligned}$$

$$= -\kappa_{\|} \sum_{\boldsymbol{k}} \frac{k_y^2}{L_s^2} [2(x_+ - x_s(\boldsymbol{k}))^2 + \frac{1}{2} x_-^2]$$

$$\simeq -\frac{\kappa_{\|}}{L_s^2} \left(2\Delta^2 + \frac{1}{2} x_-^2 \right) \frac{\partial^2}{\partial y_-^2}, \tag{7.36}$$

where $x_+ - x_s(\boldsymbol{k})$ is replaced with the radial scale of correlation Δ. From Eqs.(6.44) and (6.45), Green's function is defined by

$$\left[\frac{\partial}{\partial t} - \frac{\partial}{\partial x_-} D_- \frac{\partial}{\partial x_-} - \frac{\kappa_{\|}}{L_s^2} \left(2\Delta^2 + \frac{1}{2} x_-^2 \right) \frac{\partial^2}{\partial y_-^2} \right] g_t(\boldsymbol{x}_- | \boldsymbol{x}'_-) = 0, \tag{7.37}$$

with $g_{t=0}(\boldsymbol{x}_- | \boldsymbol{x}'_-) = \delta(\boldsymbol{x}_- - \boldsymbol{x}'_-)$, where the components of the relative diffusion tensor D_- except $D_- \equiv (\mathsf{D}_-)_{xx}$ are assumed to be negligible. Taking the moments of Eq.(7.37) by multiplying x_-^2 or y_-^2 and using Eqs.(6.46), (7.9) and (7.10) yields the differential equation for the normalized relative separation between two points:

$$\frac{\partial^2}{\partial t^2} \langle R_-^2(t) \rangle - \frac{2}{\tau_c} \frac{\partial}{\partial t} \langle R_-^2(t) \rangle - \frac{2}{\tau_d \tau_c} \langle R_-^2(t) \rangle = 0 \tag{7.38}$$

with the initial conditions:

$$\langle R_-^2(t=0) \rangle = k_{0x}^2 x_-^2 + k_{0y}^2 y_-^2 + k_{0z}^2 z_-^2 \equiv R_-^2, \tag{7.39}$$

and

$$\left. \frac{\partial}{\partial t} \langle R_-^2(t) \rangle \right|_{t=0} = \frac{2}{\tau_c} R_-^2 + \frac{k_{0x}^2}{\tau_d} (4\Delta^2 + x_-^2). \tag{7.40}$$

Here $\boldsymbol{x}_-$ denotes $\boldsymbol{x}_-(t=0)$. Solving these equations, we have

$$\langle R_-^2(t) \rangle = A e^{u_+ t} + B e^{u_- t}, \tag{7.41}$$

where

$$u_\pm = \frac{1}{\tau_c} \left(1 \pm \sqrt{1 + 2\mathrm{Re}^{-1}} \right), \tag{7.42}$$

$$A = \frac{1}{u_+ - u_-} \left(\left. \frac{\partial}{\partial t} \langle R_-^2(t) \rangle \right|_{t=0} - u_- R_-^2 \right), \tag{7.43}$$

and

$$B = \frac{1}{u_+ - u_-} \left(u_+ R_-^2 - \left. \frac{\partial}{\partial t} \langle R_-^2(t) \rangle \right|_{t=0} \right). \tag{7.44}$$

Since $u_+ > 0 > u_-$, we approximate the solution with the dominant term:

$$\langle R_-^2(t)\rangle \simeq A\mathrm{e}^{u_+ t}. \tag{7.45}$$

Thus from Eq.(7.43),

$$A = C[\alpha k_{0x}^2 \cdot 4\Delta^2 + (1+\alpha)k_{0x}^2 x_-^2 + k_{0y}^2 y_-^2 + k_{0z}^2 z_-^2], \tag{7.46}$$

and

$$\alpha \equiv \frac{\mathrm{Re}^{-1}}{1+\sqrt{1+2\mathrm{Re}^{-1}}}, \qquad C \equiv \frac{1+\sqrt{1+2\mathrm{Re}^{-1}}}{2\sqrt{1+2\mathrm{Re}^{-1}}} \tag{7.47}$$

are obtained. Eq.(7.45) and $\langle R_-^2(t=\tau_{cl})\rangle = 1$ give the clump lifetime,

$$\tau_{cl}(\boldsymbol{x}_-) = \begin{cases} \dfrac{\tau_c}{1+\sqrt{1+2\mathrm{Re}^{-1}}} \ln\left\{\dfrac{1}{C[\alpha k_{0x}^2 \cdot 4\Delta^2 + (1+\alpha)k_{0x}^2 x_-^2 + k_{0y}^2 y_-^2 + k_{0z}^2 z_-^2]}\right\} \\ \qquad (\text{ arg of ln} > 1\ ) \\ 0 \qquad\qquad (\text{ otherwise }). \end{cases} \tag{7.48}$$

We fined that, in the large Reynolds number limit, $\alpha \to 0$ and $C \to 1$ from Eq.(7.47) and the clump lifetime given by Eq.(7.48) coincides with that given by Eq.(7.13) since the parallel diffusion is neglected in this limit and the two Green's functions defined by Eqs.(7.8) and (7.37) become identical. Thus, as mentioned in Sec.7.2, the wavenumber spectrum of the density fluctuation has the same form as that given by Eq.(7.15) in this limit. However, when the Reynolds number is small, the parallel diffusion term becomes important and makes the clump lifetime at $\boldsymbol{x}_- = 0$ finite in contrast with the case of the large Reynolds number. The approximate solution to the two-point renormalized equation is given by

$$\langle n^*(1)n^*(2)\rangle \simeq \tau_{cl}(\boldsymbol{x}_-)S^0, \tag{7.49}$$

where the same approximation as in Eq.(7.14) is employed. Using Eq.(7.49), we obtain the wavenumber spectrum:

$$\langle n^* n^*\rangle_{\boldsymbol{k}} \equiv \int \frac{dx_-}{\Delta} \int dy_- \int dz_- \mathrm{e}^{-ik_y y_- - ik_z z_-} \langle n^*(1)n^*(2)\rangle$$

$$= S^0 \int \frac{dx_-}{\Delta} \int dy_- \int dz_- \mathrm{e}^{-ik_y y_- - ik_z z_-} \tau_{cl}(\boldsymbol{x}_-)$$
$$= \frac{8\pi\tau_c S^0}{\left(1+\sqrt{1+2\mathrm{Re}^{-1}}\right) k_{0y}k_{0z}} F(\boldsymbol{k}), \tag{7.50}$$

where

$$F(\boldsymbol{k}) \equiv \frac{1}{C\Delta k_{0x}\sqrt{(1+\alpha)C}} \int_0^\xi \rho d\rho J_0(\beta\rho/\sqrt{C})$$
$$\times \left(\sqrt{\xi^2-\rho^2} - \sqrt{1+\rho^2-\xi^2}\cos^{-1}\sqrt{1+\rho^2-\xi^2}\right), \tag{7.51}$$

with

$$\xi^2 \equiv 1 - C\alpha k_{0x}^2 \cdot 4\Delta^2 \qquad \beta = \sqrt{(k_y/k_{0y})^2 + (k_z/k_{0z})^2}. \tag{7.52}$$

As mentioned above, this has the same form as Eq.(7.15) when $\mathrm{Re} \to \infty$.

In order to evaluate the turbulent diffusivity D, we use the following time evolution equation of the fluctuation energy obtained from the model equations (7.26) and (7.27),

$$\frac{d}{dt}(E_n + E_K)$$
$$= \int d^3x \left[\rho_s c_s \frac{d\ln n_0}{dx} n^* \frac{\partial\phi^*}{\partial y} - \kappa_{\|}|\nabla_{\|}(n^*-\phi^*)|^2\right]$$
$$= \int dx \int \frac{d^2k}{(2\pi)^2} \left[\rho_s c_s \left(-\frac{d\ln n_0}{dx}\right) k_y \Im(\phi^*_{\boldsymbol{k}} n^*_{-\boldsymbol{k}}) - \kappa_{\|} k_{\|}^2 |n^*_{\boldsymbol{k}} - \phi^*_{\boldsymbol{k}}|^2\right], \tag{7.53}$$

where

$$E_n \equiv \frac{1}{2}\int d^3x n^{*2}, \qquad E_K \equiv \frac{1}{2}\int d^3x \rho_s^2 (\nabla_\perp \phi)^2. \tag{7.54}$$

Since the stationary turbulence is considered, $d(\langle E_n\rangle + \langle E_K\rangle)/dt = 0$. Hence we balance the first term with the second term in the integrand of Eq.(7.53),

$$\rho_s c_s \left(-\frac{d\ln n_0}{dx}\right) k_y \Im(\phi^*_{\boldsymbol{k}} n^*_{-\boldsymbol{k}}) \simeq \kappa_{\|} \frac{k_y^2}{L_s^2 k_{0x}^2} |n^*_{\boldsymbol{k}} - \phi^*_{\boldsymbol{k}}|^2, \tag{7.55}$$

where we used $k_{\|} \simeq k_y/(L_s k_{0x})$. In contrast to the reduced MHD model, our model equations (7.26) and (7.27) do not have the symmetry of the parity in (y,z)-space and therefore the phase difference between $\phi^*_{\boldsymbol{k}}$ and $n^*_{\boldsymbol{k}}$ is different from $\pi/2$. It is assumed that

$$n^*_{\boldsymbol{k}} = R_{\boldsymbol{k}} \phi^*_{\boldsymbol{k}} \mathrm{e}^{-i\delta_{\boldsymbol{k}}}, \tag{7.56}$$

where $R_{\boldsymbol{k}}$ is a real function and $\delta_{\boldsymbol{k}}$ denotes the phase difference. Substituting this into Eq.(7.55) and assuming that $|R_{\boldsymbol{k}}| \ll 1$, we obtain

$$R_{\boldsymbol{k}} \simeq \frac{\kappa_{\|} k_y^2/(L_s^2 k_{0x}^2)}{k_y \rho_s c_s (-d\ln n_0/dx)\sin\delta_{\boldsymbol{k}}} = \frac{1}{\omega_{*\boldsymbol{k}} \tau_{d\boldsymbol{k}} \sin\delta_{\boldsymbol{k}}}. \tag{7.57}$$

where $\omega_{*\boldsymbol{k}} \equiv k_y \rho_s c_s (-d\ln n_0/dx)$ is the electron diamagnetic drift frequency and $\tau_{d\boldsymbol{k}} \equiv L_s^2 k_{0x}^2/(\kappa_{\|} k_y^2)$ the parallel diffusion time for the mode with the wavenumber $\boldsymbol{k}$. $|R_{\boldsymbol{k}}| \ll 1$ means that $\delta_{\boldsymbol{k}}$ is not close to zero. Nonlinear calculations of our model equations confirm $|R_{\boldsymbol{k}}| \ll 1$ or $|\phi^*_{\boldsymbol{k}}| \gg |n^*_{\boldsymbol{k}}|$ for the case of $d\Omega/dx > 0$.[32],[43] From Eqs.(7.35), (7.56) and (7.57), we obtain

$$\begin{aligned} S^0 &= 2\rho_s c_s \left(-\frac{d\ln n_0}{dx} - \frac{d\Omega}{dx}\right) \int \frac{d^2k}{(2\pi)^2} k_y \Im\langle \phi^* n^* \rangle_{\boldsymbol{k}} \\ &\quad + 2\kappa_{\|} \int \frac{d^2k}{(2\pi)^2} k_{\|}^2 \Re\langle \phi^* n^* \rangle_{\boldsymbol{k}} \\ &= 2\rho_s^2 c_s^2 \left(-\frac{d\ln n_0}{dx} - \frac{d\Omega}{dx}\right)\left(-\frac{d\ln n_0}{dx}\right) \frac{L_s^2 k_{0x}^2}{\kappa_{\|}} \int \frac{d^2k}{(2\pi)^2} \langle n^* n^* \rangle_{\boldsymbol{k}} \sin^2\delta_{\boldsymbol{k}}. \end{aligned} \tag{7.58}$$

where $\sin\delta_{\boldsymbol{k}} > R_{\boldsymbol{k}} \cos\delta_{\boldsymbol{k}}$ is assumed and the second term proportional to $\kappa_{\|}$ becomes small for $|R_{\boldsymbol{k}}| \ll 1$. Substituting this into Eq.(7.50), we obtain

$$\begin{aligned} \langle n^* n^* \rangle_{\boldsymbol{k}} &= \frac{16\pi S^0 F(\boldsymbol{k})}{\left(1+\sqrt{1+2\mathrm{Re}^{-1}}\right) k_{0y} k_{0z}} \rho_s^2 c_s^2 \left(-\frac{d\ln n_0}{dx} - \frac{d\Omega}{dx}\right) \\ &\quad \times \left(-\frac{d\ln n_0}{dx}\right) \frac{L_s^2}{D\kappa_{\|}} \int \frac{d^2k'}{(2\pi)^2} \langle n^* n^* \rangle_{\boldsymbol{k}'} \sin^2\delta_{\boldsymbol{k}'}. \end{aligned} \tag{7.59}$$

Integrating the both sides of this equation over $\boldsymbol{k}$, we obtain the turbulent diffusivity

$$D = \rho_s^2 c_s^2 \left(-\frac{d\ln n_0}{dx} - \frac{d\Omega}{dx}\right)\left(-\frac{d\ln n_0}{dx}\right) \frac{L_s^2}{\kappa_{\|}} \left(\frac{2}{\pi} \int \frac{dk_y}{k_{0y}} \int \frac{dk_z}{k_{0z}} F(\boldsymbol{k}) \sin^2\delta_{\boldsymbol{k}}\right)$$

$$= 4\rho_s^2 c_s^2 \left(-\frac{d\ln n_0}{dx} - \frac{d\Omega}{dx}\right)\left(-\frac{d\ln n_0}{dx}\right)\frac{L_s^2}{\kappa_\parallel}\sin^2\delta_{\boldsymbol{k}_0}, \tag{7.60}$$

where we assumed that $\sin^2\delta_{\boldsymbol{k}} \simeq \sin^2\delta_{\boldsymbol{k}_0}$ by using a representative phase difference $\delta_{\boldsymbol{k}_0}$ and $\mathrm{Re} \gg 1$, which is consistent with $|R_{\boldsymbol{k}}| \ll 1$. In a cylindrical configuration, this is expressed as

$$D = 4D_{cl}\frac{q^2}{\epsilon^2}\left(\frac{r}{q}\frac{dq}{dr}\right)^{-2}\left(\frac{-r}{n_0}\frac{dn_0}{dr} - r\frac{d\Omega}{dr}\right)\left(\frac{-r}{n_0}\frac{dn_0}{dr}\right)\sin^2\delta_{\boldsymbol{k}_0}. \tag{7.61}$$

Usually the scale length of the density gradient is shorter than that of magnetic curvature in stellarator/heliotron or $|(r/n_0)(dn_0/dr)| \gg |rd\Omega/dr|$. Then Eq.(7.61) reduces to

$$D = 4D_{cl}\frac{q^2}{\epsilon^2}\left(\frac{r}{q}\frac{dq}{dr}\right)^{-2}\left(\frac{-r}{n_0}\frac{dn_0}{dr}\right)^2\sin^2\delta_{\boldsymbol{k}_0}. \tag{7.62}$$

which is identical to the results of Yagi et al.[12] obtained by applying the scale invariance argument to Eqs.(7.26) and (7.27) with $\nabla\Omega = 0$. We will examine a different assumption for the relation between $n_{\boldsymbol{k}}^*$ and $\phi_{\boldsymbol{k}}^*$, i.e., $|R_{\boldsymbol{k}}| \sim 1$. In this case,

$$2\tan\frac{\delta_{\boldsymbol{k}}}{2} \simeq k_y\rho_s c_s\left(-\frac{d\ln n_0}{dx}\right)\frac{L_s^2 k_{0x}^2}{\kappa_\parallel k_y^2} = \omega_{*\boldsymbol{k}}\tau_{d\boldsymbol{k}}. \tag{7.63}$$

By using Eqs.(7.35), (7.63) and $|R_{\boldsymbol{k}}| \sim 1$ and assuming that $|d\ln n_0/dx| > |d\Omega/dx|$, the source term beocmes

$$S^0 = 2\kappa_\parallel\frac{k_y^2}{L_s^2 k_{0x}^2}\int\frac{d^2k}{(2\pi)^2}\langle n^* n^*\rangle_{\boldsymbol{k}}\left(1 + 2\sin^2\frac{\delta_{\boldsymbol{k}}}{2}\right). \tag{7.64}$$

where $k_\parallel \simeq k_{0y}/(L_s k_{0x})$ is used. It is remarked that $\tau_c S^0$ in Eq.(7.50) is proportional to Re^{-1} in this case and Eq.(7.50) gives only the Reynolds number. It is impossible to estimate the turbulent diffusivity and the fluctuation level within the context of the renormalized theory in Chapter 6. A similar example was discussed by Terry and Diamond[21] for the resistive drift wave turbulence and an additional assumption was introduced to determine the turbulent diffusivity.

7.4 Conclusions

The clump lifetime approximation to obtain the solution of the two-point renormalized equation was employed to evaluate the wavenumber spectrum and the turbulent diffusivity in the resistive interchange mode turbulence described by the ordinary reduced MHD model and the resistive drift and the resistive interchange mode turbulence by the reduced two-fluid model. The form of the wavenumber spectrum is essentially determined by the clump lifetime and thus depends only on the form of the propagator for the fluctuation. In addition to the clump lifetime approximation, the second equation, which determines the relation between the electrostatic potential and the pressure or density fluctuation, is required for the calculation of the turbulent diffusivity. In order to obtain this relation, Lee and Diamond et al.[24] relied on the argument such as the balance between the dominant terms in the energy evolution equation, which is essentially the same as the mixing length estimation. Terry et al.[22] gave an approximation that the mode structure satisfies the relation between the pressure and the potential involved in the reduced MHD equation.

In the reduced MHD model, we followed Lee and Diamond to obtain the relation between the electrostatic potential and the pressure fluctuation. We used the fact that the phase difference is $\pi/2$ due to the parity conservation with respect to the (y, z)-space. The resulting expression for the turbulent diffusivity agrees with that obtained by the mixing length argument or the scale invariance approach as for the parameter dependence. A constant factor in the expression of turbulent diffusivity, which cannot be determined by the scale invariance, is about 4 by the two-point renormalized theory. This value is smaller than that obtained by Carreras et al. by combining the one-point renormalized theory with the marginal stability analysis.[25]

In the Hasegawa-Wakatani equations, which include the electron parallel motion and variable phase difference between the potential and density fluctuation, the loss of parity conservation makes it difficult to determine the diffusivity in contrast with the case of the reduced MHD model. The equation relating the potential to the density fluctuation cannot be obtained only by the balance between the terms in the energy evolution equation and the additional consideration about the phase difference is required to obtain the diffusivity. Since experimental data of the edge turbulence show that the typical phase difference lies between zero and $\pi/2$, the Hasegawa-Wakatani

model is more promising to explain the observed edge turbulence in Heliotron E than the RMHD model.

Though the two-point renormalized theory for studying turbulent diffusion developed in Refs.[21]–[24] is systematic and quantitative, the second equation giving the relation between the different fluctuations required for calculating the turbulent diffusivity is still heuristic. We need further study for this point.

7.A The Parity Conservation in the Reduced MHD Model

Equations (7.1) and (7.2) can be written as

$$\frac{\partial}{\partial t}\boldsymbol{\Phi} = \boldsymbol{F}[\boldsymbol{\Phi}], \tag{7.65}$$

where

$$\boldsymbol{\Phi}(x,y,z,t) \equiv \begin{bmatrix} \tilde{p}(x,y,z,t) \\ (\nabla_\perp^2\phi)(x,y,z,t) \end{bmatrix}, \tag{7.66}$$

and $\boldsymbol{F}$ represents a nonlinear operator on $\boldsymbol{\Phi}$

$$\boldsymbol{F}[\boldsymbol{\Phi}] \equiv \begin{bmatrix} \dfrac{c}{B_0}\left(\nabla\phi\times\hat{z}\cdot\nabla\tilde{p} + \dfrac{\partial\phi}{\partial y}\dfrac{dp_0}{dx}\right) \\ \dfrac{B_0}{\rho_m c}\left(\dfrac{c}{B_0}\nabla\phi\times\hat{z}\cdot\nabla\nabla_\perp^2\phi - \dfrac{B_0}{c\eta}\nabla_\parallel^2\phi - \dfrac{d\Omega}{dx}\dfrac{\partial\tilde{p}}{\partial y}\right) \end{bmatrix}. \tag{7.67}$$

Now, we define a parity operator $\boldsymbol{P}$ by

$$\boldsymbol{P}[\boldsymbol{\Phi}] \equiv \begin{bmatrix} \tilde{p}(x,-y,-z) \\ -(\nabla_\perp^2\phi)(x,-y,-z) \end{bmatrix}. \tag{7.68}$$

Eqs.(7.67) and (7.68) give

$$\boldsymbol{F}\boldsymbol{P} = \boldsymbol{P}\boldsymbol{F}. \tag{7.69}$$

From Eq.(7.69), we have

$$\frac{\partial}{\partial t}\boldsymbol{P}\boldsymbol{\Phi} = \boldsymbol{F}[\boldsymbol{P}\boldsymbol{\Phi}], \tag{7.70}$$

for an arbitrary solution $\boldsymbol{\Phi}(x,y,z,t)$ of Eq.(7.65). Thus, we find that

$$\boldsymbol{P}\boldsymbol{\Phi} = \boldsymbol{\Phi}, \tag{7.71}$$

is valid at arbitrary time if it is satisfied at initial time because of the uniqueness of the solution with respect to the initial condition. For Fourier modes $\{\tilde{p}_{\boldsymbol{k}}, \phi_{\boldsymbol{k}}\}$, we obtain

$$\begin{aligned} &\tilde{p}_{\boldsymbol{k}} = \tilde{p}_{-\boldsymbol{k}} = \tilde{p}_{\boldsymbol{k}}^* = (\text{real function}) \\ &\phi_{\boldsymbol{k}} = -\phi_{-\boldsymbol{k}} = -\phi_{\boldsymbol{k}}^* = (\text{pure imaginary function}), \end{aligned} \tag{7.72}$$

from Eqs.(7.68) and (7.71). Thus, we find that the phase diference between $\tilde{p}_{\boldsymbol{k}}$ and $\phi_{\boldsymbol{k}}$ is $\pi/2$.

The parity conservation (7.69) is related to the facts that the full MHD equations are invariant with respect to the reversal of directions for magnetic field $\boldsymbol{B}$, current $\boldsymbol{j}$ and electric field $\boldsymbol{E}$:

$$(\boldsymbol{B}, \boldsymbol{j}, \boldsymbol{E}) \to (-\boldsymbol{B}, -\boldsymbol{j}, -\boldsymbol{E}), \tag{7.73}$$

and that the system under consideration is invariant with the transform of variables, $(y, z) \to (-y, -z)$, since we have assumed that p_0 and Ω depend only on x. It is noted that the invariance with respect to (7.73) is not valid in the generalized Ohm's law and therefore the symmetry like Eq.(7.69) does not exist in the model equations (7.26) and (7.27). This is related to the appearance of the terms with $(n^* - \phi^*)$ in Eqs.(7.26) and (7.27).

Chapter 8

Concluding Remarks

In this thesis we have studied linear and nonlinear properties of the ideal and resistive interchange instabilities based on the fluid descriptions of the toroidally confined plasma. As a fluid model we have derived the reduced two-fluid model which can correctly describe the ion and electron diamagnetic drift. These effects are not included in the single fluid MHD model but they are not negligible in the high temperature plasma produced in the present and future large devices. Our model for the large aspect ratio toroidal plasmas applicable to both stellarators and tokamaks obeys the physically reasonable energy balance law and has several familiar reduced fluid models such as RMHD, Hasegawa-Mima and Hasegawa-Wakatani equations as limiting forms. Thus we can remark that our model is a general and self-consistent one which deserves further analytical and numerical studies.

Based on the reduced two-fluid model, the stabilizing effects of the ion diamagnetic drift on the ideal interchange instabilities have been studied both analytically and numerically. We have found that the dispersion relation and the stability criterion obtained by the local mode analysisi agree with the results of the numerical calculation using the shooting method. The stabilization by the ion diamagnetic drift is related to restoring the Boltzmann distribution for ions under the isothermal assumption. As an example Heliotron E currentless plasma with the equilibrium pressure profile of the form $p(r) = p(0)(1 - (r/a)^2)$ is considered. It was shown that the stability beta limit determined by the $m = 1/n = 1$ ideal interchange mode is $\beta(0) = 2.2\%$ in the ideal MHD case with no ion diamagnetic drift effects. It can be improved up to $\beta(0) = 5.1\%$ if those effects are included in the case

of the deuterium plasma with the average electron density $\bar{n}_e = 10^{13} cm^{-3}$.

By using Hasegawa-Wakatani equations including the average magnetic curvature of the helical field lines, we have found the resistive interchange instability coupled to the electron diamagnetic drift. This instability may explain the turbulence observed in the peripheral region of the Heliotron E plasma.[9] We have derived the dispersion relation for this localized instability by the sheared slab approximation, which is compared with the numerical calculation in the cylindrical geometry. It was shown that in the weakly collisional limit the real part of the eigenfrequency approaches to the curvature drift frequency and the imaginary part or the linear growth rate is proportional to the collision frequency. In this limit the phase difference between the density perturbation and the electrostatic potential goes from $\pi/4$ to $\pi/2$. It is interesting to compare these results with those obtained by the MHD model. In the MHD model the resistive interchange instability has the growth rate proportional to the 1/3 power of the collision frequency and the phase difference is always $\pi/2$.

The nonlinear evolution of the ideal and resistive interchange instabilities has been studied numerically. It was shown by the single-helicity nonlinear calculations that the ion diamagnetic drift lowers the saturation level of the ideal interchange modes and decreases the contributions from the higher harmonic modes to the total kinetic energy. These results are consistent with the linear dispersion relation which states that the stabilizing effects are stronger for higher mode numbers. The saturation is related to the flattening of the pressure profile around the mode resonant surface. By the multi-helicity nonlinear calculations using the Hasegawa-Wakatani equations, we have studied the electrostatic turbulence driven by the resistive interchange modes coupled to the electron diamagnetic drift. We have seen that in the saturation state the $m = 0$ mode becomes dominant and the stationary radial electric field is generated. This may be explained by the self-organization process[43] and the production of the $m = 0$ mode is not obtained by the conventional RMHD model. The decrease of the energy distributed over the high poloidal mode numbers due to the energy condensation to the $m = 0$ mode is expected to improve the particle confinement. The radial electric field produces the $\boldsymbol{E} \times \boldsymbol{B}$ shear flow in the poloidal direction , which may cause the secondary instability and make the characteristics of the turbulence more complex. These promblems are the subject of future studies.

We have presented the systematic formulation of the renormalized theo-

ries for the strong plasma turbulence. In our formulation we have considered the general model equation which includes the convective nonlinearity and derived the exact integral equation for the nonlinear propagator, from which the renormalized expansion of the propagator is obtained naturally by the iterative procedure. Based on this expansion, the one-point and two-point renormalized theories were given in a unified manner. The clump lifetime approximation to the solution of the two-point renormalized equation was explained. As an example, the renormalized theories were applied to the Vlasov equation. We found that the Dupree's results such as the resonance broadening and the clump lifetime in the phase space were reproduced.

Using the renormalized theories and the clump lifetime approximation, we have estimated the wavenumber spectrum and the turbulent diffusivity in the resistive interchange mode driven turbulence based on the conventional RMHD model and the Hasegawa-Wakatani model. We have found that the wavenumber spectra of the pressure or desity fluctuation take the similar forms in the both models while the turbulent diffusivities are different from each other. In the RMHD model the turbulent diffusivity is proportional to the product of the pressure gradient and the magnetic curvatuare. On the other hand in the Hasegawa-Wakatani model that is roughly proportional to the second power of the density gradient and therefore larger by the order of the aspect ratio $\epsilon^{-1} = R_0/a$. These predictions shoud be compared with the results of the numerical simulations or experiments in future studies. The phase difference between the density (or pressure) and potential fluctuation is $\pi/2$ in the RMHD model. Since experimental data of the edge turbulence show that the typical phase difference lies between zero and $\pi/2$, the Hasegawa-Wakatani model is more promising to explain the observed edge turbulence in Heliotron E than the RMHD model. In our derivations of the wavenumber spectrum and the turbulent diffusivity, several heuristic and qualitative arguments such as balancing between the dominant terms in the energy evolution equation are included in order to obtain the relation between the electrostatic potential and the pressure (or density) fluctuation. We remark that furthur developments of the renormalized theories are required to describe the plasma turbulence and the resultant anomalous transport with more quantitative accuracy.

Finally we will comments several points of implications of our results to the present or future experiments in helical systems. First is that the ion diamagnetic drift (or ion finite Larmor radius) effect might improve

stability against the interchange modes in high T_i and low density plasmas. In Heliotron E, comparison between a plasma with $T_i = 1 \sim 2keV$ and $\bar{n}_e = 2 \sim 3 \times 10^{13} cm^{-3}$ and a plasma with $T_i = 400 \sim 500eV$ and $\bar{n}_e = 5 \sim 6 \times 10^{13} cm^{-3}$ is possible to study the ion diamagnetic drift stabilization of the interchange modes. Second is that reduction of the density gradient in the magnetic hill region will be essential to decrease the anomalous transport driven by the resistive interchange turbulence in the future devices. Third point is that the radial electric field could modify the properties of turbulence and there is a possibility that the anomalous transport may be controlled by it. We hope that future experimental studies will reveal these points.

References

[1] H. R. Strauss, Phys. Fluids **19**, 134 (1976).

[2] H. R. Strauss, Phys. Fluids **20**, 1354 (1977).

[3] H. R. Strauss, Plasma Phys. **22**, 733 (1980).

[4] L. Spitzer, Jr., Phys. Fluids **1**, 253 (1958).

[5] K. Uo, Kakuyugo-Kenkyu **1**, 20 (1958).

[6] P. C. Liewer, Nucl. Fusion **25**, 543 (1985).

[7] E. Mazzucato, Phys. Rev. Lett. **36**, 792 (1976).

[8] C. M. Surko and R. E. Slusher, Phys. Rev. Lett. **37**, 1747 (1976).

[9] H. Zushi, T. Mizuuchi, O. Motojima, M. Wakatani, F. Sano, M. Sato, A. Iiyoshi, and K. Uo, Nucl. Fusion **28**, 433 (1988).

[10] J. W. Connor and J. B. Taylor, Nucl. Fusion **17**, 1047 (1977).

[11] J. W. Connor and J. B. Taylor, Phys. Fluids **27**, 2676 (1984).

[12] M. Yagi, M. Wakatani, and A. Hasegawa, J. Phys. Soc. Jpn. **56**, 973 (1987).

[13] M. Yagi, M. Wakatani, and K. C. Shaing, J. Phys. Soc. Jpn. **57**, 117 (1988).

[14] J. W. Connor, Plasma Phys. Contr. Fusion **30**, 619 (1988).

[15] T. H. Dupree, Phys. Fluids **9**, 1773 (1966).

[16] T. H. Dupree, Phys. Fluids **10**, 1049 (1967).

[17] T. H. Dupree, Phys. Fluids **11**, 2680 (1968).

[18] T. H. Dupree, Phys. Fluids **15**, 334 (1972).

[19] J. A. Krommes, in *Handbook of Plasma Physics*, edited by R. H. Sudan and A. A. Galeev (North-Holland, Amsterdam, 1984), Vol.2, p.183.

[20] P. H. Diamond, R. D. Hazeltine, Z. G. An, B. A. Carreras, and H. R. Hicks, Phys. Fluids **27**, 1449 (1984).

[21] P. W. Terry and P. H. Diamond, Phys. Fluids **28**, 1419 (1985).

[22] P. W. Terry, P. H. Diamond, K. C. Shaing, L. Garcia, and B. A. Carreras, Phys. Fluids **29**, 2501 (1986).

[23] R. D. Sydora, J. N. Leboeuf, Z. G. An, P. H. Diamond, G. S. Lee, and T. S. Hahm, Phys. Fluids **29**, 2871 (1986).

[24] G. S. Lee and P. H. Diamond, Phys. Fluids **29**, 3291 (1986).

[25] B. A. Carreras, L. Garcia, and P. H. Diamond, Phys. Fluids **30**, 1388 (1987).

[26] H. Sugama and M. Wakatani, J. Phys. Soc. Jpn. **57**, 2010 (1988).

[27] M. Wakatani and A. Hasegawa, Phys. Fluids **27**, 611 (1984).

[28] A. Hasegawa and K. Mima, Phys. Fluids **21**, 87 (1978).

[29] M. N. Rosenbluth, N. A. Krall, and N. Rostoker, Nucl. Fusion Suppl. Pt.1, 143 (1962).

[30] R. M. Kulsrud, Phys. Fluids **6**, 904 (1963).

[31] M. Wakatani, H. Sugama, and A. Hasegawa, Phys. Fluids **29**, 905 (1986).

[32] H. Sugama, M. Wakatani, and A. Hasegawa, Phys. Fluids **31**, 1601 (1988).

[33] J. M. Greene and J. L. Johnson, Phys. Fluids **4**, 875 (1961).

[34] S. I. Braginskii, in *Reviews of Plasma Physics*, edited by M. A. Leontovich (Consultants Bureau, New York, 1965), Vol.1, p.205.

[35] R. D. Hazeltine, M. Kotschenreuter, and P. J. Morrison, Phys. Fluids **28**, 2466 (1985).

[36] C. T. Hsu, R. D. Hazeltine, and P. J. Morrison, Phys. Fluids **29**, 1480 (1986).

[37] G. Rewoldt, M. Wakatani, and J.L. Johnson, Plasma Phys. Contr. Fusion **29**, 1643 (1987).

[38] B. R. Suydam, in *Proceedings of the Second United Nations International Conference on the Peaceful Uses of Atomic Energy*, Geneva, 1958 (Columbia University Press, New York, 1959), Vol.31, p.157.

[39] H. P. Furth, J. Killeen, and M. N. Rosenbluth, Phys. Fluids **6**, 459 (1963).

[40] L. Chen, P. N. Guzdar, J. Y. Hsu, P. K. Kaw, C. Oberman, and R. White, Nucl. Fusion **19**, 373 (1979).

[41] L. Chen, M. S. Chance, and C. Z. Cheng, Nucl. Fusion **20**, 901 (1980).

[42] T. S. Hahm and L. Chen, Phys. Fluids **28**, 2432 (1985).

[43] A. Hasegawa and M. Wakatani, Phys. Rev. Lett. **59**, 1581 (1987).